

NANOPHOTONICS
AND
MICRO/NANO OPTICS
INTERNATIONAL CONFERENCE
/ OCT 25-27, 2022
FIAP JEAN MONNET, PARIS

BOOK OF ABSTRACTS

Table of Contents

Shedding Nanolight on Quantum Materials	1
<u>Prof. Dimitri Basov</u>	
Quantum Control of Levitated Nanoparticles	2
<u>Prof. Lukas Novotny</u>	
Synchronization of spin-driven limit cycle oscillators optically levitated in vacuum	3
Dr. Oto Brzobohaty, Mr. Martin Duchan, Dr. Petr Jákl, Dr. Vojtěch Svak, Prof. Pavel Zemanek, <u>Dr. Stephen Simpson</u>	
Evolution of the phonon-photon coupling regime in microcavities filled with hexagonal boron nitride	4
<u>Ms. María Barra-Burillo</u> , Mr. Unai Muniain, Dr. Sara Catalano, Dr. Marta Autore, Prof. Fèlix Casanova, Prof. Luis E. Hueso, Prof. Javier Aizpurua, Dr. Ruben Esteban, Prof. Rainer Hillenbrand	
Optical shaping of surface-scattered low-energy electrons	5
<u>Mr. Adamantios P. Synanidis</u> , Dr. P. André D. Gonçalves, Prof. F. Javier García de Abajo	
Two-photon pumped exciton-polariton condensation	6
Mr. Nadav Landau, Mr. Dmitry Panna, Dr. Sebastian Brodbeck, Prof. Christian Schneider, Prof. Sven Höfling, <u>Prof. Alex Hayat</u>	
Vacuum-induced Power Broadening in Core-shell Nanoparticles	7
Dr. Felix Stete, Dr. Wouter Koopman, Dr. Carsten Henkel, Prof. Oliver Benson, <u>Dr. Günter Kewes</u> , Prof. Matias Bargheer	
Real-time Interfacial Nanothermometry Using DNA-PAINT Microscopy	8
<u>Mr. Sjoerd Nooteboom</u> , Dr. Yuyang Wang, Dr. Swayandipta Dey, Dr. Peter Zijlstra	
Nanoantenna enhanced single-molecule biosensing using transient DNA interactions	10
<u>Mr. Vincenzo Lamberti</u> , Dr. Peter Zijlstra, Dr. Mathias Dolci	
Hybrid gold-DNA origami nanostructures for colorimetric sensing	12
<u>Ms. Claudia Corti</u> , Ms. Elise Gayet, Dr. Nesrine Aissaoui, Dr. Sylvie Marguet, Dr. Gaetan Bellot, Dr. Sébastien Bidault	
Real-time optoplasmonic single-molecule sensors for discerning the physicochemical interactions of multifunctional Glyphosate molecules with gold nanoparticles	14
<u>Ms. Kalani Perera</u> , Dr. Sivaraman Subramanian, Dr. Srikanth Pedireddy, Prof. Frank Vollmer	
Subcellular cardiac sensing with biointegrated nanolasers	16
<u>Prof. Marcel Schubert</u> , Dr. Soraya Caixeiro, Ms. Vera Titze, Prof. Malte Gather	
Supersymmetric reshaping and higher-dimensional rearrangement of photonic lattices	17
<u>Dr. Tom Wolterink</u> , Dr. Matthias Heinrich, Prof. Alexander Szameit	
Deeply subwavelength 2D microscopy enabled by artificial intelligence	18
<u>Mr. Sergei Kurdiomov</u> , Dr. Nikitas Papasimakis, Dr. Jun-Yu Ou, Prof. Nikolay Zheludev	

Imaging single molecules on nanoparticles: exploiting PSF deformations for precise localization	19
Mr. Teun Huijben, Ms. Sarojini Mahajan, Mr. Masih Fahim, Dr. Peter Zijlstra, Prof. Rodolphe Marie, Dr. Kim I. Mortensen	
Optical near-field characterization of plasmonic modes in a two-wire system	20
Mr. Marc Noordam, Prof. L. Kuipers	
Strain-modulation of the Photoluminescence of 2D Hybrid Metal-Halide Perovskite Flakes	22
Ms. María Barra-Burillo, Dr. Davide Spirito, Dr. Francesco Calavalle, Dr. Costanza L. Manganelli, Dr. Marco Gobbi, Prof. Rainer Hillenbrand, Prof. Fèlix Casanova, Prof. Luis E. Hueso, Dr. Beatriz Martín-García	
Quantum Optical Scattering applied to Integrated Photonics	23
Dr. A. C. Amaro de Faria Jr	
Origin of thermal and cold modification induced by femtosecond laser ablation in diamond	25
Dr. Ahmed Abdelmalek, Prof. Bedrane Zeyneb, Dr. Lebogang Kotsedi, Dr. El-Hachemi Amara, Prof. Malik Maaza	
Effects of Crystalline Structure on Second-Harmonic Generation in Thin GaAs Nanowires	26
Dr. Bin Zhang, Dr. Jan Stehr, Dr. Ping-Ping Chen, Dr. Xingjun Wang, Dr. Fumitaro Ishikawa, Prof. Weimin Chen, Prof. Irina Buyanova	
Light extraction and injection enhancement using metallic nanocubes	27
Dr. François Réveret, Dr. Mohammad Khaywah, Dr. Audrey Potdevin, Dr. Rachid Mahiou, Prof. Youcef Ouerdane, Dr. Anthony Désert, Prof. Stephane Parola, Prof. Geneviève Chadeyron, Prof. Emmanuel Centeno, Dr. Rafik Smaali, Dr. Antoine Moreau	
Nanoplasmonics for efficient gas sensing and detection.	28
Dr. Benjamin Demirdjian, Dr. Igor Ozerov, Mr. Frédéric Bedu, Mr. Alain Ranguis, Dr. Claude R. Henry	
Angular dependence of localized surface plasmon resonance extinction in anisotropic silver nanoplates	29
Mr. luca salemi, Mr. Orazio Samperi, Dr. Marcello Condorelli, Mr. Mario Pulvirenti, Prof. Luisa D'Urso, Prof. Giuseppe Compagnini	
Ultra-fast photochemistry in the strong light-matter coupling regime	31
Mr. Arpan Dutta, Mr. Ville Tiainen, Dr. Luis Duarte, Dr. Nemanja Markesevic, Dr. Ruth Tichauer, Mr. Hassan Qureshi, Dr. Gerrit Groenhof, Dr. Jussi Toppari	
Finite difference time domain simulations of GaAs-based ridge waveguide with Bragg gratings	32
Ms. Yasmin Rahimof, Mr. Sten Wenzel, Dr. Igor Nechepurenko, Dr. Bassem Arar, Dr. Andreas Wicht	
Designing an opto-spintronic semiconductor nanostructure with nearly 100% electron and photon spin polarization at room temperature	33
Dr. Y Huang, Dr. V Polojärvi, Dr. S Hiura, Mr. P Höjer, Dr. A Aho, Dr. R Isoaho, Dr. T Hakkarainen, Prof. M Guina, Dr. S Sato, Dr. J Takayama, Prof. A Murayama, Prof. Irina Buyanova, Prof. Weimin Chen	
Van der Waals materials for applications in nanophotonics	34
Dr. Panaiot Zotev, Dr. Yue Wang, Mr. Toby Severs Millard, Dr. Daniel Andres-Penares, Dr. Luca Sortino, Dr. Nic Mullin, Mr. Donato Conteduca, Dr. Mauro Brotons-Gisbert, Mr. Sam Randerson, Mr. Mostafa Shagar, Prof. Jamie Hobbs, Prof. Brian Gerardot, Prof. Thomas Krauss, Prof. Alexander Tartakovskii	

Nanoimaging of vibrational strong coupling between propagating phonon polaritons and organic molecules	35
Mr. Andrei Bylinkin, Dr. Martin Schnell, Dr. Marta Autore, Dr. Francesco Calavalle, Dr. Peining Li, Dr. Javier Taboada-Gutiérrez, Dr. Song Liu, Prof. James H. Edgar, Prof. Fèlix Casanova, Prof. Luis E. Hueso, Dr. Pablo Alonso González, Dr. Alexey Y. Nikitin, Prof. Rainer Hillenbrand	
Full control of the electric and magnetic light-matter interactions through a plasmonic mirror on a near-field tip	36
Mr. Benoît Reynier, Mr. Eric Charron, Mr. Obren Markovic, Mr. Xingyu Yang, Dr. Bruno Gallas, Dr. Sébastien Bidault, Dr. Mathieu Mivelle	
Anapole states in gap-surface plasmon resonators	38
Dr. Torgom Yezekyan, Dr. Vladimir Zenin, Dr. Jonas Beermann, Prof. Sergey Bozhevolnyi	
Efficient distributed feedback lasers with parity-time symmetry breaking	39
Mr. Yaoyao Liang, Dr. Quentin Gaimard, Dr. Jean-Rene Coudeville, Dr. Alexandre Garreau, Dr. Arnaud Wilk, Prof. Henri Benisty, Prof. Abderrahim Ramdane, Prof. Anatole Lupu	
Laser-induced Self-organized Quasi-random Plasmonic Nanomaterials: Hybridization of Plasmonic and Photonic Modes	40
Mr. Van Doan Le, Mr. Yaya Lefkir, Prof. Nathalie Destouches	
Optical horn antenna for extremely high single molecule detection rates	41
Dr. sunny tiwari, Mr. prithu roy, Dr. Jean Benoit Claude, Dr. Jérôme Wenger	
Aluminum bowties for broadband SEIRA sensing	42
Mrs. Melissa Najem, Mr. Franck Carcenac, Prof. Thierry Taliercio, Dr. Fernando Gonzalez-Posada Flores	
Aluminum Nanostructure for Deep-Ultraviolet Nanophotonics and its Application in Label-Free Single-Molecule Biophysics	43
Mr. prithu roy, Dr. Jean Benoit Claude, Dr. Jérôme Wenger	
Introduction of mesoporous gold materials for plasmonic applications	44
Dr. Olga Guselnikova, Dr. Joel Henzie, Prof. Yusuke Yamauchi	
Plasmonic cavity based molecular junction for combined transport and spectroscopy	46
Ms. Sakthi priya Amirtharaj, Mrs. Xie Zhiyuan, Dr. Wen Chen, Dr. Emanuel Lörtscher, Prof. Christophe Galland	
THz time-domain spectroscopy modulated with semiconductor plasmonic perfect absorbers	48
Dr. Fernando Gonzalez-Posada Flores, Dr. Dominique Coquillat, Mrs. Melissa Najem, Prof. Thierry Taliercio	
Satisfying solutions to inverse design problems in photonics	50
Ms. Pauline Bennet, Dr. Olivier Teytaud, Mr. Vage Karakhanyan, Dr. Thierry Grosjean, Dr. Rafik Smaali, Prof. Emmanuel Centeno, Dr. Antoine Moreau	
AI based forward prediction and inverse design of complex metasurfaces	52
Dr. Tianning Zhang, Dr. Chunyun Kee, Prof. Yee sin Ang, Prof. Ricky ANG	
Inverse-designed dielectric cloaks for entanglement generation	54
Mr. Alberto Miguel, Prof. Antonio I. Fernández-Domínguez, Prof. Francisco José García Vidal, Mr. Jaime Abad Arredondo	

Universal active metasurface modulation with ultimate performance in reflection	55
<u>Dr. Mahmoud Elsawy, Dr. Christina Kyrou, Dr. Elena Mikheeva, Dr. Remi Colom, Dr. Jean-Yves Duboz, Dr. Stéphane Lanteri, Dr. Patrice Genevet</u>	
A Chiral Inverse Faraday Effect Mediated by an Inverse-designed Plasmonic Antenna	57
<u>Mr. Ye Mou, Mr. Xingyu Yang, Dr. Bruno Gallas, Dr. Mathieu Mivelle</u>	
Geometry optimization of the magnetic Purcell factor in high index dielectric nanostructures	58
<u>Dr. Yoann Brûlé, Dr. Peter Wiecha, Dr. Aurélien Cuche, Prof. Vincent Paillard, Prof. Gérard Colas des Francs</u>	
Optimal nanophotonics: the road from theory to practice	60
<u>Prof. Alejandro Rodriguez</u>	
Biphoton generation in nanostructures at telecom wavelength	61
<u>Prof. Rachel Grange</u>	
Nonlinear Topological Photonics	62
<u>Dr. Mikael Rechtsman</u>	
TBD	63
<u>Prof. Laura Na Liu</u>	
Plasmon Empowered Nanophotonics	64
<u>Prof. Sergey Bozhevolnyi</u>	
Topological plasmonics: Watching the ultrafast vector dynamics of plasmonic skyrmions	65
<u>Prof. Harald Giessen</u>	
Isotropic and anisotropic regime in the limit of weak disorder	66
<u>Dr. Afifa Yedjour</u>	
New plasmonic-magnetic nanomaterials for Raman analysis of surfaces	67
<u>Prof. Andrzej Kudelski</u>	
FRET-mediated Collective Blinking of Self-Assembled Stacks of Semiconducting Nanoplatelets	69
<u>Mr. Zakarya Ouzit, Dr. Jiawen Liu, Mr. Guillaume Baillard, Mr. Juan Pintor, Dr. Lilian Guillemeney, Mr. Benoît Wagnon, Dr. Benjamin Abécassis, Dr. Laurent Coolen</u>	
Chirality of absorption bands of functionalized CdSe monitored through photoluminescence intensity	70
<u>Ms. Lingfei Cui, Mr. Leonardo Curti, Dr. Benoit Fleury, Dr. Yoann Prado, Dr. Emmanuel Lhuillier, Dr. Benjamin Abécassis, Prof. Catherine Schwob, Dr. Mathieu Mivelle, Dr. Bruno Gallas</u>	
Novel ways to image the brain	71
<u>Mr. Sam Crowther</u>	
Effect of charging on electronic structure and plasmonic properties of derivatized anthracenes	72
<u>Mr. Gokul Raj Mini Rajendran, Dr. Pavol Tisovský, Dr. Lukáš Félix Paštka, Dr. Milan Sýkora</u>	
Fano Resonances in Wire Metamaterials	74
<u>Dr. David Fernandes, Mr. Francisco Faim, Dr. Sylvain Lannebère, Dr. Tiago A. Morgado</u>	
Label-free detection of virus with specificity by self-assembly single nanostructure	75
<u>Dr. Yali Sun, Dr. Zeying Zhang, Prof. Meng Su, Prof. Yanlin Song, Dr. Dmitry Zuev</u>	

Superfluorescence from Mie-resonant lead halide superlattices	76
<u>Mr. Pavel Tonkaev</u>	
Mueller Matrix Ellipsometry for accurate metrology of arrays of Au patches supporting Gap Surface Plasmons	77
<u>Mr. Per Walmsness, Mr. Nathan Hale, Prof. Morten Kildemo</u>	
Hyperbolic Meta-Antennas for Light-Matter Interaction Engineering	78
<u>Mrs. Sema Ebrahimi, Mrs. Sema Ebrahimi, Dr. Alina Muravitskaya, Dr. Ali Adawi, Dr. Anne-Laure Baudrion, Prof. Pierre-Michel Adam, Dr. Jean-Sebastien Bouillard</u>	
Amplified spontaneous emission in CsPbBr₃ decorated metasurfaces	80
<u>Dr. Giammarco Roini, Mr. Gabriele Calusi, Prof. Ivano Alessandri, Prof. Anna Vinattieri</u>	
Metasurfaces integration for high field of view and ultrafast LiDAR	81
<u>Mr. Emil Marinov, Dr. Renato Juliano Martins, Mr. Aziz Ben Youssef, Dr. Patrice Genevet</u>	
Cascaded-mode optics: generalizing near-field optical design and optical resonators	82
<u>Prof. Vincent Ginis, Prof. Ileana-Cristina Benea-Chelmu, Dr. Jinsheng Lu, Dr. Marco Piccardo, Prof. Federico Capasso</u>	
Infrared Plasmons in Ultrahigh Conductive PdCoO₂ Metallic Oxide	83
<u>Dr. Salvatore Macis, Dr. Luca Tomarchio, Prof. Stefano Lupi</u>	
Tuning of the quasi-trapped mode response of dielectric metasurfaces	84
<u>Dr. Andrey B. Evlyukhin</u>	
Angle-resolved optical properties of the regular arrays of diamond-shaped silver nano-particles	85
<u>Dr. Iryna Gozhyk, Mr. Leo Laborie, Dr. Paul Jacquet, Dr. Barbara Bouteille, Dr. Jeremie Teisseire, Dr. Rémi Lazzari, Dr. Jacques Jupille, Dr. Philippe Gogol, Dr. Beatrice Dagens</u>	
DNA-templated ultracompact optical antennas for unidirectional single-molecule emission	86
<u>Mr. Fangjia Zhu, Dr. Maria Sanz-Paz, Dr. Mauricio Pilo-Pais, Prof. Antonio I. Fernández-Domínguez, Prof. Fernando Stefani, Prof. Guillermo Acuna</u>	
A quantum circuit architecture by integrating nanophotonic devices and two-dimensional molecular network	88
<u>Dr. Wei Wu</u>	
Semiconductors nanocrystals in microcavity for microlasers development	90
<u>Mr. Charlie Kersuzan, Mr. Sergei Celaj, Dr. Thomas Pons, Prof. Agnes Maitre</u>	
Size-dependent Electronic Properties of Strongly Confined Graphene Quantum Dots	92
<u>Dr. Milan Sýkora</u>	
Coupling of strain-induced single-photon emitters in a MoSe₂ monolayer to a low-loss plasmonic waveguide	94
<u>Mr. Paul Steinmann, Mr. Yuhao Zhang, Mr. Hans-Joachim Schill, Prof. Stefan Linden</u>	
An integrated single photon source at room temperature	95
<u>Dr. Christophe Couteau</u>	

Directed and enhanced photoluminescence of quantum nanoemitters using all-dielectric nanostructures	96
Dr. Romain HERNANDEZ, Dr. Mélodie Humbert, Dr. Peter Wiecha, Dr. Franck Fournel, Dr. Vincent Larrey, Dr. Guilhem Larrieu, Prof. Vincent Paillard, Prof. Laurence Ressier, Dr. Aurélien Cuche	
Deterministic generation of frequency entangled photonic multi-qudit states in modulated qubit arrays	98
Mr. Denis Ilin, Dr. Alexander poshakinskiy, Prof. Alexander Poddubny, Prof. Ivan Iorsh	
Electrical Generation of Surface Phonon Polaritons	100
Dr. Christopher Gubbin, Prof. Simone De Liberato	
Collective strong coupling in a plasmonic nanocavity: where is quantum ?	101
Mr. Alberto Alexander Diaz Valles, Dr. Hugo Varguet, Dr. Benjamin Rousseaux, Prof. Stéphane Guérin, Prof. Hans-Rudolf Jauslin, Prof. Gérard Colas des Francs	
DNA origami assembled nanoantennas for manipulating single-molecule spectral emission	103
Dr. Maria Sanz-Paz, Mr. Fangjia Zhu, Dr. Mauricio Pilo-Pais, Prof. Guillermo Acuna	
Observation of microcavity fine structure	104
Mr. Corné Koks, Prof. Martin van Exter	
Strong coupling between polaritons and both vibrational and electronic excitations of organic molecules	106
Mr. Andrei Bylinkin, Dr. Francesco Calavalle, Ms. María Barra-Burillo, Mr. Roman Kirtaev, Dr. Elizaveta Nikulina, Dr. Evgenii Modin, Prof. James H. Edgar, Prof. Fèlix Casanova, Prof. Luis E. Hueso, Prof. Valentin Volkov, Prof. Paolo Vavassori, Dr. Igor Aharonovich, Dr. Pablo Alonso González, Prof. Rainer Hillenbrand, Dr. Alexey Y. Nikitin	
Polaron-enhanced exciton-polariton optical nonlinearity in perovskite photonic crystal slab	107
Mr. Mikhail Masharin, Dr. Vanik Shahnazaryan, Dr. Fedor Benimetskiy, Prof. Ivan Shelykh, Prof. Sergey Makarov, Dr. Anton Samusev, Dr. Anton Samusev	
Quantum Hydrodynamic Theory for Plasmonics: from Molecule-Coupling to Nonlinear Optics	109
Dr. Cristian Ciraci, Dr. Henrikh Baghramyan, Dr. Muhammad Khalid, Dr. Fabio Della Sala	
Bimetallic plasmonic metasurface for asymmetric second-harmonic generation	110
Dr. Sergejs Boroviks, Mr. Andrei Kiselev, Dr. Karim Achouri, Prof. Olivier J.F. Martin	
Non-Hermitian anharmonicity induces photon blockade in hybrid metalldielectric cavities	112
Dr. Anael Ben-Asher, Prof. Antonio I. Fernández-Domínguez, Dr. Johannes Feist	
Plasmon enhanced SHG of BaTiO₃ nanocubes	113
Dr. Laureen Moreaud, Mr. Guillaume Boudan, Dr. William Djampa-Tapi, Mr. Aurélien Loirette-Pelous, Dr. Alexandra Bogicevic, Dr. Mondher Besbes, Prof. Jean-Jacques Greffet, Prof. Nicolas Lequeux, Dr. Thomas Pons, Dr. Christine Bogicevic, Prof. François Marquier, Dr. Simon Vassant, Dr. Céline Fiorini	
Nonlinear meta-holograms for the generation of second harmonic vortex beams	115
Ms. Laure Coudrat, Dr. Pascal Filloux, Dr. Romain Dezert, Dr. Adrien Borne, Dr. Tana Ranos, Dr. Julien Claudon, Dr. Jean-Michel Gérard, Dr. Aloyse Degiron, Prof. Giuseppe Leo	
Photon Pair Correlations in Semiconductor-Superconductor Light Sources	117
Dr. Shlomi Bouscher, Mr. Dmitry Panna, Dr. Ronen Jacovi, Dr. Ankit Kumar, Prof. Sebastian Klembt, Prof. Sven Höfling, Prof. Alex Hayat	

An Achiral Magnetic Photonic Antenna as a Tunable Nanosource of Superchiral Light	118
Ms. Lingfei Cui, Dr. Bruno Gallas, Dr. Mathieu Mivelle, Mr. Xingyu Yang, Mr. Benoît Reynier, Dr. Catherine Schwob, Dr. Sébastien Bidault	
An Inverse Faraday effect generated by linearly polarized light through a plasmonic nano-antenna	119
Mr. Xingyu Yang, Mr. Ye Mou, Mr. Homero Zapata, Mr. Benoît Reynier, Dr. Bruno Gallas, Dr. Mathieu Mivelle	
Opening Gap Nanopatch Antenna: A Surface Plasmon Polariton Source	120
Ms. Nhung Vu, Dr. Bruno Bérini, Dr. Stephanie Buil, Dr. Frédéric Lerouge, Prof. Emmanuel Cottancin, Dr. Michel Pellarin, Dr. Julien Laverdant	
Optoinduced magnetization in metal from the spin and orbital angular momenta of light	121
Mr. Vage Karakhanyan, Mr. Clément Eustache, Dr. Yannick Lefier, Dr. Thierry Grosjean	
Giant increase of absorption cross section of CdSe /CdS single nanocrystal within a plasmonic antenna	122
Dr. Amit Raj Dhawan, Dr. Michel Nasilowski, Prof. Benoit Dubertret, Prof. Agnes Maitre	
The glowing fate of hot electrons	124
Dr. Alexandre Bouhelier, Dr. Adrian Agreda, Dr. Deepak Sharma, Mr. Florian Dell’Ova, Dr. Konstantin Malchow, Dr. HAMDAD Sarah, Prof. Gérard Colas-des-Francs, Dr. Erik Dujardin	
Nanoaperture Tweezers: From Single Proteins to Single Quantum Emitters	125
Prof. Reuven Gordon	
“Hot” carriers in metal nanostructures – when they matter, and when they do not...	126
Prof. Yonatan Sivan	
Purcell Effect in Colloidal Plasmonic and Dielectric Resonators	127
Dr. Sébastien Bidault	
Aggregation of Gold Nanoparticles Induced by Halide Salts	128
Dr. Vittorio Scardaci, Dr. Marcello Condorelli, Ms. Lucrezia Catanzaro, Prof. Giuseppe Compagnini	
Electric field enhancement of dielectric nanoparticle with nanometer-sized low index slot	129
Mr. Seokhyeon Hong, Mr. Youngsoo Kim, Mr. Seung Hyeon Hong, Mr. Sanghyeok Yu, Ms. Bo Kyung Kim, Prof. Soon-Hong Kwon	
PSF distortion and mislocalization by dielectric nanoparticles in single-molecule microscopy	131
Mr. Masih Fahim, Mr. Teun Huijben, Dr. Kim I. Mortensen, Prof. Jonas N. Pedersen, Prof. Rodolphe Marie	
Single-photon superradiance: effects of the dielectric environment and accuracy of the rotating-wave approximation	132
Mr. Mads A. Jørgensen, Dr. Devashish Pandey, Dr. Sanshui Xiao, Dr. Nicolas Stenger, Dr. Martijn Wubs	
The Handedness (Chirality) Of A Neuronal Molecule Using Plasmonic Chains	133
Mrs. Shahin Ghamari, Dr. Hsin Yu Wu, Prof. Frank Vollmer	
Efficient Si metasurface mirror design for practical realization	135
Ms. Mariia Matiushechkina, Dr. Andrey B. Evlyukhin, Dr. Vladimir Zenin, Prof. Boris Chichkov, Prof. Michèle Heurs	
Fabrication of dielectric metasurfaces with 2π phase control	136
Ms. Shan Song	

Thermo-optical simulation of Bragg gratings for monolithically integrated extended cavity diode lasers	138
<u>Dr. Igor Nechepurenko, Ms. Yasmin Rahimof, Mr. Sten Wenzel, Dr. Bassem Arar, Dr. Andreas Wicht</u>	
Glyphosate IR spectroscopy with a plasmonic sensor optical transductor based in functionalized semi-conductor nanoantennas	139
<u>Dr. Anis Taleb Bendiab, Mrs. Cécile Pohar, Dr. Marion Mortamais, Dr. Nicola Marchi, Dr. Julie Perroy, Dr. AMARIA BAGHDADLI, Prof. Thierry Taliercio, Dr. Fernando Gonzalez-Posada Flores</u>	
Plasmonic nanoparticles for the exploration of strong field physics	141
<u>Dr. Sylvie Marguet, Prof. Bruno Palpant, Dr. Ludovic Douillard</u>	
Extremely large broadband emission of CdSe/CdS nanocrystals under high excitation	142
<u>Mr. Damien Simonot, Mr. Poncia Nyembo, Dr. Celine Roux-Byl, Dr. Thomas Pons, Dr. Simon Huppert, Prof. Agnes Maitre</u>	
The nonlinear optical response and non-equilibrium electron dynamics in ITO	144
<u>Dr. Subhajit Sarkar, Dr. Ieng-Wai Un, Prof. Yonatan Sivan</u>	
Raman amplification for trapped radiation in crystalline Si single nanoparticle	145
<u>Dr. Giovanni Mannino, Dr. Marcello Condorelli, Prof. Giuseppe Compagnini, Prof. Giuseppe Faraci</u>	
Speeding up trapping of nanoparticles in nanoaperture optical tweezers by applying a voltage	147
<u>Ms. Elham Babaei, Prof. Reuven Gordon</u>	
Comprehensive in-situ study of solution-based quantum dots with plasmonic tweezers	148
<u>Ms. Parinaz Moazzezi, Mr. Hao Zhang, Dr. Juanjuan Ren, Ms. Brett Henderson, Dr. Cristina Cordoba, Mr. Vishal Yeddu, Prof. Arthur Blackburn, Prof. Makhsud Saidaminov, Prof. Irina Paci, Prof. Stephen Hughes, Prof. Reuven Gordon</u>	
Double nanohole optical tweezers probe for protein-ligand binding	149
<u>Mr. Samuel Mathew, Prof. Laura Itzhaki, Prof. Iveta Bahar, Mr. Anupam Banerjee, Dr. Moshin Naqvi, Dr. Janet Kumita, Dr. Michael Ohlmeyer, Dr. Demelza Wright, Ms. Elham Babaei, Mr. Mirali Seyed Shariadoust, Prof. Reuven Gordon</u>	
Topological engineering of plasmonic waveguide arrays	150
<u>Mrs. Anna Sidorenko, Mrs. Helene Wetter, Prof. Stefan Linden, Dr. Julian Schmitt</u>	
Enhanced second-harmonic generation from photonic crystal slabs via double-resonance bound states in the continuum	151
<u>Mr. Ji Tong Wang, Dr. Feng Xia Li, Prof. Nicolae C. Panoiu</u>	
Tip-induced and electrical control of the photoluminescence yield of monolayer WS2	153
<u>Dr. Ricardo Javier Peña Román, Dr. Rémi Bretel, Dr. Delphine Pommier, Dr. Luis E. Parra López, Dr. Etienne Lorchat, Dr. Elizabeth Boer-Duchemin, Dr. Gérald Dujardin, Prof. Luiz F. Zagonel, Dr. Guillaume Schull, Prof. Stéphane Berciaud, Dr. Eric Le Moal</u>	
Direct investigation of trivial and non-trivial photonic modes in symmetry protected edge states at telecom wavelengths at the nanoscale	154
<u>Ms. Sonakshi Arora, Dr. Thomas Bauer, Mr. Rene Barczyk, Prof. Ewold Verhagen, Prof. L. Kuipers</u>	
Mie-exciton polaritons with monolayer WSe2 hybridized by van der Waals nanophotonic structures	156
<u>Dr. Yadong Wang, Mr. Sam Randerson, Dr. Panaiot Zotev, Dr. Xuerong Hu, Dr. Yue Wang, Prof. Thomas Krauss, Prof. Alexander Tartakovskii</u>	

Shedding Nanolight on Quantum Materials

Tuesday, 25th October - 09:00: Plenary Session - Oral

Prof. Dimitri Basov¹

1. Columbia University

TBD

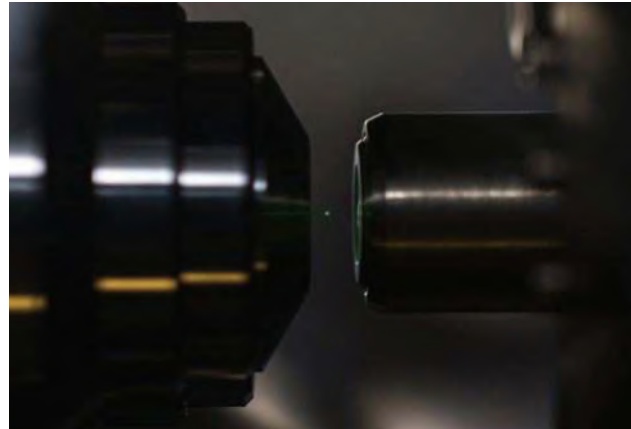
Quantum Control of Levitated Nanoparticles

Tuesday, 25th October - 09:40: Plenary Session - Oral

Prof. Lukas Novotny¹

1. ETH Zurich

We aim at generating macroscopic quantum superpositions using levitated nanoparticles in ultrahigh vacuum. Using both active and cavity-based feedback control we cool the particle's center-of-mass temperature to its quantum ground state and observe quantum signatures in the spectrum of the scattered light. The vacuum-trapped nanoparticle is an ideal model system for studying non-equilibrium processes, nonlinear dynamics and ultrasmall forces.



Particle.jpg

Synchronization of spin-driven limit cycle oscillators optically levitated in vacuum

Tuesday, 25th October - 10:50: Strong light-matter interactions at the nanoscale - Oral

Dr. Oto Brzobohaty¹, Mr. Martin Duchan¹, Dr. Petr Jákl¹, Dr. Vojtěch Svák¹, Prof. Pavel Zemanek¹, Dr. Stephen Simpson¹

¹ Institute of Scientific Instruments of the CAS, v. v. i. Královopolská 147 612 64 Brno Czech Republic

In this article we demonstrate an archetypal non-equilibrium effect: synchronization of a pair of noisy limit cycle oscillators. The oscillators comprise dielectric microspheres optically trapped in two pairs circularly polarized, counter-propagating optical beams. Non-conservative, azimuthal spin forces push the oscillators out of equilibrium [1]. For modest beam powers the stochastic motion is weakly correlated with each particle showing a tendency towards orbital circulation. At a critical, threshold power each oscillator undergoes a Hopf bifurcation, resulting in limit cycle oscillations [2]. Orbiting nanoparticles are coupled through optical and hydrodynamic interactions and the motion of the spheres becomes increasingly strongly correlated. Weak optical and hydrodynamic interactions between the particles result in the formation of a synchronized state, which is robust with respect to various minor asymmetries. In particular, we show that small frequency differences between the oscillators result in characteristic detuning behaviour whereby the synchronized state is increasingly susceptible to phase jumps in favour of the faster oscillator [3, 4].

In principle, arrays of such Non-Hermitian elements can be arranged, paving the way for opto-mechanical topological materials or, possibly, time crystals. In addition, the preparation of synchronized states in levitated optomechanics could lead to new and robust sensors or alternative routes to the entanglement of macroscopic objects could be developed.

Fig. 1: Overview of the experiment, describing the synchronized motion of two particles in parallel, counter-propagating, circularly polarized traps. (a) Basic geometry and coordinate system, (b) sections of experimentally measured orbits, (c) relative phase plotted against time, showing a discrete phase jump.

[1] V. Svák, O. Brzobohatý, M. Šiler, P. Jákl, J. Kaňka, P. Zemánek, and S. Simpson, *Nature communications* 9, 1 (2018).

[2] S. H. Simpson, Y. Arita, K. Dholakia, and P. Zemánek, *Physical Review A* 104, 043518 (2021).

[3] A. Pikovsky, M. Rosenblum, and J. Kurths, “Synchronization: a universal concept in nonlinear science,” (2002).

[4] S. Gupta, A. Campa, and S. Ruffo, *Statistical physics of synchronization*, 48 (2018).

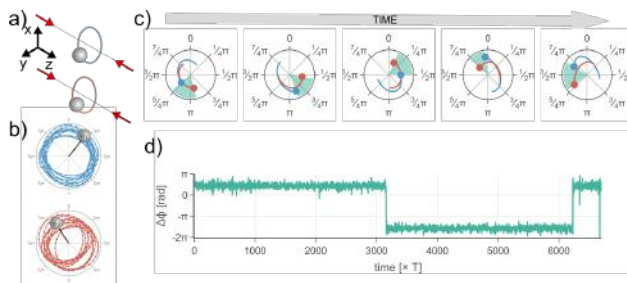


Fig1.png

Evolution of the phonon-photon coupling regime in microcavities filled with hexagonal boron nitride

Tuesday, 25th October - 11:07: Strong light-matter interactions at the nanoscale - Oral

Ms. María Barra-Burillo¹, Mr. Unai Muniain², Dr. Sara Catalano¹, Dr. Marta Autore¹, Prof. Fèlix Casanova³, Prof. Luis E. Hueso³, Prof. Javier Aizpurua⁴, Dr. Ruben Esteban⁴, Prof. Rainer Hillenbrand⁵

1. CIC nanoGUNE BRTA, **2.** Donostia International Physics Center, **3.** CIC nanoGUNE BRTA / IKERBASQUE, **4.** Donostia International Physics Center / Materials Physics Center, **5.** CIC nanoGUNE BRTA / IKERBASQUE / UPV-EHU

Recently, it has been widely studied how some properties of molecular materials, such as chemical reactivity¹ or phase transitions², can be affected by strongly coupling molecular vibrations to a microcavity mode. Coupling between phonons and microcavity modes has been much less studied, but it may offer intriguing possibilities for fundamental studies and applications^{3,4}. Here, we perform a theoretical and experimental study of the evolution of the coupling regime in classical Fabry-Pérot microcavities⁵. We use the van der Waals compound hexagonal boron nitride (hBN) to controllably obtain high-quality layers via mechanical exfoliation. Remarkably, a thin layer of 10 nm of hBN placed in the middle of the microcavity is already enough to achieve strong coupling, thus proving that strong coupling regime can be reached with only a very small amount of phononic material. Further, ultrastrong coupling regime is achieved from 100 nm of hBN on. Finally, the study of fully filled cavities yields a polariton dispersion that matches that of phonon polaritons in bulk hBN, highlighting that the maximum light-matter coupling in microcavities is limited to the coupling strength between photons and the bulk material. Tunable cavity phonon polaritons could become a versatile platform for studying how the coupling strength between photons and phonons may modify the properties of polar crystals.

1. Thomas, A. *et al.* Tilting a ground-state reactivity landscape by vibrational strong coupling. *Science*. **363**, 615–619 (2019).
2. Wang, S. *et al.* Phase transition of a perovskite strongly coupled to the vacuum field. *Nanoscale* **6**, 7243–7248 (2014).
3. Bakker, H. J., Hunsche, S. & Kurz, H. Coherent phonon polaritons as probes of anharmonic phonons in ferroelectrics. *Rev. Mod. Phys.* **70**, 523–536 (1998).
4. He, Y. *et al.* Rapid change of superconductivity and electron-phonon coupling through critical doping in Bi-2212. *Science*. **362**, 62–65 (2018).
5. Barra-Burillo, M. *et al.* Microcavity phonon polaritons from the weak to the ultrastrong phonon–photon coupling regime. *Nat. Commun.* **12**, 6206 (2021).

Optical shaping of surface-scattered low-energy electrons

Tuesday, 25th October - 11:24: Strong light-matter interactions at the nanoscale - Oral

Mr. Adamantios P. Synanidis¹, Dr. P. André D. Gonçalves¹, Prof. F. Javier García de Abajo¹

1. ICFO – Institut de Ciències Fotòniques, The Barcelona Institute of Science and Technology, 08860 Castelldefels, Barcelona, Spain

Fueled by recent advances in instrumentation and conceptual design, electron microscopy is swiftly advancing towards the goal of a combined sub-Å-sub-fs-sub-meV resolution [1]. In this context, the interaction between free electrons and light is emerging as a powerful route to manipulate the electron wave function and imprint some degree of coherence on the excitations created in a specimen, opening opportunities for studying novel aspects of electron-light interactions and potentially enabling disruptive modalities of electron microscopy [2]. While most works so far have focused on high-energy electrons (several keV's), whose phenomenology follows simple rules dictated by the nonrecoil approximation, here we investigate low-energy electrons interacting with light modes (polaritons or photons) and reveal emerging electron-light-matter phenomena associated with recoil effects.

We consider low-energy electrons impinging on an illuminated planar surface and calculate the resulting transmitted and reflected electrons by developing a Green function formalism that rigorously describes the electron-light and electron-surface interactions. We apply this formalism to several types of surfaces corresponding to different experimental scenarios, including totally and partially reflecting smooth planar interfaces as well as atomically-thin layers producing electron Bragg scattering [3].

We find that strong electron-light interactions lead to inelastically reflected and transmitted electron waves characterized by the absorption or emission of a net number of photons, similar to what is observed in photon-induced near-field electron microscopy (PINEM) [2] (see Fig. 1). For two-dimensional atomic layers, Bragg peaks are multiplexed according to such number of photon exchanges. Interestingly, in contrast to fast electrons, surface scattering provides low-energy electrons with the ability to interact with freely propagating modes –an effect that we investigate by studying electron scattering by an atomic monolayer in the presence of unscattered external light. Our work reveals the central role played by recoil in electron-light interactions at low electron energy, including the ability to enhance the coupling due to the breaking of momentum conservation along the out-of-plane direction.

[1] F. J. García de Abajo and V. Di Giulio, *ACS Photonics* **8**, 945 (2021).

[2] B. Barwick *et al.*, *Nature* **462**, 902 (2009).

[3] J. B. Pendry, *Low Energy Electron Diffraction* (Academic Press, London, 1974).

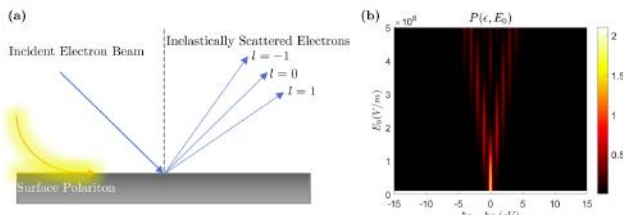


Figure 1. (a) We consider the interaction between surface polaritons and low-energy electrons scattered from a planar surface, giving rise to multiple photon exchanges (a net number of quanta l). (b) For a flat surface, the probability associated with the absorption or emission of 1 photons of energy $\hbar\omega_0 = 1\text{ eV}$ each (horizontal axis) follows a characteristic quantum billiard pattern as we increase the light intensity (vertical axis).

Figure 1.png

Two-photon pumped exciton-polariton condensation

Tuesday, 25th October - 11:41: Strong light-matter interactions at the nanoscale - Oral

Mr. Nadav Landau¹, Mr. Dmitry Panna¹, Dr. Sebastian Brodbeck², Prof. Christian Schneider³, Prof. Sven Höfling², Prof. Alex Hayat¹

1. Department of Electrical Engineering, Technion – Israel Institute of Technology, Haifa, 3200003, Israel, **2.** Technische Physik, Physikalisches Institut and Wilhelm Conrad Röntgen Research Center for Complex Material Systems, Universität Würzburg, D-97074 Würzburg, Germany, **3.** Institute of Physics, Carl von Ossietzky Universität Oldenburg, D-26111 Oldenburg, Germany

We report the first experimental observation of two-photon pumped polariton condensation, demonstrated by angle-resolved photoluminescence in a GaAs-based microcavity. Our results pave the way towards polariton-based THz lasing and coherent control of collective quantum states with individual qubits.

Two-Photon Absorption (TPA) is widely utilized nowadays for investigation of solid-state quantum-confined structures, revealing various “dark” states of matter inaccessible to conventional spectroscopy but important for quantum information processing. Recently, a condensate of strongly-coupled light-matter exciton-polaritons [1] was proposed to stimulate highly efficient THz emission, in a transition from a two-photon excited 2p “dark” exciton state [2]. This scheme could enable doubly-stimulated THz emission far more efficient than existing sources [3], and introduces new possibilities for nonlinear optics with polariton condensates, so far relying on underlying inter-particle interactions [4]. It further provides a testbed for “dark” state-condensate interactions and can implement coherent control of collective quantum states with individual qubits. So far, several groups have demonstrated TPA-based excitation of non-condensed polaritons [5], yet condensation via TPA was not achieved.

Here we demonstrate two-photon pumped polariton condensation, achieved by TPA-based excitation. We show this in a planar GaAs-based microcavity by pumping with ultrafast pulses at half the exciton energies. The resulting angle-resolved photoluminescence (PL) (Fig. 1a-c) exhibits a clear threshold as a function of TPA power, coinciding with an interaction-induced blueshift and a spectral linewidth narrowing (Fig. 1d-f), characteristic of a transition from a polariton thermal distribution to polariton condensation. TPA is evidenced in the quadratic input-output dependence below and above threshold (Fig. 1g), and second-harmonic generation is ruled out by both this threshold behaviour and by the emission peak energy showing no dependence on pump wavelength.

[1] Kasprzak, J. et al. *Nature* 443, 409 (2006).

[2] Kavokin, A. V. et al. *Phys. Rev. Lett.* 108, 197401 (2012).

[3] Tonouchi, M. *Nat. Photonics* 1, 97 (2007).

[4] Savvidis, P. G. et al. *Phys. Rev. Lett.* 84, 1547 (2000).

[5] Leménager, G. et al. *Opt. Lett.* 39, 307 (2014); Gautham, C. et al. *Optica* 4, 118 (2017).

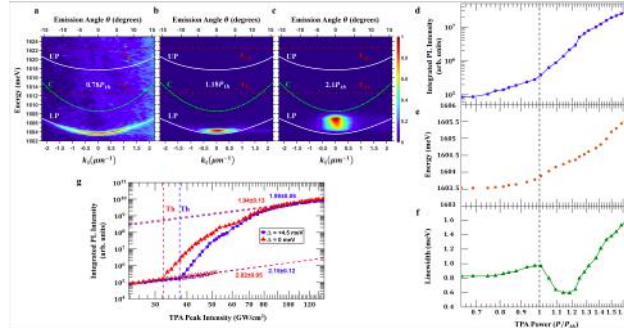


Fig2.png

Vacuum-induced Power Broadening in Core-shell Nanoparticles

Tuesday, 25th October - 11:58: Strong light-matter interactions at the nanoscale - Oral

Dr. Felix Stete¹, Dr. Wouter Koopman¹, Dr. Carsten Henkel¹, Prof. Oliver Benson², Dr. Günter Kewes², Prof. Matias Bargheer¹

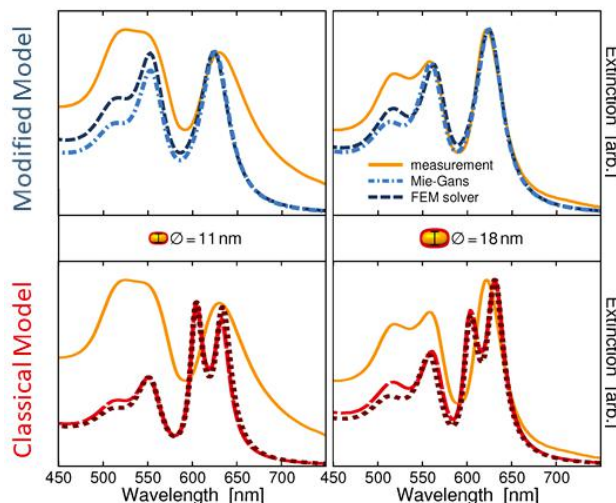
1. Institut für Physik & Astronomie, Universität Potsdam, **2.** Humboldt University of Berlin

Hybrid plasmon-exciton nanoparticles reaching the strong coupling regime, have been intensively studied in the last years. While the construction of a full quantum description of such systems is extremely challenging, it was often stated that simple classical models of two coupled oscillators cover the essential physics. In particular, such models are realized by solving Maxwell's equations with a material featuring a Lorentzian-shaped permittivity for the excitonic part.

Here, we show that this purely classical model easily breaks down. We introduce a modified permittivity based on Bloch equations for the excitonic part that takes into account power broadening. To this end, we present data of J-Aggregate (TDBC) coated gold nanorods. In our attempt to accurately simulate the experimental extinction spectra with the classical and with the modified model, the striking difference between the two models becomes apparent: instead of a prominent third peak [1] between the hybridized modes produced by the classical model, no peak emerges with the modified model.

We interpret, that the included powerbroading must be induced by the vacuum light field and suspect, that this essentially non-linear effect should be observable even before the onset of strong coupling.

[1] T. J. Antosiewicz, S. P. Apell, and T. Shegai, “Plasmon–Exciton Interactions in a Core–Shell Geometry: From Enhanced Absorption to Strong Coupling,” ACS Photonics 1, 454–463 (2014)



Nanop2022.png

Real-time Interfacial Nanothermometry Using DNA-PAINT Microscopy

Tuesday, 25th October - 10:50: Optical sensing - Oral

Mr. Sjoerd Nooteboom¹, Dr. Yuyang Wang¹, Dr. Swayandipta Dey¹, Dr. Peter Zijlstra¹

¹ Eindhoven University of Technology

Due to their plasmon resonances, metallic nanoparticles (NPs) serve as a sensitive optical platform for a range of single-particle and single-biomolecule sensors that exploit plasmon-enhanced fluorescence[1] or label-free mechanisms.[2] The optical excitation required for these applications induces local heating around the NPs due to the thermoplasmonic effect.[3] In the context of single-biomolecule applications, such local heating must be carefully controlled because it can affect the structure and function of biomolecules conjugated near the NP interface. Therefore, quantitative understanding is required of the interplay between optical excitation and the interfacial temperature of the NPs. Several methods exist that probe the temperature of single NPs,[4] but none of them provide real-time interfacial thermometry.

Here,[5] we present a nanothermometry method that achieves exactly this goal by monitoring the temperature-dependent dissociation rate (k_{off}) of single-molecule DNA interactions (DNA-PAINT,[6] see Figure 1). The observation of the fluorescently labeled DNA is aided by plasmonic fluorescence enhancement.

Figure 2 shows DNA-PAINT intensity-time traces of the same gold nanorod (AuNR) measured at different laser powers. At higher laser power, the DNA dissociation rate is significantly higher due to plasmonic heating of the AuNR surface.

After calibrating the dependence of k_{off} on temperature, we can deduce the temperature of any single AuNR from the k_{off} value observed in a timetrace. Thus, we can measure the interfacial temperature of single NPs in real-time, with intervals of a few minutes and a precision of 1 Kelvin. Figure 3 shows an example, where the bottom panel displays alternations in laser power, and the top panel displays the interfacial temperature of one AuNR measured with our method. The interfacial temperature clearly follows the alternations in power, confirming the real-time potential of our nanothermometry method, which can be applied to a wide range of nanoscale structures.

[1]Koenderink, A.F. *ACS Photonics* **2017**, *4* (4), 710–722.

[2]Beuwer, M.A. et al. *Nano Lett.* **2015**, *15* (5), 3507–3511.

[3]Baffou, G. et al. *Nat. Mater.* **2020**, *19* (9), 946–958.

[4]Jauffred, L. et al. *Chem. Rev.* **2019**, *119* (13), 8087–8130.

[5]Nooteboom, S.W. et al. *Small* **2022**, *18* (31), 2201602.

[6]Jungmann, R. et al. *Nano Lett.* **2010**, *10* (11), 4756–4761.

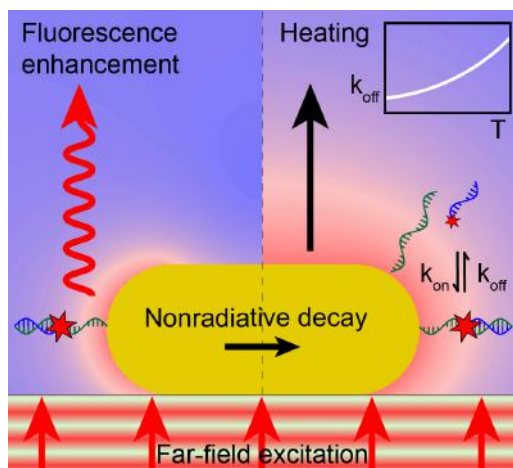


Figure 1 - overview of the method.png

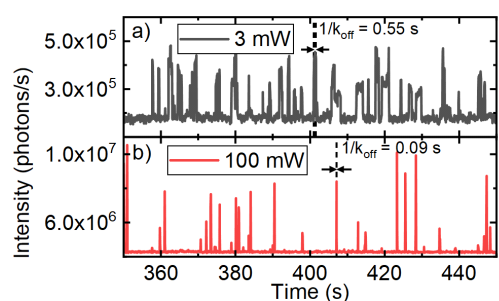


Figure 2 - effect of laser heating on dissociation rate.png

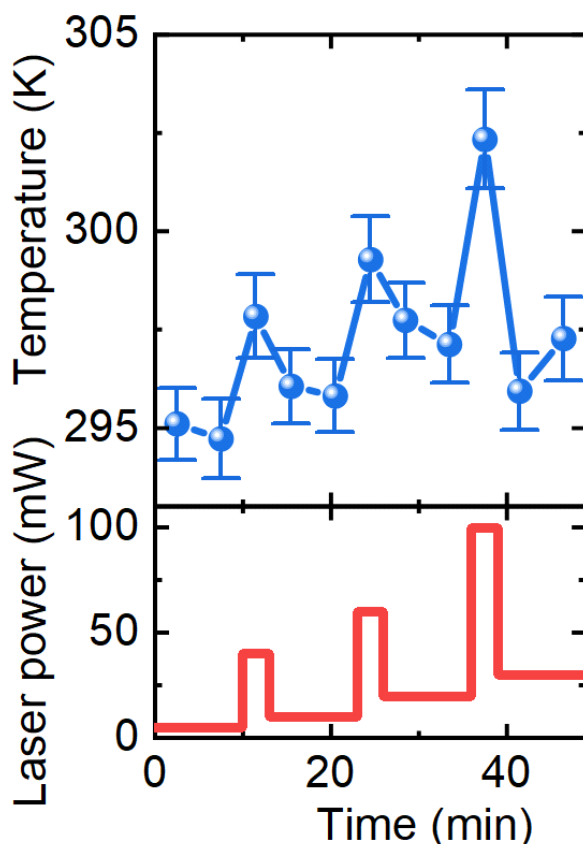


Figure 3 - monitoring real-time laser heating.png

Nanoantenna enhanced single-molecule biosensing using transient DNA interactions

Tuesday, 25th October - 11:07: Optical sensing - Oral

Mr. Vincenzo Lamberti¹, Dr. Peter Zijlstra², Dr. Mathias Dolci¹

1. Department of Applied Physics, Eindhoven University of Technology (TU/e), The Netherlands, 2. Eindhoven University of Technology

Single-molecule biosensors employing fluorescence microscopy enable direct counting of molecular targets such as nucleic acids^[1] and proteins^[2]. Whereas highly specific sandwich assays have been developed using fluorescence probes^[3], these assays provide intrinsically low single-molecule signals. As a result, existing single-molecule fluorescence approaches are not compatible with complex biological fluids such as blood serum since background autofluorescence dominates the optical response. Coincidentally, the signal's collection requires research-grade optical microscopies, incompatible with foreseen applications such as integrated R&D and point-of-care devices.

Here, we propose a particle-based sandwich assay using plasmon-enhanced fluorescence (PEF), enabling single-molecule biosensing with a strongly enhanced signal-to-noise ratio (Fig 1a). The biosensor consists of immobilized gold nanorods (Fig 2a) decorated with ssDNA capture probes. The presence of ssDNA analyte is detected in a sandwich assay by a short imager probe (Fig 1b). Fluorescent probe transiently interacts with the bound analyte resulting in a time-trace for every single particle (Fig 2b), showing bursts due to plasmon-enhanced fluorescence. The advantage of this new approach is (a) the plasmon resonance provides ~20-fold enhanced fluorescence intensity^[4] compared to a good fluorophore, (b) the transient interaction of the imager probe results in an assay that is essentially immune to photobleaching^[5], and (c) the simultaneous probing of hundreds of nanorods provides high statistics for an accurate concentration measurement.

The kinetics of the interactions (bright time and dark time, Fig 2b) are statistically analyzed at single-particle level to extract the target concentration and generate a dose-response curve (Fig 3). The current limit of detection is ~100pM, limited by a combination of non-specific interactions and affinity of the sandwich assay. We show that the enhanced signal-to-noise ratio enables single-molecule sensing directly in complex biological fluids (blood serum) with negligible background, whereas the strong signals enable device's miniaturization in the future.

- [1] Hayward, S. L. et al. J. Am. Chem. Soc, 140(37), 11755–11762. (2018).
- [2] Chatterjee, T., et al. PNAS, 117(37), 22815–22822. (2020).
- [3] Johnson-Buck, A., et al. Nature Biotechnology, 33(7), 730–732. (2015).
- [4] Taylor, A. B., & Zijlstra, P. ACS Sensors, 2(8), 1103–1122. (2017).
- [5] Horáček, M. et al. Nanoscale, 12(6), 4128–4136. (2020).

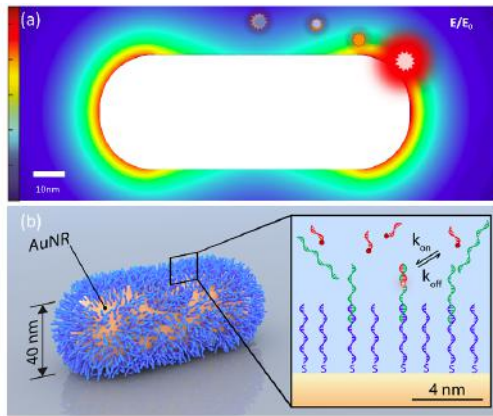


Fig. 1. (a) Amplitude of the electric near-field of a gold nanorod and plasmon-enhanced fluorescence representation. Field color map form deep blue to orange. Fluorescence color map from orange to red. Scale bar 10nm. (b) Visual representation of dynamic DNA sandwich assay. Detection of temporary bound analyte is probed by low-affinity complementary imagers.

Fig 1.png

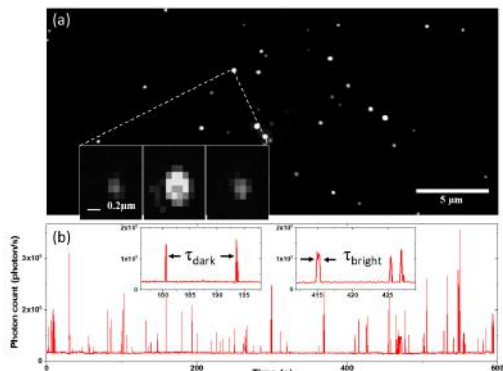


Fig. 2. (a) Typical FoV showing diffraction-limited spots that represent the photoluminescence of a single AuNR. Insets show timesteps of intensity burst due to plasmon enhanced fluorescence. (b) Experimental fluorescence time-traces corresponding to an analyte concentration of 10nM. Kinetic information are obtained by the analysis of dark and bright times.

Fig 2.png

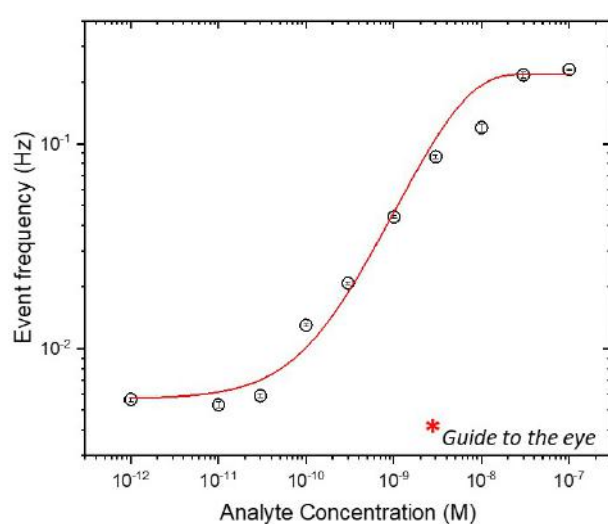


Fig. 3. Dose response curve for DNA sandwich assay in buffer based on particle average number of events in 10 min. Error bars represents standard error in particle-to-particle heterogeneity.

Fig 3.jpg

Hybrid gold-DNA origami nanostructures for colorimetric sensing

Tuesday, 25th October - 11:24: Optical sensing - Oral

Ms. Claudia Corti¹, Ms. Elise Gayet¹, Dr. Nesrine Aissaoui², Dr. Sylvie Marguet³, Dr. Gaetan Bellot⁴, Dr. Sébastien Bidault¹

1. Institut Langevin, ESPCI Paris, CNRS, **2.** CBS - Centre de Biochimie Structurale, CNRS, INSERM, Montpellier, **3.** Univ. Paris-Saclay, CEA, CNRS, NIMBE, F-91191 Gif-sur-Yvette, France, **4.** CBS - Centre de Biochimie Structurale - CNRS - INSERM - Montpellier

Colorimetric sensing based on plasmonic nanostructures allows the detection of target biomolecules using a simple optical readout but requires ensemble measurements, limiting the overall sensitivity of this approach. To develop a colorimetric sensing platform compatible with single-molecule detection, we assemble gold nanosphere dimers on a 3D Y-shaped DNA origami that acts as a nanoscale actuator (Fig. 1-a). Indeed, DNA origamis are a flexible platform to produce nanostructures that shift their morphology when interacting with specific target molecules, such as DNA/RNA strands, proteins, or specific cations [2]. To translate such conformational changes in colorimetric information, we exploit the nanoscale dependence of plasmon coupling between the two gold nanospheres. We recently demonstrated that darkfield microscopy allows the far-field monitoring of nanoscale distance changes in single gold dimers on a simple color camera [3].

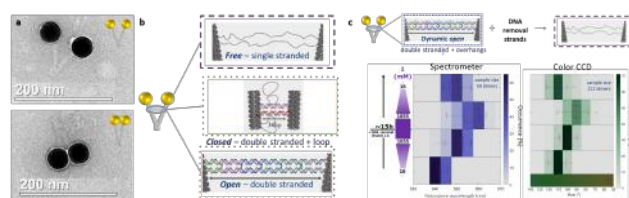
The Y-shaped DNA origami scaffold features an active site with a conformation that can be tuned by hybridizing specific DNA single strands (Fig. 1-b). The overall morphology of the hybrid nanostructure is governed by the geometry of the DNA origami but also by steric and electrostatic repulsion between gold nanospheres. We observe that the conformation of the active site is only visible in the optical response of the nanostructures for high ionic strengths when these steric and electrostatic repulsions are reduced.

Colorimetric sensing of DNA single strands is performed at high ionic strengths using a strand displacement reaction (Fig. 1-c). These measurements are performed both in single nanostructure scattering spectroscopy or by monitoring the hue of single dimers in darkfield images, providing similar statistical responses (Fig. 1-c) and opening exciting perspectives for the colorimetric sensing of individual DNA strands on a color camera.

Figure: (a) EM images with negative staining of 40nm gold particle dimers in open (top) and closed (bottom) conformations. (b) Schemes of the different conformations of the DNA origami active site and (c) strand displacement reaction monitored by single nanostructure spectroscopy (left) or colorimetric sensing (right).

References

- [1] Y. Ke et al. 2016. Nat. Commun. 7:10935.
- [2] L. Lermusiaux et al. 2015. ACS Nano 9:978.
- [3] L. Lermusiaux et al. 2018. Langmuir 34:14946.



Tem images and schemes of dna origami designs - monitoring of strand displacement reaction.png

Real-time optoplasmonic single-molecule sensors for discerning the physicochemical interactions of multifunctional Glyphosate molecules with gold nanoparticles

Tuesday, 25th October - 11:41: Optical sensing - Oral

Ms. Kalani Perera¹, Dr. Sivaraman Subramanian¹, Dr. Srikanth Pedireddy¹, Prof. Frank Vollmer¹

1. Living Systems Institute, University of Exeter

Understanding the surface properties of plasmonic metal nanoparticles is gaining increased attention in chemical and biological applications. Current sensing platforms lack precise interactions of molecules with the plasmonic nanoparticles in real time. Herein, we track the binding preference of multifunctional molecules such as Glyphosate (GLY) via oxyanions ($\text{COO}^-/\text{PO}_4^{2-}$) and amine in real-time and at the single-molecule level. This is possible by monitoring the frequency shifts of optical Whispering Gallery Modes (WGM) upon the interaction of a molecule on the gold nanorod (AuNR) surface. Transient molecule-AuNR interactions lead to spike-like events in the WGM-sensor signal time traces, and permanent interactions lead to step-like events. GLY has multi-ionic states at varying pH, which interact differently with the AuNR surface. We probe the interactions of GLY with AuNRs by changing the medium pH from 2-11 and identified the interaction of oxyanions at lower pH (<10) and the involvement of amine interactions at higher pH (>10.6), resulting in step-like WGM-sensor signals. The interactions of oxyanions $\text{COO}^-/\text{PO}_4^{2-}$ and amine were further supported by density functional theory (DFT). In the lower pH (<10) medium, pH was adjusted with HCl/NaOH and the ionic strength was maintained with NaCl, which was shown to promote the chemisorption process of GLY towards the gold surface. However, the higher binding ability towards gold was found to be at pH>10 (carbonate), in which GLY has amine lone pair along with the oxyanions to coordinate with the gold surface which has the highest binding energy even compared to the buffer molecule and is recognised as a step-like signal in the WGM-sensor traces. Furthermore, permanent interactions (pH<10) can be altered to reversible/transient interactions by using various buffer molecules (citrate, phosphate and carbonate), signified by the spike-like WGM-sensor signals, which are crucial for real-time sensing applications. These single-molecule experiments showed that the buffer molecules occupy the gold binding sites, which hinders the gold binding sites for GLY and eventually promotes a physisorption process that was further clarified by the DFT study. Therefore, it is apparent that our WGM-sensor was able to show that some of the GLY interactions with AuNR are mediated by the buffer molecules.

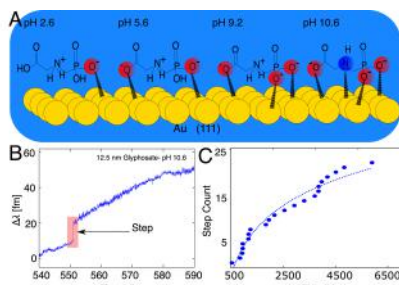


Figure 1 (A) A conceptual illustration of phosphine oxyanion (pH 2.6), carboxylate amino-Au-phosphine oxyanion (pH 5.6), carboxylate amino-Au-phosphine oxyanion (pH 9.2) and carboxylate amino-Au-phosphine oxyanion; and amino-Au (pH 10.6) left to right, respectively. (B) Discrete signals in the WGM resonator trace from the covalent bond formation of the oxyanions and amine functional group with the Au surface at pH 10.6. (C) Cumulative step counts and fitted saturation curve for amine and oxyanion AuNPs interaction at pH 10.6. Experiments were conducted at room temperature.

Image 1 nanop.png

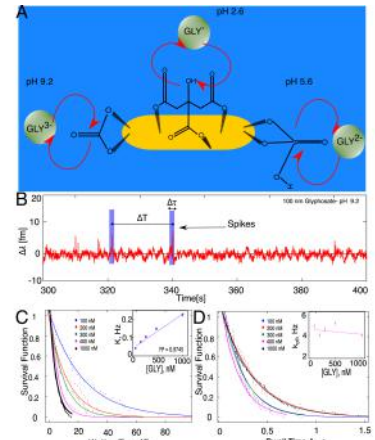


Figure 2 (A) conceptual illustration of the pre-occupancy of the carbonate (left) and phosphate (right). Citrate (up) with the gold binding sites and the reverse reaction of the corresponding ionic states of the GLY at pH 9.2, 5.6 and 2.6, respectively. (B) Spike signals in the WGM resonator trace data (the reversible reaction) due to the repulsion interaction of the carbonate molecule and GLY molecule at pH 9.2 (C) Survivor function and corresponding exponential fit to the time separation of spike events; 100 nM GLY (Blue), 200 nM GLY (Red), 300 nM GLY (Green), 500 nM GLY (Pink), and 1000 nM GLY (Black). Inset shows the regression slope of spike event rate (K) versus GLY concentration ($R^2 = 0.9746$). (D) Survivor function and corresponding exponential fit to the time separation of spike events; 100 nM GLY (Blue), 200 nM GLY (Red), 300 nM GLY (Green), 500 nM GLY (Pink), and 1000 nM GLY (Black). Inset illustrates the behaviour of the offset rate (k_{off}) versus GLY concentration. Experiments were conducted at room temperature.

Image 2 nanop.png

Subcellular cardiac sensing with biointegrated nanolasers

Tuesday, 25th October - 11:58: Optical sensing - Oral

Prof. Marcel Schubert¹, Dr. Soraya Caixeiro¹, Ms. Vera Titze², Prof. Malte Gather¹

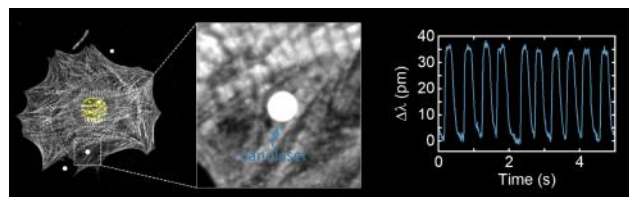
1. University of Cologne, Humboldt Centre for Nano and Biophotonics, **2.** University of St Andrews

Sensing cardiac contractility on the single cell level remains a challenging task due to fast tissue dynamics as well as strong light scattering and absorption. As a new approach to overcome these limitations, micro and nanodisk laser particles can be used as single cell barcoding and sensing devices. Based on generating laser light directly inside biological tissue, this spectroscopic sensing approach provides unique advantages over established imaging-based technologies [1].

Here, we show the integration of microscopic whispering gallery mode lasers into cardiac cells and tissue. Our experiments provide insights into the optical properties of cardiac cells during contraction. Correlating these optical characteristics to the structure of myofibrillar proteins allows us to extract cardiac contractility profiles with cellular resolution and high temporal dynamics. We demonstrate repeated measurements of single cells over the course of several days by using the multimode emission pattern as optical barcodes to identify individual cells. In addition, due to the high intensity of the biointegrated microlasers, the optical signal can be detected deep inside cardiac tissue. To demonstrate the advantage over multi-photon microscopy approaches, we characterise cardiac contractility *in vivo* in zebrafish embryos as well as in thick cardiac slices. Furthermore, by reducing the laser particle size to the dimensions of individual myofibrils - highly organized protein structures of heart muscle cells that induce cardiac contractions - we are able to perform subcellular contractility measurements. We further demonstrate the modification of the nanolaser quantum well composition to improve their spectral characteristics, resulting in emission spectra that are ideal for deep-tissue and multiphoton applications [2]. Finally, we present new microlasers that extend the range of detectable biomechanical parameters, opening new avenues for future applications of microlasers in cardiovascular research.

[1] M. Schubert et al, *Nature Photonics*, 14, 452 (2020).

[2] V. M. Titze et al, *ACS Photonics*, 9, 952 (2022).



Nanolaser contractility sensing.png

Supersymmetric reshaping and higher-dimensional rearrangement of photonic lattices

Tuesday, 25th October - 10:50: Advanced imaging - Oral

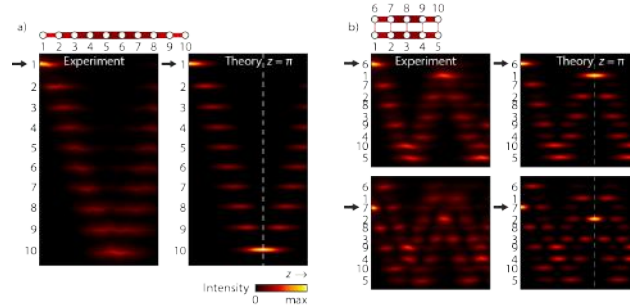
Dr. Tom Wolterink¹, Dr. Matthias Heinrich¹, Prof. Alexander Szameit¹

¹. University of Rostock

Dynamics in wave-mechanical systems are governed by the full set of its modes and their eigenvalues. The key task of imaging between two specific planes can be accomplished via the structure of the eigenvalue spectrum, in particular if the spectrum is equidistantly spaced similar to that of the harmonic oscillator. In finite-size discrete systems, the so-called Jx lattice fulfils this condition and allows for the perfect coherent transfer of quantum and classical states alike. However, implementing large-scale Jx arrays remains experimentally challenging, as this necessitates precise realization of a large number of different yet finely tuned nearest-neighbour interaction strengths across a substantial dynamic range. To overcome these limitations, we leverage the concept of supersymmetric (SUSY) photonics and present a method to design families of compact two-dimensional systems that share the spectral and dynamic features of one-dimensional Jx arrays while requiring dramatically fewer distinct coupling values.

Our approach relies on iteratively applying discrete SUSY transformations to the Hamiltonian of the Jx array, resulting in a sequence of higher-order superpartners and isolated sites, followed by reattachment of these sites in a series of inverse SUSY transformation steps in the orthogonal direction, thereby constructing 2D arrays. We experimentally realize these systems in arrays of evanescently coupled waveguides fabricated by femtosecond-laser direct writing and investigate their imaging properties by recording the intensity dynamics of guided light through fluorescence microscopy.

We find that, while exhibiting systematically different dynamics, in each of the conventional Jx array and the 2D superpartner arrays, light coalesces to the single target waveguide on the opposite side of the array at the imaging distance, realizing the desired perfect state transfer enabled by their identical spectra. Yet, the 2D superpartner exhibits these features more faithfully, as a result of its lower number of distinct couplings that makes it less susceptible to perturbations. Therefore, our method readily allows for increased robustness to perturbations and fabrication inaccuracies and provides the tools to maintain coherence during state transfer in larger-scale photonic circuits.



Light dynamics in 1d and 2d jx arrays.png

Deeply subwavelength 2D microscopy enabled by artificial intelligence

Tuesday, 25th October - 11:07: Advanced imaging - Oral

Mr. Sergei Kurdiomov¹, Dr. Nikitas Papasimakis¹, Dr. Jun-Yu Ou¹, Prof. Nikolay Zheludev²

1. University of Southampton, 2. University of Southampton, Nanyang Technological University

Optical imaging with spatial resolution beyond the Abbe-Rayleigh diffraction limit ($\sim\lambda/2$) constitutes a long-standing challenge in microscopy. To this end, a wide range of techniques have been developed, including fluorescence-based methods (STED, STORM), structured illumination, near-field imaging, and scanning approaches [1, 2]. Here we introduce a novel artificial intelligence (AI)-enabled scanning microscopy approach and demonstrate numerically an improvement of x1.4 over standard techniques (scanning confocal microscopy). In our approach, the imaging target (a Siemens star in an otherwise opaque screen, see Fig. 1a,b) is scanned with a 640 nm tightly focused laser beam with spot size of 600 nm (at $1/e^2$) and the resulting diffraction patterns are recorded at a distance of 1280 nm. The recorded patterns, corresponding to different relative positions of the sample and laser beam, are then analysed by a convolutional neural network, which reconstructs the target (Fig. 1c). During reconstruction, the target is considered to consist of sets (superpixels) of 3x3 (fully opaque or transparent) pixels. The superpixel size is 360 nm x 360 nm. To account for the effect of the surroundings on the diffraction pattern of each superpixel, the network is trained on a dataset of diffraction patterns from different superpixels with randomly selected neighbouring pixels, resulting in dataset size of 12,288. The resolution of the method was evaluated using fringe visibility analysis at different radii of the Siemens star target [3]. To quantify resolution, a visibility threshold of 0.07 was selected, at which fringes become invisible by eye [4] (see red dashed line in Fig. 1e). This corresponds to a resolution of 170 nm ($\sim\lambda/4$) (Fig. 1e). Confocal imaging of the same target (see Fig. 1d) results in resolution of 235 nm, x1.4 lower than our approach. In summary, we demonstrate an AI-enabled scanning microscopy approach outperforming the conventional diffraction limit by x2. We expect our approach finds applications in nanotechnology and biomedical sciences.

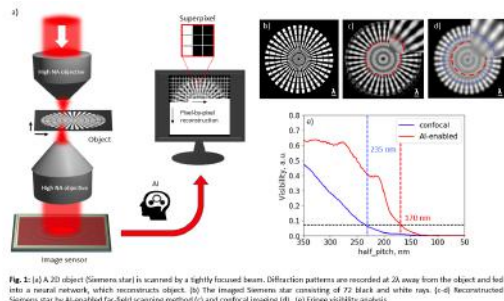


Fig1 with caption.png

References

- L. Schermelleh, A. Ferrand, T. Huser, C. Eggeling, M. Sauer, O. Biehlmaier, and G. P. C. Drummen, "Super-resolution microscopy demystified," *Nat Cell Biol* **21**(1), 72–84 (2019).
- N. I. Zheludev and G. Yuan, "Optical superscillation technologies beyond the diffraction limit," *Nat Rev Phys* **4**(1), 16–32 (2022).
- R. Horstmeyer, R. Heintzmann, G. Popescu, L. Waller, and C. Yang, "Standardizing the resolution claims for coherent microscopy," *Nature Photon* **10**(2), 68–71 (2016).
- E. T. F. Rogers, S. Quraishi, K. S. Rogers, T. A. Newman, P. J. S. Smith, and N. I. Zheludev, "Far-field unlabeled super-resolution imaging with superscillatory illumination," *APL Photonics* **5**(6), 066107 (2020).

References.png

Imaging single molecules on nanoparticles: exploiting PSF deformations for precise localization

Tuesday, 25th October - 11:24: Advanced imaging - Oral

Mr. Teun Huijben¹, Ms. Sarojini Mahajan², Mr. Masih Fahim¹, Dr. Peter Zijlstra², Prof. Rodolphe Marie¹, Dr. Kim I. Mortensen¹

1. Department of Health Technology, Technical University of Denmark (DTU), Denmark, 2. Department of Applied Physics, Eindhoven University of Technology (TU/e), The Netherlands

Nanoparticles (NPs) have proven their applicability in biosensing, drug delivery, catalysis and photo-thermal therapy. Importantly, the exact behaviour of each NP depends heavily on the number and distribution of chemical groups on its surface. Such parameters are traditionally characterized using ensemble-averaging assays, which do not capture the particle-to-particle heterogeneity resulting from variations in particle synthesis and statistical stochasticity.

Single-molecule localization microscopy, on the other hand, is ideally suited for the study of the fluorescently-labeled surface functionalizations of individual NPs in their native, typically aqueous, environment. In this technique, sequentially, sparse subsets of the fluorophores are active, and their positions are localized with high precision by fitting a Gaussian point-spread function (PSF). However, the NP acts as a scatterer near the fluorophore and consequently distorts and displaces the point-spread function (PSF) [1,2,3]. This leads to mislocalizations, when the PSF is fitted with a two-dimensional Gaussian, which is common practice in the field. Here, we present the first fully analytical description of the PSF of a fluorophore near a spherical NP of any material and size. In contrast to popular numerical approaches, our method is exact, 3 orders of magnitude faster, free and open source. This method 1) serves as an exact fitting algorithm for distorted PSFs and 2) reduces mislocalizations by serving as a predictive tool for optimal experimental design (e.g., NP material, size, and fluorophore). We show that by using the analytical PSF as a fitting tool for experimental DNA-PAINT data on spherical gold NPs, the position of the emitters on the NP surface can be retrieved (Figure 1). Here, we exploit that the PSF shape depends on the relative position of the emitter to the NP, thereby encoding 3D information about the functionalization of the NP surface.

We anticipate that this tool will be instrumental for future characterization of plasmonic biosensors, NP near-fields [4], NP geometry [5] and surface functionalization [6].

- [1] Fu. ACS Nano (2017).
- [2] Lim. Nano Letters (2016).
- [3] Raab. Nature Communications (2017).
- [4] Wertz. ACS Photonics (2016).
- [5] Taylor. JPhysChem (2018).
- [6] Post. Nature Communications (2019).

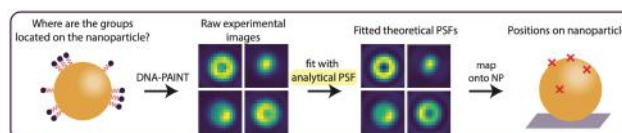


Figure 1. Single-molecule localization microscopy is used to study the surface functionalization of nanoparticles. By using our fully analytical PSF model to fit experimental data of DNA-PAINT on 100nm gold nanoparticles, the position of individual groups can be determined. Pixel size is 65 nm.

Single molecule localization on nanoparticles.png

Optical near-field characterization of plasmonic modes in a two-wire system

Tuesday, 25th October - 11:41: Advanced imaging - Oral

Mr. Marc Noordam¹, Prof. L. Kuipers¹

1. TU Delft

Propagating surface plasmon modes are promising for nanophotonic circuit applications due to their high spatial confinement at the visible and near-infrared frequencies. An interesting candidate for a surface plasmon based circuit is a two-wire transmission line (TWTL) consisting of two parallel nanowires. In this system the plasmonic modes of the single nanowires hybridize into a symmetric mode and an anti-symmetric mode, see fig. 1a for the simulated local electric fields. Since the plasmonic modes are confined to the interface between the metal and dielectric, their propagation behavior cannot be directly observed in the two-wire system using far-field microscopy. In this study we characterize the propagation behavior of the symmetric and anti-symmetric mode in a two-wire system using a near-field optical microscope.

Here, we use an amplitude, phase and polarization resolved near-field optical microscope to measure the local fields in the x and y polarization direction. Figure 1b shows a SEM image of the nanofabricated two-wire system and a sketch of the optical setup is displayed in fig. 1c. In fig. 2 the measured local near-field is plotted for the propagating symmetric (top) and anti-symmetric (bottom) mode for the x (left) and y (right) polarization. From fig. 2 it can be observed that the measured field symmetries and intensity patterns of the symmetric and anti-symmetric modes correlate well with the simulated mode patterns from fig. 1a for both polarizations.

Next to the observation of the field symmetry of the plasmonic mode we also measure the (anti-)symmetric mode behavior in two-wire system circuit elements such as an antenna (see fig. 3) and a filter system (see fig. 4). For the antenna element we observe the excitation of a superposition of the anti-symmetric and symmetric mode depending on the polarization angle of the incoming beam and we observe constructive and deconstructive interference in the individual wires. For the filter system we observe selective filtering of either the symmetric or the anti-symmetric mode depending on if the filter element is located at the outside or in the middle of the two-wire system.

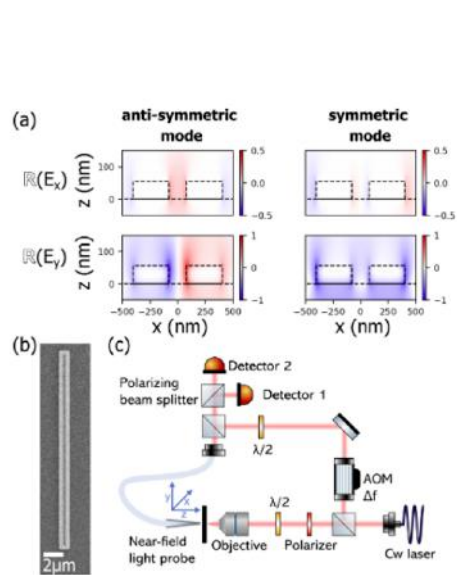


Figure 1.png

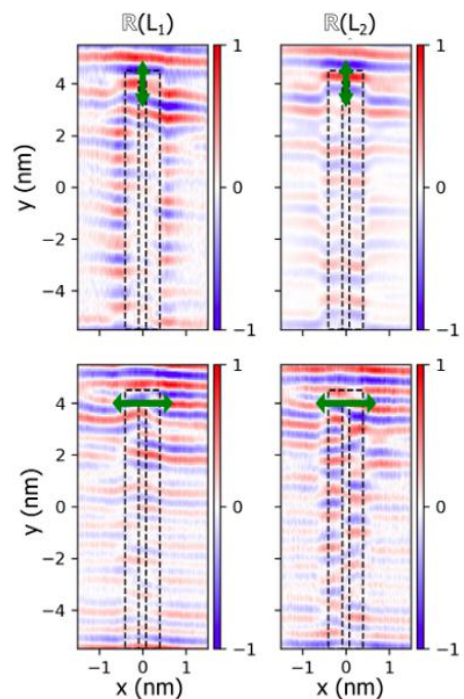


Figure 2.png

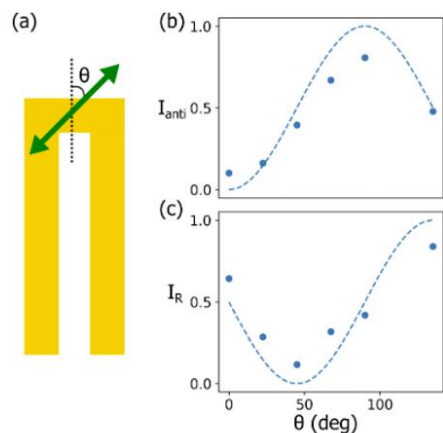


Figure 3.png

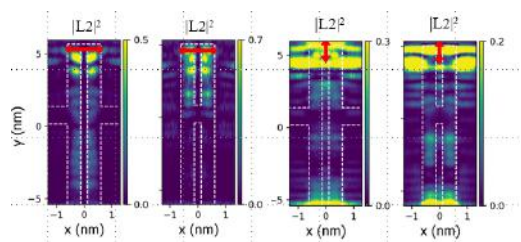


Figure 4.png

Strain-modulation of the Photoluminescence of 2D Hybrid Metal-Halide Perovskite Flakes

Tuesday, 25th October - 13:45: Poster Session - Poster

Ms. María Barra-Burillo¹, Dr. Davide Spirito², Dr. Francesco Calavalle¹, Dr. Costanza L. Manganelli², Dr. Marco Gobbi³, Prof. Rainer Hillenbrand⁴, Prof. Fèlix Casanova⁵, Prof. Luis E. Hueso⁵, Dr. Beatriz Martín-García¹

1. CIC nanoGUNE BRTA, **2.** IHP–Leibniz-Institut für innovative Mikroelektronik, **3.** CIC nanoGUNE BRTA / IKERBASQUE / Materials Physics Center, **4.** CIC nanoGUNE BRTA / IKERBASQUE / UPV-EHU, **5.** CIC nanoGUNE BRTA / IKERBASQUE

In the last few years, layered hybrid organic-inorganic metal halide perovskites (HOIPs) have emerged as promising materials in the development of optoelectronic devices, namely due to their tunable bandgap and high carrier mobility. Different techniques to engineer and tune their optical properties, and in particular their photoluminescence (PL), have been proposed, for instance, the variation of their organic-inorganic composition [1], or the application of mechanical strain [2]. Indeed, strain engineering has demonstrated to be an effective strategy to modulate the optoelectronic properties of 2D materials [3], but it has been barely explored on hybrid metal-halide perovskites. Here, we investigate the tuning of micro-photoluminescence of 2D lead-bromide HOIP flakes subject to biaxial strain [4]. For this purpose, we fabricate a rigid platform with SiO₂ microrings on which flakes are placed by viscoelastic stamping, leading to the formation of domes. At low temperatures, we find that a strain < 1% can change the PL emission from a single peak (unstrained) to three well-resolved peaks. Combining temperature-dependent micro-PL and Raman mapping and reverse mechanical engineering strain modeling, we confirm that the emergence of the two new PL peaks is related to tensile and compressive thermomechanically generated strain coexisting along the flake. Our findings provide new insight into the relevance of the material selection and the strain-engineering approach towards the design of strain-based optoelectronic and sensing devices using 2D HOIPs.

References

- Smith, M. D., Connor, B. A. & Karunadasa, H. I. Tuning the Luminescence of Layered Halide Perovskites. *Chem. Rev.* **119**, 3104–3139 (2019).
- Tu, Q. *et al.* Probing Strain-Induced Band Gap Modulation in 2D Hybrid Organic–Inorganic Perovskites. *ACS Energy Lett.* **4**, 796–802 (2019).
- Roldán, R., Castellanos-Gomez, A., Cappelluti, E. & Guinea, F. Strain engineering in semiconducting two-dimensional crystals. *J. Phys. Condens. Matter* **27**, 313201 (2015).
- Spirito, D., Barra-Burillo, M., *et al.* Tailoring Photoluminescence by Strain-Engineering in Layered Perovskite Flakes. *Nano Lett.* **22**, 4153–4160 (2022).

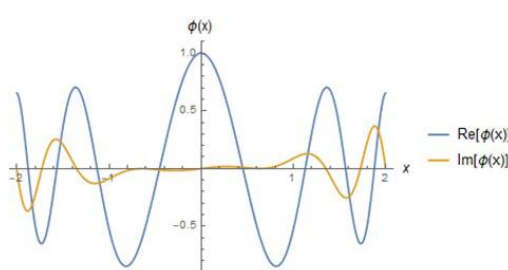
Quantum Optical Scattering applied to Integrated Photonics

Tuesday, 25th October - 13:45: Poster Session - Poster

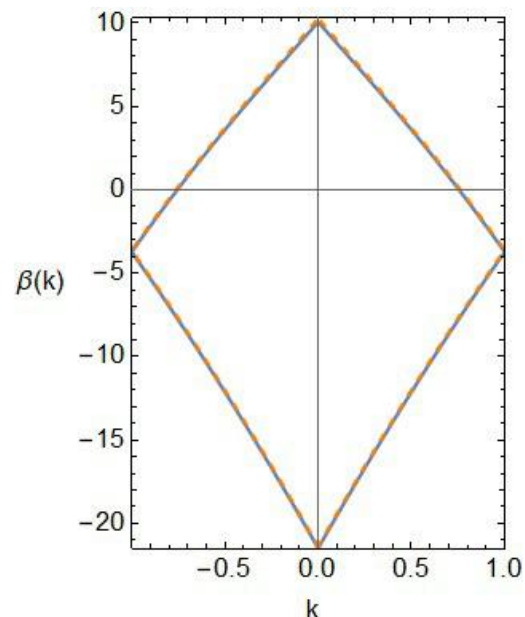
Dr. A. C. Amaro de Faria Jr¹

1. Federal Technological University of Paraná - UTFPR-P / Advanced Studies Institute - IEAv

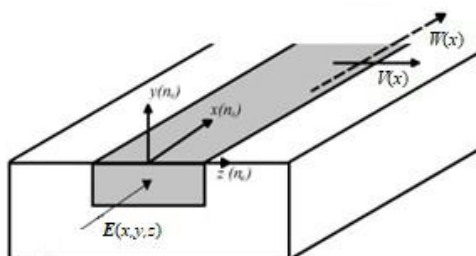
In this work we investigate the modeling of optical structures, such as optical fibers and crystalline lattices, whose optical potential exhibit a certain type of symmetry known as parity-time (PT) symmetry. These optical potentials describe the scattering of light in the structure by modulating the refractive index of the system and thus generating a nonlinear optical beam that propagates along the waveguide. These optical beams have low dispersion and low energy loss, and maintain their shape during propagation. Due to such properties these nonlinear optical pulses can be applied in the development of optical filters, as well as in the transmission and processing of nonlinear optical signals, because they have a well-defined band structure, depending on the degree of discrimination that is desired. These systems, which exhibit well-defined band structure, can be employed in integrated optics, incorporating the possibilities generated from quantum and nonlinear optics. Such applications can also innovate the perspectives and demands of quantum computing. We analyze some of these original nonlinear optical systems that exhibit PT symmetry, whose solution spectra are stable and exhibit a well-defined characteristic band structure that can be employed in the development of optical sensors and filters based on the discrimination range of their wavelengths which can be properly, regulated controlled and defined. The figures show the profile of the optical potentials, the solution spectrum, and the band structure of the corresponding systems. These nonlinear and quantum optical effects occurs due to the refractive index modulation of the lattice responsible for the optical scattering and the emergence of the effect. The result is a nonlinear optical spectrum with a characteristic band structure that can be adequately discriminated. The method can be applied to the design of optical structures from the nonlinear optical scattering potentials presenting a stable solution spectrum and a defined band structure. The stability of the solution spectrum, enables its application in emerging demands of quantum computing due to the semi-classical character of the nonlinear Schrödinger equation as well as opens new perspectives for the application of quantum optics in optical sensors and integrated optics.



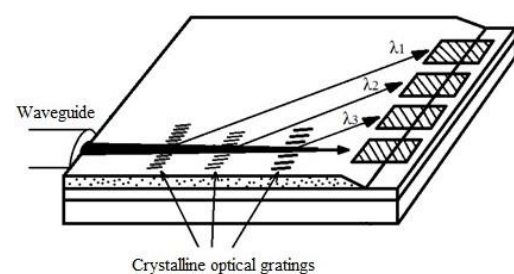
Spectrum solution.jpg



Structure band.jpg



Waveguide.jpg



Sensor.jpg

Origin of thermal and cold modification induced by femtosecond laser ablation in diamond

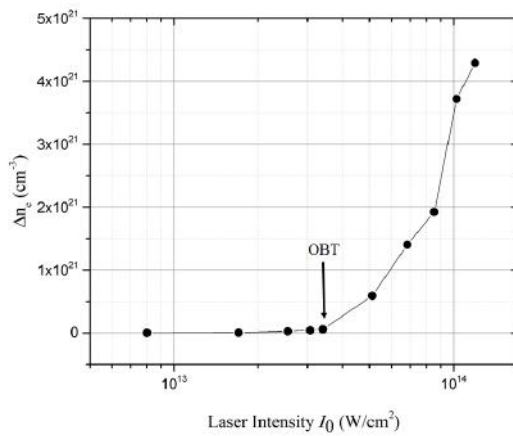
Tuesday, 25th October - 13:45: Poster Session - Poster

Dr. Ahmed Abdelmalek¹, Prof. Bedrane Zeyneb¹, Dr. Lebogang Kotsedi², Dr. El-Hachemi Amara³, Prof. Malik Maaza⁴

1. Theoretical Physics Laboratory, Physics Dpt., Sciences Faculty, Tlemcen University, Algeria, **2.** NANOAFNET, iThemba LABS-National Research Foundation, Old Faure Road, 7129, Somerset West, **3.** Centre de Développement des Technologies Avancées, CDTA, PO. Box 17 Baba-Hassen, Algiers 16303, Algeria, **4.** NANOAFNET, Ithemba iThemba LABS-National Research Foundation, Old Faure Road, 7129, Somerset West

The fundamental processes induced by direct femtosecond laser excitation on diamond surface has been investigated using the electron density rate equation. The calculation showed that there are two ablation regimes induced by the femtosecond laser pulse in transparent materials when the laser fluence increases. we suggest that at high fluence, the avalanche process is the main responsible for the thermal effect while at low fluence, the laser-surface interaction can be considered as cold leading to high precision manufacturing. This study provides a better understanding and control of laser-induced nano-micromachining.

The results obtained are shown in Figure 1. The curve clearly shows that there are two different excitation regimes when the laser intensity increases, i.e. when the laser energy increases.



Obt2.png

Effects of Crystalline Structure on Second-Harmonic Generation in Thin GaAs Nanowires

Tuesday, 25th October - 13:45: Poster Session - Poster

Dr. Bin Zhang¹, Dr. Jan Stehr¹, Dr. Ping-Ping Chen², Dr. Xingjun Wang², Dr. Fumitaro Ishikawa³, Prof. Weimin Chen¹, Prof. Irina Buyanova¹

1. Linköping University, **2.** Shanghai Institute of Technical Physics, **3.** Ehime University

Nonlinear optical processes, including second harmonic generation (SHG), can be utilized in a wide range of classical and quantum applications. Using nanowires (NWs) for such applications is advantageous for efficient miniaturization. Moreover, the ability to grow NWs with different lattice structures allows one to explore non-linearity of crystallographic polytypes that cannot be fabricated in bulk under conventional growth conditions. The (Al)GaAs material system is especially appealing as non-linear media, as GaAs exhibits large bulk second-order nonlinear optical susceptibility. Though essential for optimization, ascertaining the origin of SHG in thin NWs, including GaAs-based NWs, is not trivial due to sensitivity of non-linear properties to surfaces, interfaces, defects, etc. Until now, however, impacts of these effects on non-linear properties of GaAs NWs are still largely unexplored and are investigated in this work.

The investigated GaAs NWs were grown by molecular beam epitaxy (MBE). Both zinc blende (ZB) and wurtzite (WZ) NWs with diameters of around 80 - 100 nm were studied. Their crystallographic structure was characterised by using transmission electron microscopy (TEM). It is found [1] that the SHG intensity is significantly stronger in WZ NWs as compared with ZB NWs (by about 7 times), reaching the value of $2.5 \times 10^{-5} \text{ W}^{-1}$. This value is among the highest reported in the literature, including complex waveguide and nanoresonator structures, as well as hybrid plasmonic structures. Such enhancement was directly verified by correlative SHG intensity mapping and TEM characterization performed on the same polymorphic NWs. The dominant parallel SHG is proven to be enhanced in WZ via electric-field induced SHG, which is activated by the axial built-in electric field related to spontaneous polarization in WZ NWs and can be controlled optically and potentially electrically. This SHG enhancement is found to be robust and does not require high structural quality of the NWs, as the presence of structural defects in fact facilitates SHG by enhancing the internal electric field. Our results, therefore, demonstrate great potential of thin GaAs NWs for nonlinear nanophotonics and show that their non-linear properties can be manipulated via lattice engineering.

[1] B. Zhang et al., Adv. Funct. Mater. 31, 2104671 (2021).

Light extraction and injection enhancement using metallic nanocubes

Tuesday, 25th October - 13:45: Poster Session - Poster

Dr. François Réveret¹, Dr. Mohammad Khaywah¹, Dr. Audrey Potdevin¹, Dr. Rachid Mahiou¹, Prof. Youcef Ouerdane², Dr. Anthony Désert³, Prof. Stephane Parola³, Prof. Geneviève Chadeyron¹, Prof. Emmanuel Centeno⁴, Dr. Rafik Smaali⁴, Dr. Antoine Moreau⁴

1. ICCF - CNRS, INP, Université Clermont Auvergne, **2.** Laboratoire Hubert Curien - CNRS, Université Jean Monnet, **3.** Laboratoire de Chimie - ENS, CNRS, Université Lyon 1, **4.** IP - CNRS, INP, Université Clermont Auvergne

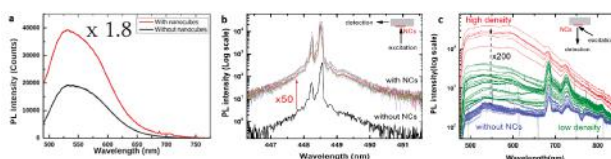
Phosphor materials are widely used as luminescent coating (LC) in lighting, display, illumination, marking or Li-Fi [1]. Due to the refractive index mismatch between LC and the air, a strong amount of light is trapped in the structure. Large part of photons is guided in both LC and substrate and escape mostly from the edge. This leak could represent up to 80% of the emitted photons [2]. After a brief review of the existing solutions in the literature to extract guided photons, the interest of using metallic nanoparticles (MNPs) will be presented. Most of published works report the improvement of light extraction by using plasmonic resonance of MNPs. In this study, we show that MNPs could be used efficiently as optical scatterers [3]. A light extraction enhancement by a factor of 1.8 has been evidenced (figure 1a) when silver nanocubes (NCs) are simply deposited on the LC surface. The role of the NCs density will be highlighted and compared with simulations. As shown in figure 1b, we can quantify a large light injection improvement when Ag NCs are dispersed on a transparent material (quartz substrate), a factor 50 is found. Moreover, we observe a strong light extraction enhancement of a feebly luminescent quartz material by a factor up to 200 depending on the Ag NCs density (figure 1c).

Figure 1: (a) Emission spectra of YAG:Ce LC with and without nanocubes. (b) Light injection improvement on a quartz substrate decorated with Ag nanocubes. (c) Enhancement of light extraction of a quartz substrate depending on the Ag nanocubes density.

[1] Ma, L.; Yu, P.; Wang, W.; et al. *Laser & Photonics Reviews* **2021**, *15* (5), 2000367

[2] Dantelle, G.; Fleury, B.; Boilot, J.-P.; et al. *ACS Applied Materials & Interfaces* **2013**, *5* (21), 11315.

[3] Khaywah, M.; Potdevin, A.; Réveret, F.; et al. *The Journal of Physical Chemistry C* **2021**, *125* (14), 7780.



Light injection and extraction enhancement.png

Nanoplasmonics for efficient gas sensing and detection.

Tuesday, 25th October - 13:45: Poster Session - Poster

Dr. Benjamin Demirdjian¹, Dr. Igor Ozerov¹, Mr. Frédéric Bedu¹, Mr. Alain Ranguis¹, Dr. Claude R. Henry¹

1. CINaM

Understanding how gas molecules such as water, oxygen, or carbon monoxide interact with nanoparticles (NPs) remains an important challenge in the studies of atmospheric chemistry and catalysis reactions.

When gas molecules are directly adsorbed onto Au nanodisks (direct nanoplasmonic sensing DNPS) or when they interact with NPs supported on Au nanodisks (indirect nanoplasmonic sensing INPS, figure 1), they modify the local dielectric properties of the surrounding media. Such a modification induces a wavelength shift of the localized surface plasmon resonance (LSPR) of Au nanodisks which can be easily detected by UV-Vis spectroscopy.

We measured water adsorption isotherms by DNPS following the Au LSPR shift when water molecules adsorb/desorb on Au nanodisks [1]. With high sensitivity, we used INPS to follow also the interaction of water molecules on soot NPs that are a significant contributor to global warming in the atmosphere.

Then, CO and oxygen adsorption as well as CO oxidation, on Pt NPs, have also been followed by INPS coupled with mass spectrometry [2]. We obtained a quantitative and very sensitive probe even for a very low Pt NPs density.

For both DNPS and INPS, we could detect small molecule quantities such as a few hundredths of an adsorbed monolayer. Moreover, we can use nanoplasmonic sensing in a large range of pressure and temperature.

FDTD calculations are performed to interpret LSPR spectra and to optimize the physical parameters of our plasmonic nanosensors.

References

- [1] B. Demirdjian, F. Bedu, A. Ranguis, I. Ozerov, C. R. Henry, *Langmuir* 34, 5381-5385 (2018)
- [2] B. Demirdjian, I. Ozerov, F. Bedu, A. Ranguis and C. R. Henry, *ACS Omega* 6, 13398-13405 (2021)

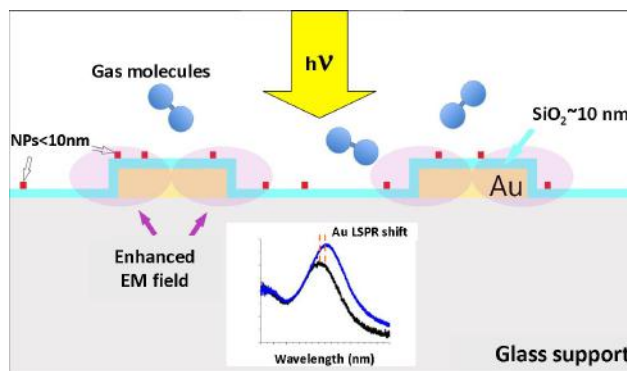


Figure1 inps indirectnanoplasmonicsensing.jpg

Angular dependence of localized surface plasmon resonance extinction in anisotropic silver nanoplates

Tuesday, 25th October - 13:45: Poster Session - Poster

Mr. luca salemi¹, Mr. Orazio Samperi¹, Dr. Marcello Condorelli¹, Mr. Mario Pulvirenti¹, Prof. Luisa D'Urso¹, Prof. Giuseppe Compagnini¹

1. Department of Chemical Science, University of Catania

Introduction

Noble metal nanoparticles exhibit localized surface plasmon resonances in the visible and near infrared spectrum at wavelengths depending on the metal's optical properties, the surrounding medium's refractive index, the shape and size of the nanoparticle itself. The plasmon resonances of anisotropic nanoparticles are generally associated to the orientation and polarization of the beam and to the symmetries of the nanoparticle, which govern the coupling with the external electromagnetic field.

In this work we present the angle dependence of the dipolar and quadrupolar plasmon extinction in some chemically prepared silver nanoplates, uniformly deposited on a substrate.

Methods

We have synthesized some colloidal silver nanoplates via a chemical nucleation and growth process in the presence of a capping agent. The particles have been deposited on a chemically functionalized glass substrate. Angular dependent extinction measurements have been performed to characterize the plasmonic behaviour through a home made apparatus. The experimental results have been compared with numerical simulations (Comsol).

AFM micrographs are presented to evaluate the geometrical disposition of the nanoparticles on the substrate.

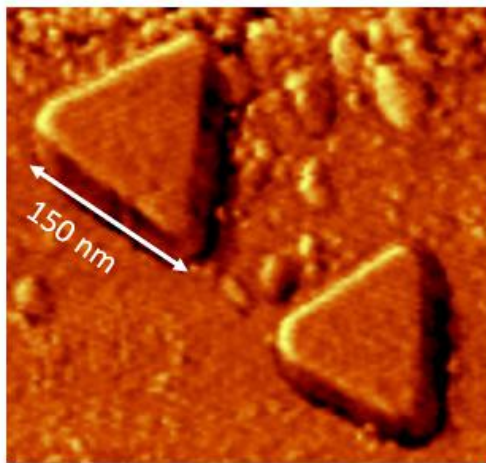
Results and discussion

AFM micrographs show that the particles are adsorbed preferentially with their flatness parallel to the surface of the substrate, even though with a random distribution of in-plane orientation. The corresponding extinction spectrum performed at normal incidence only shows plasmonic peaks associated with in-plane oscillation of the field.

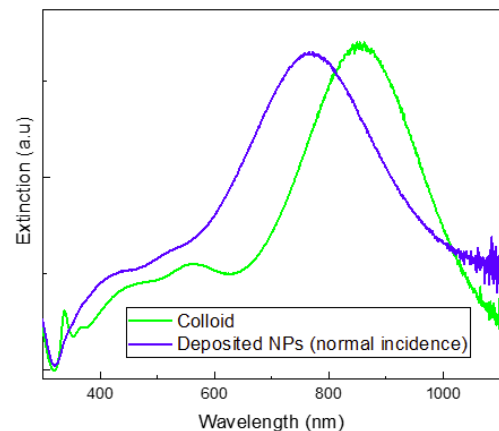
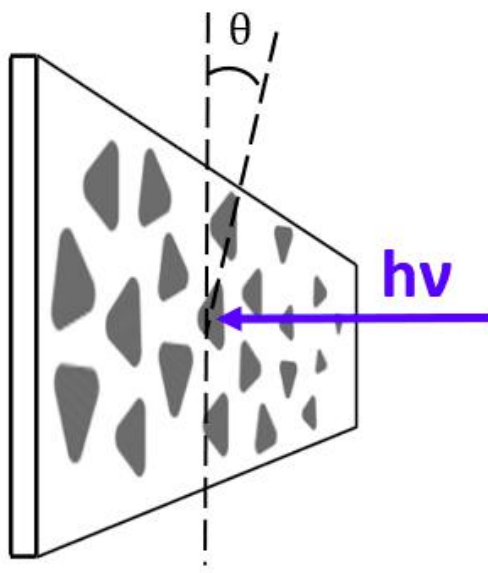
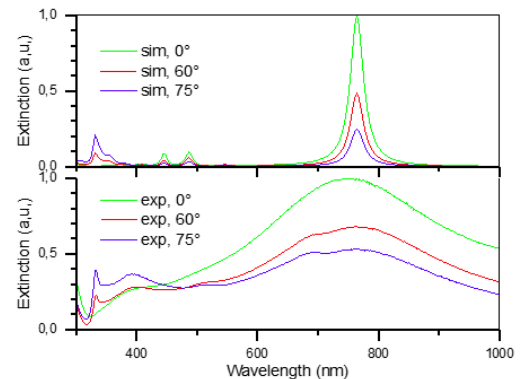
Extinction spectra performed as a function of the incidence angle demonstrate a strong dependence of the relative dipole to quadrupole intensity, and the appearance of minor plasmonic features.

The results have been compared with the typical extinction spectra of the same plates in the colloidal form and finite elements method simulations have been performed to correlate all the experimental results.

The observation open a possible discussion on the use of ordered plasmonic monolayer in the field of chemical and biological sensing such as refractive index sensing and surface-enhanced Raman scattering approaches.



Afm.png



Ultra-fast photochemistry in the strong light-matter coupling regime

Tuesday, 25th October - 13:45: Poster Session - Poster

Mr. Arpan Dutta¹, Mr. Ville Tiainen¹, Dr. Luis Duarte², Dr. Nemanja Markesovic¹, Dr. Ruth Tichauer¹, Mr. Hassan Qureshi³, Dr. Gerrit Groenhof¹, Dr. Jussi Toppari¹

1. University of Jyväskylä, 2. University of Helsinki, 3. University of Turku

Strong light-matter coupling between photoactive molecules and cavity modes results in the formation of hybrid light-matter states ‘polaritons’ with energies above and below the original state [1]. Such modification of the excited state can alter the chemical behavior of the molecule. In this work, we investigate the influence of strong light-matter coupling on an ultrafast photochemical reaction, i.e., the excited-state intramolecular proton transfer (ESIPT), of 10-hydroxybenzo[h]quinoline (HBQ), which happens when HBQ is excited by ultraviolet light around 375 nm. After the process the molecule radiatively decays back to the ground state by emitting around 620 nm, which is used as a measure of the reaction efficiency. To obtain the strong light-matter coupling with varying coupling strengths, we embedded different concentrations of HBQ within metallic Fabry-Pérot microcavities tuned to have the first order cavity mode in resonance with the HBQ excited state. The change in the potential energy surface due to polariton formation would suggest increase of the reaction barrier with increased coupling and thus hindering of the ESIPT. However, our experiments show enhancement of the emission yield [2] with increased coupling. More detailed excitation spectroscopy reveals that upon excitation of a polariton state, the excitation localizes onto a HBQ molecule which undergoes ESIPT. Furthermore, this process seems to be fully independent of the type and nature of the excited polariton state and only depends on the spectral overlap between the polariton and the molecular dark states [3]. Since this overlap is increasing with increased HBQ concentration, we see enhancement of ESIPT as a function of the coupling strength. Our findings are important in the context of polaritonic chemistry, where influencing photochemical reactions via strong light-matter coupling is crucial.

References

- [1] R. F. Ribeiro, et al., Chem. Sci., 9, 6325-6339 (2018)
- [2] S. Wang, et al., J. Phys. Chem. Lett., 5, 1433-1439 (2014)
- [3] G. Groenhof, et al., J. Phys. Chem. Lett., 10, 5476-5483 (2019)

Finite difference time domain simulations of GaAs-based ridge waveguide with Bragg gratings

Tuesday, 25th October - 13:45: Poster Session - Poster

Ms. Yasmin Rahimof¹, Mr. Sten Wenzel¹, Dr. Igor Nechepurenko¹, Dr. Bassem Arar¹, Dr. Andreas Wicht¹

1. Ferdinand-Braun-Institute (FBH)

Ultra-narrow linewidth lasers are main components for optical atomic clocks and atom interferometry-based quantum sensors. Owing to their high energy efficiency and small form factor, diode lasers are one of the most promising integral technologies to be used in space applications. Taking a step forward in the field of diode lasers, extended cavity diode lasers (ECDL) have recently been implemented on a single GaAs chip to realize a monolithic ECDL (mECDL). The mECDL was fabricated with two-step epitaxy technology which has a narrow 3dB linewidth of 25 kHz @ 1 ms at 1064 nm wavelength [1].

The chip facet located next to the active section serves as the front mirror while the Bragg-grating within the passive section composes the back mirror of the resonator. As a result of using the 2 mm long surface Bragg grating section, the longitudinal single mode operation is achieved. Apodisation of the grating coupling coefficient and chirp of the Bragg period can further improve the gratings reflectivity spectrum [2]. In order to simulate this structure, coupled mode theory, the transfer matrix method and the eigenmode expansion method can be implemented [3-5]. All methods are based on approximations and have limited precision. To develop a precise model, finite difference time domain (FDTD) [6] method can be used for 3D simulations.

In this study, to avail a better control on the reflection spectrum, periodic and aperiodic surface Bragg gratings in ridge waveguides were considered. It was shown that the ripples amplitude decreased when apodisation were applied. The reflectivity spectra of the Bragg gratings were investigated by 2D and 3D FDTD modeling methods. The Bragg grating with different orders were optimized and their spectra were compared.

References:

- [1] Wenzel, S., et al. CLEO (2021): ATh4G-3.
- [2] Miyazu, J., et al. IEICE Transactions on Electronics 88.7 (2005): 1521-1522.
- [3] Kogelnik, H., et al. Journal of Applied Physics 43.5 (1972): 2327-2335.
- [4] Yamada, M., et al. Applied Optics 26.16 (1987): 3474-3478.
- [5] Wenzel, H., et al. IEEE Journal of Quantum Electronics 42.1 (2005): 64-70.
- [6] Gnan, M., et al. Optical and Quantum Electronics 38.1 (2006): 133-148.

Designing an opto-spintronic semiconductor nanostructure with nearly 100% electron and photon spin polarization at room temperature

Tuesday, 25th October - 13:45: Poster Session - Poster

Dr. Y Huang¹, Dr. V Polojärvi², Dr. S Hiura³, Mr. P Höjer¹, Dr. A Aho², Dr. R Isoaho², Dr. T Hakkarainen², Prof. M Guina², Dr. S Sato³, Dr. J Takayama³, Prof. A Murayama³, Prof. Irina Buyanova¹, Prof. Weimin Chen¹

1. Linköping University, **2.** Tampere University, **3.** Hokkaido University

An exclusive advantage of semiconductor spintronics is its potential for opto-spintronics that will allow integration of spin-based information processing and storage with photon-based information transfer and communications. Unfortunately, progresses of semiconductor spintronics have so far been severely hampered by the failure to generate nearly fully spin-polarized charge carriers in semiconductors at and above room temperature (RT) at which today's devices operate. In this work, we succeed to achieve conduction electron spin polarization exceeding 90% at RT in a semiconductor nanostructure, which remains steadily high even up to 110°C [1]. This represents the highest RT electron spin polarization ever reported in any semiconductor by any approach! This breakthrough is accomplished by a conceptually new approach of defect-engineered remote spin filtering and amplification of InAs quantum-dot (QD) electrons via an adjacent tunneling-coupled GaNAs quantum well acting as a spin filter. The extraordinary spin filtering effect in GaNAs is enabled by spin-dependent recombination via spin-polarized defects, i.e. grown-in Ga self-interstitials, which selectively deplete conduction electrons with an opposite spin orientation to that of the defect electron. In sharp contrast to the general trend of deteriorating spin polarization with increasing temperature seen in all other approaches of spin generation, our approach is gifted with an opposite temperature dependence up to RT thanks to a thermally accelerated remote spin-filtering effect as a result of thermally activated recombination via the defects. We further show that the QD electron spin can be remotely manipulated by spin control in the adjacent spin filter, paving the way for remote spin encoding and writing of quantum memory as well as for remote spin control of spin-photon interfaces. The fact that the demonstrated spin functionality is implemented in a commonly used semiconductor optoelectronic nanostructure system (i.e. InAs/GaAs QDs) based on the mature GaAs technology can greatly facilitate the integration of spin functionalities with the existing electronic and photonic devices.

[1] Y. Huang, V. Polojärvi, S. Hiura, P. Höjer, A. Aho, R. Isoaho, T. Hakkarainen, M. Guina, S. Sato, J. Takayama, A. Murayama, I.A. Buyanova and W.M. Chen, *Nature Photonics* 15, 475 (2021).

Van der Waals materials for applications in nanophotonics

Tuesday, 25th October - 14:45: Photonic & plasmonic nanomaterials - Oral

Dr. Panaiot Zotev¹, Dr. Yue Wang², Mr. Toby Severs Millard¹, Dr. Daniel Andres-Penares³, Dr. Luca Sortino⁴, Dr. Nic Mullin¹, Mr. Donato Conteduca², Dr. Mauro Brotons-Gisbert³, Mr. Sam Randerson¹, Mr. Mostafa Shagar¹, Prof. Jamie Hobbs¹, Prof. Brian Gerardot³, Prof. Thomas Krauss², Prof. Alexander Tartakovskii¹

1. The University of Sheffield, **2.** University of York, **3.** Heriot-Watt University, **4.** Ludwig-Maximilians-Universität

Nanophotonic structures enable a range of applications including optical waveguiding, Purcell enhancement of emission and low-threshold lasing. Many research fields and technologies have benefited from nano-scale resonators and waveguides fabricated from noble metals [1] or dielectrics such as silicon [2] and III-V materials [3]. While these offer a large range of opportunities for both research and technology, van der Waals materials may expand the possibilities of nanophotonics in the visible and near-infrared due to high refractive indices ($n>4$) [4], a large range of transparency windows, and numerous advantages due to their weak van der Waals attractive forces.

In order to inspire and facilitate fabrication of nanophotonic structures from layered materials, we extract the dielectric constants of a diverse set including transition metal dichalcogenides (TMDs), III-VI semiconductors, and magnetic van der Waals crystals. Employing established techniques, we fabricate nanoresonators with a range of geometries (see Fig. 1(a)) from bulk as well as twisted stacks of these materials and observe Mie resonances as well as strong coupling between the excitonic features of TMDs and anapole modes with Rabi splittings up to 140 meV, shown in Fig. 1(b),(c). After the transfer of a monolayer of WSe₂ onto WS₂ nanoantennas, we observe room temperature Purcell enhancement of emission (see Fig. 1(d)) [5] as well as low temperature formation of single photon emitters (see Fig. 1(e)) with enhanced quantum efficiencies within a system fabricated entirely of layered materials. Due to the weak van der Waals interactions of the nanoresonators and the substrate, we were able to employ an atomic force microscopy cantilever in the repositioning of double-pillar nanoantennas to achieve ultra-small gaps (~ 10 nm, left inset of Fig. 1(f)) [5]. This post-fabrication technique enables applications such as stable, low-power optical trapping of quantum emitters with Purcell enhancement factors above 150 as shown by the simulations in Fig. 1(f).

[1] Luo, Y. et al. Nature Nanotechnology, 13(2018), 1137-1142.

[2] Li, Y. et al. Nature Nanotechnology, 12(2017), 987-992.

[3] Sortino, L. et al. Nature Communications, 12(2021), 6063.

[4] Verre, R. et al. Nature Nanotechnology, 14(2019), 679-683.

[5] Zotev, P. et al. ACS Nano, 16(2022), 6493-6505.

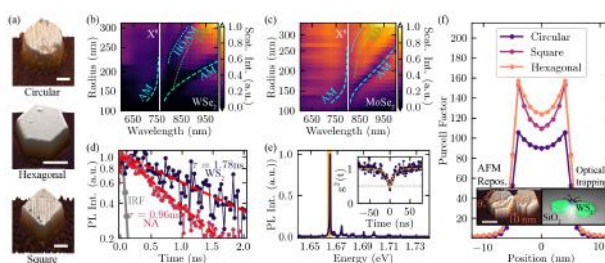


Fig.jpg

Nanoimaging of vibrational strong coupling between propagating phonon polaritons and organic molecules

Tuesday, 25th October - 15:02: Photonic & plasmonic nanomaterials - Oral

Mr. Andrei Bylinkin¹, Dr. Martin Schnell², Dr. Marta Autore², Dr. Francesco Calavalle², Dr. Peining Li², Dr. Javier Taboada-Gutiérrez³, Dr. Song Liu⁴, Prof. James H. Edgar⁴, Prof. Fèlix Casanova⁵, Prof. Luis E. Hueso⁵, Dr. Pablo Alonso González³, Dr. Alexey Y. Nikitin⁶, Prof. Rainer Hillenbrand⁷

1. CIC nanoGUNE BRTA, 20018 Donostia - San Sebastian, Spain, **2.** CIC nanoGUNE BRTA, **3.** Departamento de Física, Universidad de Oviedo, **4.** Tim Taylor Department of Chemical Engineering, Kansas State University Manhattan, **5.** CIC nanoGUNE BRTA / IKERBASQUE, **6.** Donostia International Physics Center (DIPC) / IKERBASQUE, **7.** CIC nanoGUNE BRTA / IKERBASQUE / UPV-EHU

Enhanced light-matter interaction in polar crystals attracts considerable attention since the latter support phonon polaritons (PhPs) - hybrid electromagnetic modes involving atomic vibrations. PhPs in the thin slab of van de Waals materials (vdW) demonstrate a long lifetime and ultra-high field confinement [1] which can lead to intriguing vibrational strong coupling (VSC) phenomena and potential sensing applications. Recently VSC between h-BN nano-resonators and molecular vibration has been demonstrated. However, the basic interaction between molecular vibrations and propagating PhPs in unstructured slabs of the vdW materials has not yet been studied. In this work, we use nanoimaging techniques to study the interaction between ultra-confined propagating PhPs and molecular vibrations in sub-100 nm thick organic layers. Specifically, we performed near-field polariton interferometry of PhPs in a thin continuous h-BN layer interacting with 4,4'-Bis(N-carbazolyl)-1,1'-biphenyl (CPB) molecules. In contrast to the typical far-field spectroscopy experiments, we monitor in the real space the effect of molecular absorption on PPs. Our results show that VSC leads to the formation of a hybrid mode with a pronounced anti-crossing region in its dispersion, in which propagation with negative group velocity is found. Moreover, the numerical study predicts that PhPs in few-layer h-BN films may reach strong coupling even in the case of atomically thin molecular layers, thus underlining the potential of PPs to become a platform for ultra-sensitive on-chip spectroscopy devices.

Our work shows the fundamental study of the strong-coupling between molecular vibration and propagating PhPs and demonstrates the feasibility of exploiting ultra-confined polaritons for mid-infrared waveguide sensing of molecular vibrations and strong-coupling experiments.

Full control of the electric and magnetic light-matter interactions through a plasmonic mirror on a near-field tip

Tuesday, 25th October - 15:19: Photonic & plasmonic nanomaterials - Oral

Mr. Benoît Reynier¹, Mr. Eric Charron¹, Mr. Obren Markovic¹, Mr. Xingyu Yang¹, Dr. Bruno Gallas¹, Dr. Sébastien Bidault², Dr. Mathieu Mivelle¹

1. Institut des NanoSciences de Paris, 2. Institut Langevin, ESPCI Paris, CNRS

Light-matter interactions are often considered to be mediated by the optical electric field, and electric dipole (ED) transitions only, discarding half of the energy stored in the optical magnetic field. Although interactions between light and magnetic dipole (MD) transitions are very weak, they can be studied in a certain class of materials, such as metal ions. For instance, Eu³⁺ lanthanide ions are known to sustain ED and MD excitation as well as ED and MD emission transitions. For instance, it was demonstrated that MD emission could be manipulated by tuning the local magnetic quantum environment surrounding the MDs by means of dielectric or plasmonic nano-structures [1,2]. Along the same line, it is possible to manipulate the excitation of the ED and MD by controlling the electric and magnetic fields distribution of the excitation light [3].

Here, by manipulating the spatial distributions of the electric & magnetic optical fields and their local density of states, we report the selective excitation and emission control of ED and MD transitions. This is achieved by generating a standing wave whose electric and magnetic nodes and anti-nodes do not overlap spatially.

For this purpose, using a scanning near-field optical microscope (SNOM), a plasmonic nanostructure at the end of an optical fiber tip acting as a mirror is placed on top of a Eu³⁺ doped Y₂O₃ nanoparticle (Figure 1). The 3D scanning properties of the SNOM allow to couple, in space, the electric and magnetic nodes and anti-nodes of the standing wave to the electric or magnetic transitions of the Eu³⁺ ions. By collecting luminescence, we imaged, for the first time, both electric and magnetic nodes and anti-nodes of a standing wave (Figure 2) with their associated local density of states. We have, therefore, a system granting us complete control of the electromagnetic and quantum interactions between the two components of light and matter. Also, we show an increase in collected luminescence by magnetic excitation with respect to a far-field excitation. Finally, we demonstrated that we can also control the luminescence emission by manipulating the magnetic and electric quantum environment solely through magnetic or electric excitation.

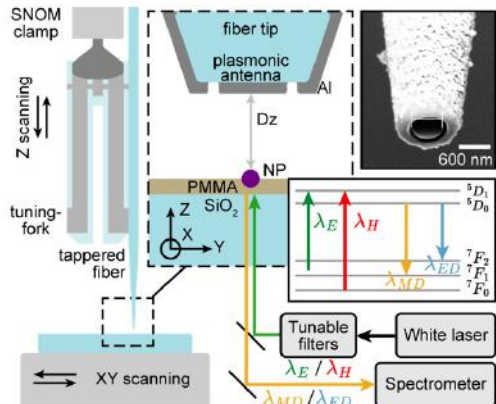


Figure 1: Schematic of the experimental set-up. A plasmonic-mirror antenna at the end of a fiber tip is approached in close proximity to a $\text{Y}_2\text{O}_3:\text{Eu}^{3+}$ doped nanoparticle using a SNOM, which allows us to position the antenna at the nanoscale with respect to the nanoparticle. Selective electric or magnetic excitation is controlled by tunable filters. The luminescence is collected and analyzed by a spectrometer for each antenna-particle position.

Fig1 - schematic of the set-up.png

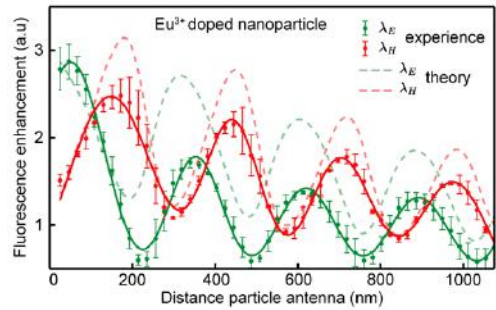


Figure 2: Luminescence enhancement of a nanoparticle excited at either λ_E or λ_H , in function of the particle-antenna distance. The electric and magnetic nodes and anti-nodes of the standing wave are imaged.

Fig2 - standing wave imaging.png

Anapole states in gap-surface plasmon resonators

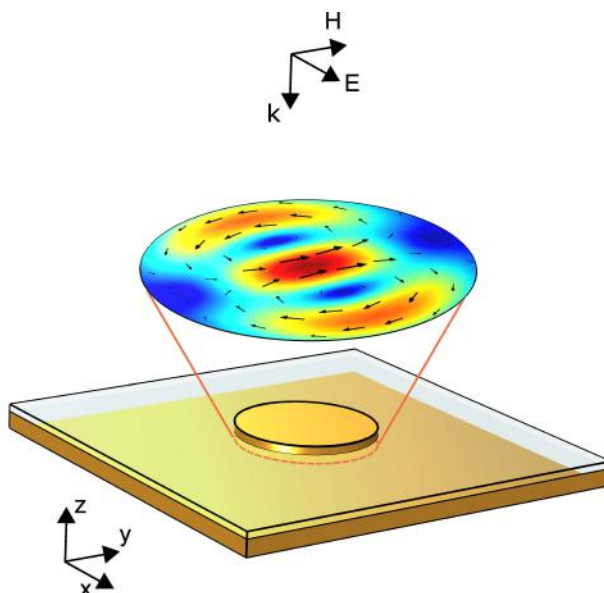
Tuesday, 25th October - 15:36: Photonic & plasmonic nanomaterials - Oral

Dr. Torgom Yezekyan¹, Dr. Vladimir Zenin¹, Dr. Jonas Beermann¹, Prof. Sergey Bozhevolnyi¹

¹. University of Southern Denmark

Anapole states associated with the destructive interference between dipole and toroidal moments result in suppressed scattering accompanied with strongly enhanced near fields. Anapole states and their applications have been thoroughly and widely investigated for dielectric particles with high refractive indexes, but very few studies are dedicated to realization of anapole states with plasmonic structures. Here the challenge is that plasmonic modes are dominated by strong electric dipole contribution, which generally cannot be suppressed by toroidal moments. In this work we succeeded in finding a configuration for realization of plasmonic anapole. This was achieved by considering

gap surface-plasmon (GSP) resonators (these resonators are widely used in plasmonics, for example, in plasmonic metasurfaces), where electric dipole moment is suppressed by symmetry, while dominated magnetic dipole moment can be suppressed with induced out-of-phase magnetic toroidal dipole moment by varying the size of the structure. We show that, in contrast to the common case of dielectric particles with out-of-phase superposition of electric and toroidal dipoles, anapole states in GSP resonators are formed due to the compensation of magnetic dipole moments. We performed multipole decomposition of scattering for the GSP sandwich resonator to highlight the occurrence of the magnetic anapole states in this structure. Unlike anapole states in dielectric particles, magnetic anapole states in GSP resonator do not provide a pronounced suppression of scattering, but feature huge electric field enhancement, which we verify by numerical simulations and two-photon luminescence measurements. The GSP resonator configuration is simple and robust in realization and tunability, making its use for exploiting anapole states very promising in a wide range of applications, ranging from nonlinear harmonic generation to absorption enhancement and sensing.



Schematic illustration of the gsp resonator .jpg

Efficient distributed feedback lasers with parity-time symmetry breaking

Tuesday, 25th October - 15:53: Photonic & plasmonic nanomaterials - Oral

Mr. Yaoyao Liang¹, Dr. Quentin Gaimard¹, Dr. Jean-Rene Coudeville¹, Dr. Alexandre Garreau², Dr. Arnaud Wilk², Prof. Henri Benisty³, Prof. Abderrahim Ramdane¹, Prof. Anatole Lupu¹

1. Centre de Nanosciences et de Nanotechnologies, CNRS, Université Paris-Saclay, Palaiseau, 91120, France, **2.** III-V Lab, 1 avenue Augustin Fresnel, 91767 Palaiseau Cedex, France, **3.** Laboratoire Charles Fabry de l'Institut d'Optique LCFIO, Université Paris-Saclay, Palaiseau, 91120, France

The ability to effectively manipulate the cavity resonant modes is of fundamental significance in laser physics. Recent progress of parity-time symmetry provides an opportunity to achieve stable single-mode lasing by strategically structuring gain and loss in the laser cavity. Here we experimentally demonstrate that when the index and gain modulations of the complex structure operate at parity-time symmetry phase, high-output single-mode lasing with relatively low threshold current can be realized in first-order distributed feedback cavities.

Fig. 1(a) is the sketch of the proposed PT-symmetry DFB laser structure. It is a standard ridge waveguide composed of a dielectric grating with two metallic gratings on its lateral sides. The grating periods are both 240 nm with a f=0.5 duty-cycle suited to operate at 1550 nm. By bringing an additional shifted gain/loss modulation to a conventional refractive Bragg grating structure, the potential can be turned into a PT symmetric condition, notably for a phase shift of $\pi/2$ between the gain and refractive index modulations, when real and imaginary parts of the material index respectively obey even and odd profiles in a unit cell [inset in Fig. 1(a)]. Fig. 1(b) shows a zoom-in micrograph of white dash region in Fig. 1(a) of the fabricated first-order PT-symmetric DFB laser structure.

Fig.1. (a) Sketch of first-order PT-symmetry DFB laser, blue (dielectric) and yellow (metallic) gratings are shown; the inset depicts the condition for PT symmetric potential. (b) Zoom-in SEM image in white dashed region in (a).

A typical light-current characteristic of our first-order PT-symmetry DFB laser with the cavity length around 1.5 mm is presented in Fig. 2(a), the lasing threshold I_{th} is around 20 mA with an output power at $I=200$ mA of nearly 20 mW per (cleaved) facet. The measured typical emission spectra in Fig. 2(b) shows a neat single mode lasing with a Side Mode Suppression Ratio (SMSR) around 50 dB. Our achievement validates the PT-symmetry strategy for use in single-mode DFB lasers with expected characteristics such as feedback immunity of high interest notably in PICs.

Fig. 2 Typical (a) Light-current characteristic and (b) Emission spectrum measured by first-order PT-symmetry DFB lasers.

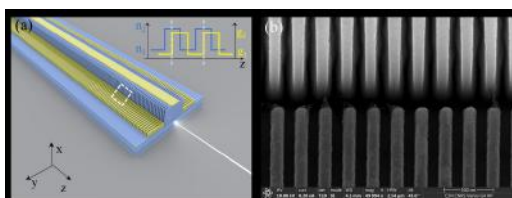


Fig1.jpg

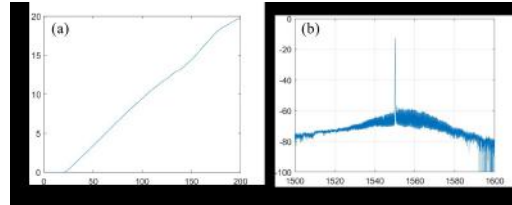


Fig2.jpg

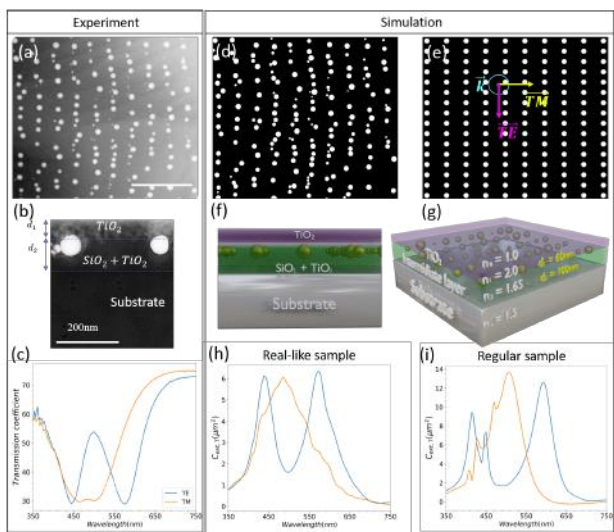
Laser-induced Self-organized Quasi-random Plasmonic Nanomaterials: Hybridization of Plasmonic and Photonic Modes

Tuesday, 25th October - 16:10: Photonic & plasmonic nanomaterials - Oral

Mr. Van Doan Le¹, Mr. Yaya Lefkir¹, Prof. Nathalie Destouches¹

1. Univ Lyon, UJM-Saint-Etienne, CNRS, Institut d'Optique Graduate School, Laboratoire Hubert Curien UMR 5516, F-42023 Saint-Etienne

Periodic plasmonic nanomaterials may support collective lattice resonances originating from the coupling between localized surface plasmon resonances of individual nanoparticles and delocalized photonic modes. The latter arise either from diffraction of the incident light by the periodic structure into waves propagating along the surface plane or excited guided modes when a waveguide layer is present. Recently, self-organized plasmonic metamaterials have been produced by laser. The latter controls the statistical properties of metallic nanoparticles present under the beam and leads to broad size distributions and spatial disorder in the nanoparticle alignment. Despite such disorders, the resulting nanostructures exhibit a strong dichroism and optical properties that are well reproduced from one laser printing to another. Here, we investigate experimentally and numerically the optical properties of laser-generated self-organized quasi-random plasmonic metamaterials. To understand the underlying physics, we highlight the coupling from near-field to far-field and compare the simulation results of the real-like sample and regular sample. The results demonstrate the coupling of plasmonic and photonic modes, whose efficiency is not reduced too much by the size and spatial disorder introduced by the laser processing. Further simulations with increasing disorder quantitatively investigate its effect on the coupling. Two kinds of real samples are investigated in which different degree of coupling between plasmonic modes and photonic modes occur. This paper proves that the inherent imperfections of laser-induced self-organized metamaterials do not dramatically hamper the collective effects, and prove that laser processing has a huge promising for real-world applications.



Plane views cross section views and spectra of experiment vs simulations.png

Optical horn antenna for extremely high single molecule detection rates

Tuesday, 25th October - 14:45: Enhanced spectroscopies - Oral

Dr. sunny tiwari¹, Mr. prithu roy¹, Dr. Jean Benoit Claude¹, Dr. Jérôme Wenger¹

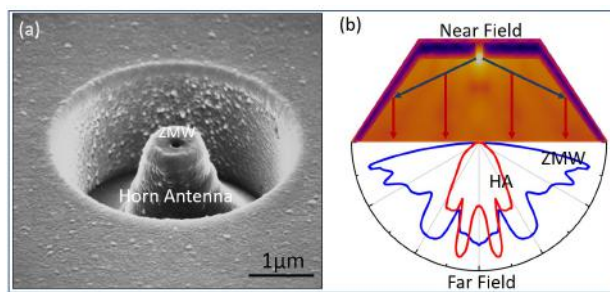
1. Institut Fresnel

Zero mode waveguides (ZMWs) are subwavelength apertures milled in metallic films which can confine light to scales much smaller than the diffraction limit¹. Molecules placed in the vicinity of ZMWs undergo enhanced emission as a consequence of the increase in the excitation and radiative rates. However, the maximum brightness signal one can extract from a single molecule further depends on how well the emission can be collected², which is crucial in probing faster molecular kinetics and achieving ultra-high count rates above one million counts per second.

Herein, we utilise optical horn antennas coupled with ZMWs which can enhance the signal from single molecules moving in an aqueous solution³. ZMW enhances the molecular fluorescence whereas the optical horn antenna redirects the majority of the emission to the collection optics into a narrow range of angles (**figure 1**). This helps in reaching extreme brightness from molecules by fetching nearly two million counts per second per molecule, thus surpassing the previous efficiency of collecting molecular emissions from single molecules. We probe the enhanced molecular emission using fluorescence correlation spectroscopy and corroborate the experimental findings using finite element method based numerical calculations. These results will have implications in observing single molecule dynamics in confined environments and in studying fast kinetics biological reactions such as biotin-streptavidin binding.

References:

1. Baibakov, Mikhail, et al. "Extending single-molecule forster resonance energy transfer (FRET) range beyond 10 nanometers in zero-mode waveguides." ACS nano 13.7 (2019): 8469-8480.
2. Novotny, Lukas, and Bert Hecht. Principles of nano-optics. Cambridge university press, 2012.
3. Barulin, Aleksandr, et al. "Ultraviolet optical horn antennas for label-free detection of single proteins." Nature Communications 13.1 (2022): 1-9.



Nanopfig.jpg

Aluminum bowties for broadband SEIRA sensing

Tuesday, 25th October - 15:02: Enhanced spectroscopies - Oral

Mrs. Melissa Najem¹, Mr. Franck Carcenac², Prof. Thierry Taliercio¹, Dr. Fernando Gonzalez-Posada Flores³

1. IES - Univ. Montpellier - CNRS, **2.** LAAS - CNRS -Toulouse, **3.** Institut for electronic and systems

Surface-enhanced infrared absorption (SEIRA) spectroscopy shows promising detection features of molecules down to low concentrations per individual nanoantenna[1]. Aluminum bowtie-shaped (Al-BT) nanoantennas are excellent building blocks for wide-spectrum SEIRA ranging from 1000 to 10.000 cm⁻¹. An engineered localized surface plasmon resonances (LSPRs) with triangle side-lengths (L) and gaps (g) provide an outstanding near E-field by “lightening-rod effect” at their sharp apex[2]. Al-BT are fabricated by electron-beam lithography followed by metallization and lift-off within a metal-insulator-metal (MIM) structure as illustrated in Fig.1a. The Al-BT array with gaps of 20 nm in the SEM image of Fig1b has a $\sim 10^3$ near-field enhancement from FDTD simulations (Lumerical). The excitation source is polarized along the BT main axis to enhance the electrical field into the gap where it is strongly localized[3]. Al-BT are optically characterized under 36x IR Fourier Transform IR (FTIR) spectrometer. Fig.1c confirms a good agreement between simulation (FDTD) and experiment (FTIR), for L from 0.3 to 2.0 μm with a step of 0.1 μm and g constant at 100 nm. For each L value, one main plasmonic resonance peak is detected and usually referred to as strong dipolar coupling. Fig.1d is the SEIRA demonstration of 5 IR lines of vanillin, L is varied from 1.4 to 2.0 μm (step of 0.1 μm). The enhancing effect occurs only when the resonant interaction between both excitations (antenna and molecular vibration) is fulfilled and it is marked by a Fano-like asymmetric profiles. The asymmetry of the line shapes is reversed when the narrow vibration is located to the right or to the left of the broadband plasmonic resonance. An enormous enhancement factors of ~ 7 orders of magnitude are achieved only by probing 2.5×10^4 molecules per tip with Al BT [1]. Such result is extremely encouraging for a lab-on-chip detection using a single plasmonic platform in comparison with the SEIRA state-of art[4].

- [1] F. Neubrech et al., *Chem. Rev.*, **2017**, *117*, 5110.
 - [2] N. J. Halas et al., *ACS Photonics*, **2016**, *3*, 354.
 - [3] B. Wang et al., *Plasmonics*, **2020**, *15*, 609.
 - [4] M. Najem et al., *Adv. Optical Mater.* **2022**, 201025.

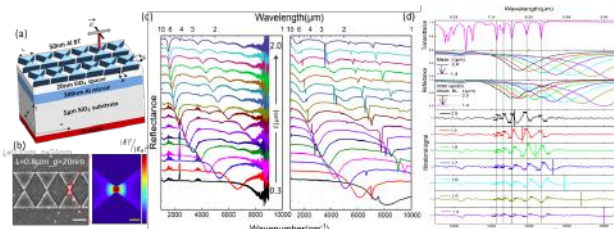


Image albt.png

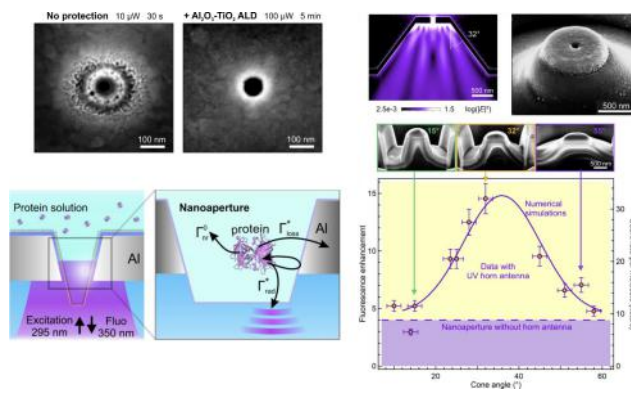
Aluminum Nanostructure for Deep-Ultraviolet Nanophotonics and its Application in Label-Free Single-Molecule Biophysics

Tuesday, 25th October - 15:19: Enhanced spectroscopies - Oral

Mr. prithu roy¹, Dr. Jean Benoit Claude¹, Dr. Jérôme Wenger¹

1. Institut Fresnel

Proteins usually contain aromatic amino acids like tryptophan and tyrosine which can be excited by deep ultraviolet light and are the source of auto-fluorescence of proteins. Thus Deep-Ultraviolet light renders the possibility to excite auto-fluorescence in proteins, a pathway to see and study protein without labeling i.e. A label-free single molecule detection technique where we can monitor the behavior of protein without modifying its property by additional dye molecules. However, simple as it might sound, the auto-fluorescence is intrinsically weak, which has been a big hindrance in this field. To deal with this problem, we have developed Al (Aluminum) based nanostructures like rectangular, circular nano-apertures and some advanced structures like Horn-antenna. We used Al, which is the most commonly used UV plasmonic-photonic material because it is earth-abundant material and has a higher faraday number in UV however, stability of Al in water or salt solution has always been an area of concern and active research, we dealt with this problem by providing nanometer oxide based insulated coating on Al structures as well as introducing ROS (Reactive Oxygen Species) quenchers to mitigate the corrosion problem. We further studied how different nano-meter thick oxides can affect the optical and physical properties of Al nanostructures. These structures render us the ability to enhance the autofluorescence signal to order or higher. This feat is achieved by exploiting features of zero-mode waveguides which provide volume confinement to atto litters and plasmonic enhancement. The zero-mode waveguides intensify the Purcell factor of label-free proteins by changing the local density of states inside the nano aperture's interaction volume. Further, we embedded the nano-aperture in a conical reflector forming a horn antenna in UV, this nanostructure helps in the collection as it directs the emitted light, from larger angles into the objective which has relatively smaller collection angles. This gives us the opportunity to study biophysical phenomena like single - proteins diffusion, fold-unfolding of proteins and binding mechanism, etc., label-free.



Final.png

Introduction of mesoporous gold materials for plasmonic applications

Tuesday, 25th October - 15:36: Enhanced spectroscopies - Oral

Dr. Olga Guselnikova¹, Dr. Joel Henzie¹, Prof. Yusuke Yamauchi¹

1. National Institute For Materials Science

Introduction of mesoporous gold materials for plasmonic applications

O. Guselnikova¹, J. Henzie¹, Y. Yamauchi¹

¹ International Center for Materials Nanoarchitectonics (WPI-MANA), National Institute for Materials Science (NIMS), 1-1 Namiki, Tsukuba, Ibaraki 305-0044, Japan

Introduction

Porous plasmonic materials demonstrate strong LSPR enhancement because of a generated ultrahigh surface area, abundant round surface tips, and pores/voids. And the combination of concave and convex features of plasmonic nano-crescent antennae can collect and focus light to generate ultra-strong near fields. Extended arrays of pores in three dimensions should enhance both local and long-range plasmon coupling effects, but little work has addressed this topic.

Methods

Mesoporous gold films were synthesized using electrochemical reduction of Au species in polymeric micelles polystyrene-b-poly(ethylene oxide). The micelles serve as a pore-directing agent to form the mesoporous structure. Mesoporous gold NPs were prepared via the chemical reduction in the presence of the diblock copolymer PS-b-PEO and L-Cysteine as thiol-containing ligand.

Results and Discussion

Mesoporous gold films and nanoparticles with a tunable pore size ranging from 5 to 30 nm facilitate mass transport of guest molecules leading to a higher number of interaction events between a molecule of interest, plasmonic surface and generated plasmons compared to non-porous ones. We prepared hybrid nanostructures of gold films with AgNPs [1], nanoporous metal-organic framework [2], and chiral shuriken structures. These hybrid porous substrates demonstrated an advantageous application for surface-enhanced Raman spectroscopy (SERS) biosensing of thiols in the presence of living cells [1], chiral drug pseudoephedrine [2] and chiral fungicide metalaxyl. For SERS application, mesoporous architecture serves a filtering function of large biomolecules from biomatrix and achieved the maximum signal enhancement. The mesoporous NPs with different pore's size [3] show advantageous porosity-induced symmetry breaking because strong electric fields of the plasmon are colocalized along concave/convex features where step-edges and kinks in the atomic structure generate numerous catalytic active sites. Plasmon-enhanced photodegradation of metanil yellow was used to demonstrate the superior photocatalytic properties of mesoporous AuNPs.

References:

- [1] ACS Appl. Mater. Interfaces 2022, in press, doi.org/10.1021/acsami.2c12804
- [2] Biosens. Bioelec., 2021, 180, 113109
- [3] Chem. Mater. 2022, 34, 16, 7256–7270

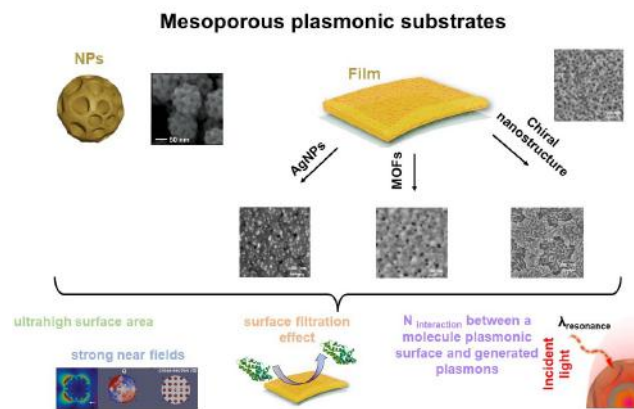


Fig aum.jpg

Plasmonic cavity based molecular junction for combined transport and spectroscopy

Tuesday, 25th October - 15:53: Enhanced spectroscopies - Oral

Ms. Sakthi priya Amirtharaj¹, Mrs. Xie Zhiyuan¹, Dr. Wen Chen¹, Dr. Emanuel Lörtscher², Prof. Christophe Galland¹

1. Laboratory of Quantum and Nano-optics, Ecole Polytechnique Fédérale de Lausanne, CH-1015 Lausanne, Switzerland, 2.

IBM Research – Zurich, Säumerstrasse 4, CH-8803 Rüschlikon, Switzerland

Introduction-

Molecular junctions are a promising platform for single molecule sensing and nanoscale electronics. For a long time, the poor reproducibility and complexity in the fabrication of molecular junctions have prevented the commercialization of these devices. We have developed a novel macroscopic molecular junction device exhibiting a few molecule features with state-of-the-art stability at room temperature. The device geometry allows good optical access and enables detection of Raman signal from a few hundreds of molecules, thanks to the plasmonic enhancement of the nanoparticle cavity. Thus, we can reliably probe the optical and electronic properties of the molecules. We further demonstrate simultaneous monitoring of surface enhanced Raman scattering (SERS) along with the conductance of the molecules in real-time.

Methods-

The device comprises a self-assembled monolayer (SAM) of biphenyl-4,4-dithiol molecules bridged between gold electrodes and a nanoparticle, forming molecular junctions encompassed in a plasmonic cavity. Despite using a SAM, only a small number of molecules establish successful contact with the gold nanoparticle, and makes it a few molecular device. The on-chip molecular junctions can be easily observed under our custom microscope, which can perform spectroscopic and conductance measurements at the same time.

Results and discussion-

We have formed molecular junctions (figure 1) as described in the methods and verified the presence of molecule-metal contact by measuring the conductance. The devices are stable at room temperature for several days. Some of them also sustain high voltage drives up to 4.5V as shown in the current-voltage plot in figure 2. The SERS and conductance measurement performed on a molecular junction device is shown in figure 3. The spectrometer registered hundreds of counts/s/ μ W of laser power, which allowed us to make spectral data acquisitions with a 300-500ms time interval for real-time monitoring. Finally, the stability of the device with time is shown in figure 4. The robust nature of our device, added with scalability and ease of fabrication could make molecular scale devices a reality. Moreover, optical access with a well defined plasmonic cavity would help to better understand the interaction of electronic and vibrational energy levels in a metal-molecule interface to an atomic scale.

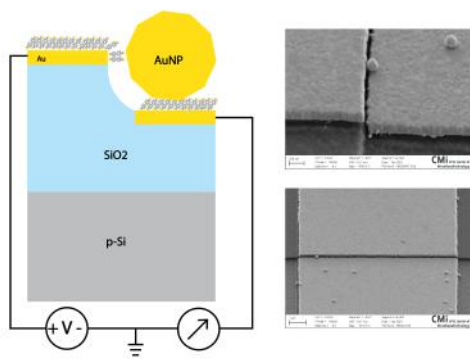


Figure 1 plasmonic cavity based molecular junction.png

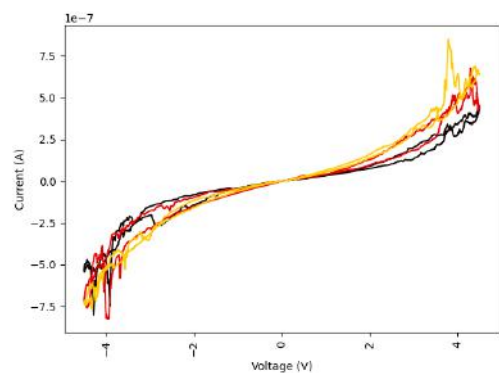


Figure 2 current-voltage characteristics at high bias voltages.png

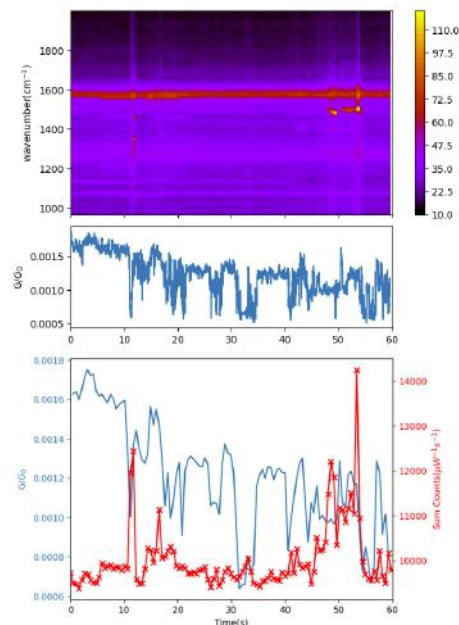


Figure 3 combined sers and conductance measurement.png

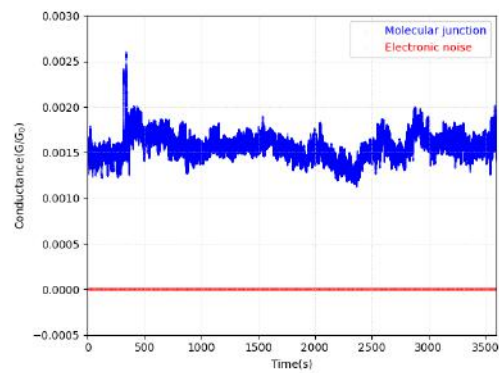


Figure 4 stability of the molecular junction at 5mv bias voltage.png

THz time-domain spectroscopy modulated with semiconductor plasmonic perfect absorbers

Tuesday, 25th October - 16:10: Enhanced spectroscopies - Oral

Dr. Fernando Gonzalez-Posada Flores¹, Dr. Dominique Coquillat², Mrs. Melissa Najem¹, Prof. Thierry Taliercio¹

1. IES - Univ. Montpellier - CNRS, 2. L2C - Univ. Montpellier - CNRS

Terahertz time domain spectroscopy (THz-TDS) remains one important pillar of terahertz photonics in many applications. [1] Plasmonic microstructures and metasurfaces are particularly promising for improving THz spectroscopy techniques, and above all encourages the THz development of biomedical and environmental sensors. [2] Traditionally, noble metals are used, but highly doped semiconductors are appropriate for a replacement in the THz range. The semiconductor plasmonic optic behaviors are tuned with different geometry, size and gap-effect interactions. Figure 1A shows a perfect absorber structure based on III-V semiconductor layers on a GaSb commercial template. A metallic mirror-like doped InAsSb layer with a GaSb spacer on top targets a photonic absorption peak in the IR dependent only on the thickness. In the THz region, the InAsSb top layer was doped and microstructured to obtain a plasmonic resonance, dependent only on the doping and structure's geometry. Figure 1B shows visible light diffraction of the 1x1 mm² microstructured arrays fabricated by electron beam lithography and dry etching. In figure 1C, the darkest 1x1 mm² squares correspond to an array of InAsSb linewidth of 14 and 16 mm with a constant pitch of 30 mm. Such contrast is related to the coupling between the plasmonic microstructure array and the incident light at a mean frequency region selected in the THz-TDS measurement. Thus, an intense color indicates a higher electric field in the C-slice view scale. In this particular C-slice view, a 2-2.05 THz mean frequency is selected. Finally, in figure 1D, the THz-TDS measurements of the minimum absorption reached (red dots) correspond with the simulation absorption map calculated by rigorous-coupled wave analysis [3]. In conclusion, perfect absorbers microstructures pave the way to use semiconductor plasmonics as support for sensing applications in the THz spectrometers.

References:

- [1] W.L.Cham et al. Rep. Prog. Phys. 70 (2007) 1325–1379.
- [2] D. M. Mittleman Nature Photonics 7, 666 (2013)
- [3] J.-P. Hugonin, & Lalanne. Light-in-complex-nanostructures RETICOLO V8 (2020).

This work is partially supported by :

- Equipex EXTRA (ANR-11-EQPX-0016)
- SEA – Region Occitanie (2020-2021)
- MUSE – PRIME@MUSE – I-Site

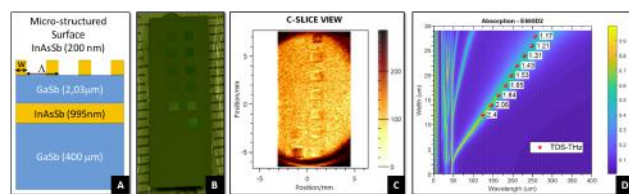


Image thz.png

Satisfying solutions to inverse design problems in photonics

Tuesday, 25th October - 14:45: Inverse design in photonics - Oral

Ms. Pauline Bennet¹, Dr. Olivier Teytaud², Mr. Vage Karakhanyan³, Dr. Thierry Grosjean³, Dr. Rafik Smaali¹, Prof. Emmanuel Centeno¹, Dr. Antoine Moreau¹

1. IP - CNRS, INP, Université Clermont Auvergne, **2.** Facebook AI Research Paris, **3.** Femto-ST, Université Bourgogne Franche-Comté

Introduction. It is almost impossible to assess whether the solution of a photonics optimization problem is the true, global optimum. It is however possible to discuss the quality of a given solution. Two criteria, at least, can be used (i) the frequency of occurrence when algorithms are run several times and (ii) a physical analysis allowing to understand its emergence[1].

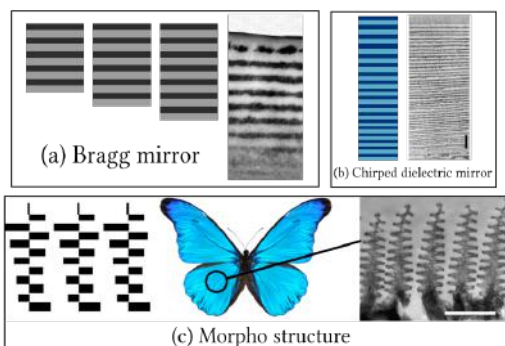
Methods. We have used global optimization algorithms (PSO, Differential Evolution, CMA-ES, Nelder Mead,...) to solve simple well posed photonics problems (how to reflect a given wavelength, reflect a broad range of wavelength, diffract a given wavelength, how to favor the absorption by a photovoltaic device, excite a long range surface mode, separate polarizations, excite a waveguide). Algorithms are run a large number of times allowing to assess the reliability of each solution.

Results. Differential Evolution, for problems with typically 10 to 100 parameters, seems to possess the property of finding truly satisfying solutions, with periodicity or regularity emerging most often. For all the problems mentioned above, it has provided designs which are understandable and which have been thoroughly analyzed physically. Some of the structures found by optimization even occur in nature (Bragg mirrors)[2]. Structures obtained by optimization are shown on the figures.

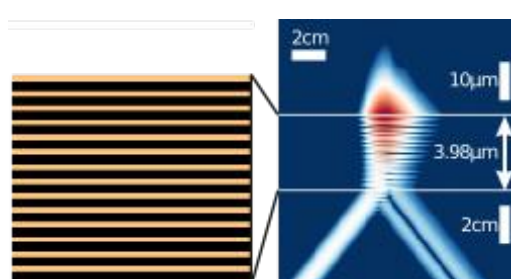
Discussion. The careful methodology we have applied to find truly satisfying solutions allows to tell whenever a problem becomes to hard for the algorithms : disorder emerges, performances deteriorate. This sheds a new light on many previously published optimization results. Furthermore, it makes possible to compare the result of an optimization by an evolutionary algorithm to the product of true evolution – and helps explain why photonic crystals are ubiquitous in natural photonic structures. From our results, it should be expected that regular or even partially periodic solutions exist for potentially any photonic problem. Finally, photonics problems turn out to be particularly useful for the benchmarking of optimization algorithms.

[1] Bennet, Pauline, et al. *Physical Review B* 103.12 (2021): 125135.

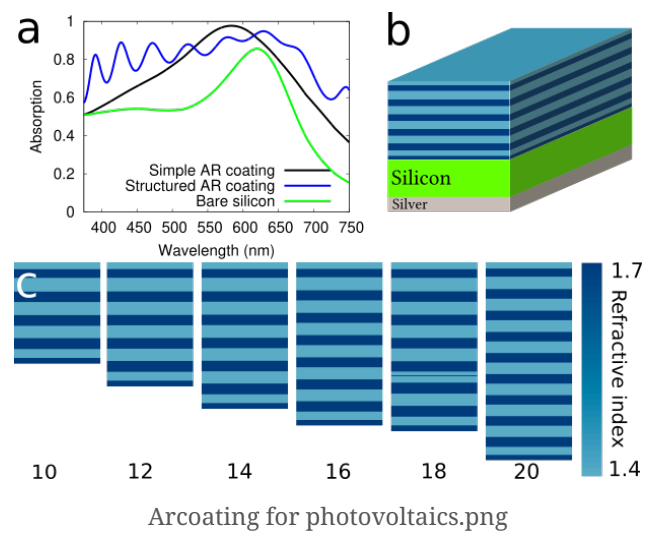
[2] Barry, Mamadou Aliou, et al. *Scientific reports* 10.1 (2020): 1-10.



Optimized structures compare to natural.png



Extreme range plasmon coupler.png



AI based forward prediction and inverse design of complex metasurfaces

Tuesday, 25th October - 15:02: Inverse design in photonics - Oral

Dr. Tianning Zhang¹, Dr. Chunyun Kee¹, Prof. Yee sin Ang¹, Prof. Ricky ANG¹

¹ Singapore University of Technology and Design

In this presentation, we report our recent works [1,2] in using complex and random metasurfaces to test the performance of various Deep Learning (DL) models for both forward prediction and inverse design. Using CST simulation, we create about 30,000 of samples with their EM reflection from 2 to 12 GHz for this type complex and random metasurfaces. Using this home-made dataset, we compare and determine the best DL models to provide high accuracy [1] for different patterns in the dataset [1]. Good prediction is obtained. However, the cross-comparison reports a shortcoming of the DCNN model in applying to any patterns, which suggests a statistic-fitting machine and lose the AI's generalization for transfer learning. In using Network Architecture Search (NAS) method and the spatial symmetry information of the complex metasurfaces, we are able to improve the performance [2]. It is found that a shallow and wide neural network will provide better performance for this type of complex and physics based metasurfaces problem, which is in contrast to the deep trends used in the traditional DL models for computer vision. Our method can now accurately identify the EM response locations from arbitrary random and complex metasurfaces while the conventional models fail to accomplish. It can also accurately predict the EM response curve by injecting correct symmetry information into the architecture design step. Thus, our DL model offers a platform to study the influence of different fundamental operations for complex metasurface design problems. Finally, we are sharing [3, 4] our home-generated physics-based dataset [SUTD polarized reflection of complex metasurfaces (SUTD-PRCM)] for future testings from the research community that we believe the best DL model is yet to be found.

[1] Tianning Zhang, Chun Yun Kee, Yee Sin Ang, and L. K. Ang*, “Deep learning-based design of broadband GHz complex and random metasurfaces”, APL photonics 6, 106101 (2021).

[2] Tianning Zhang, Chunyun Kee, Yee Sin Ang, Er Ping Li, and L.K. Ang*, Symmetry Enhanced Network Architecture Search for the design of Complex Metasurfaces, IEEE Access 10, 73533 (2022)

[3] https://github.com/veya2ztn/SUTD_PRCM_dataset

[4] <https://github.com/veya2ztn/MetaSurface>

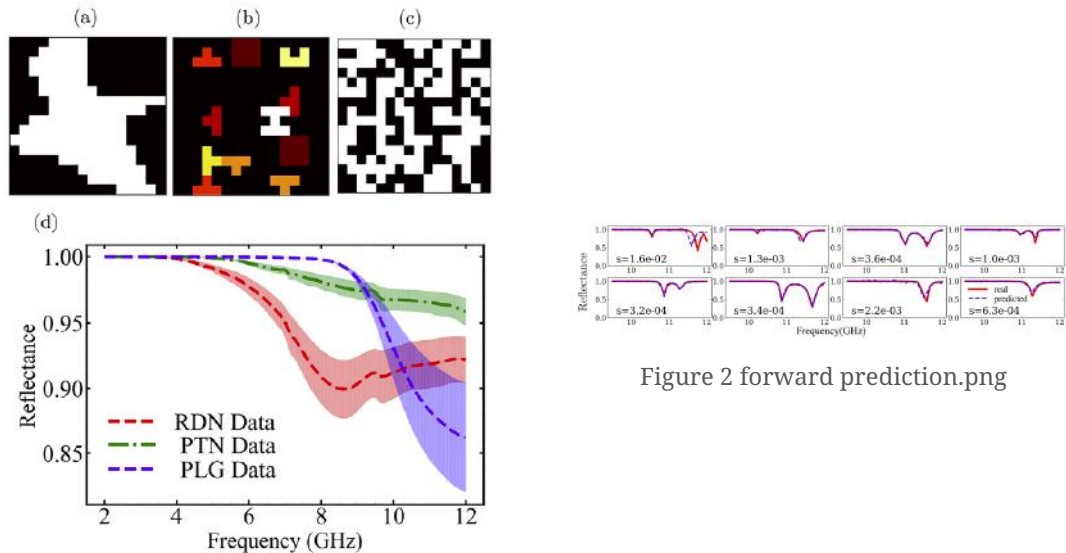


Figure 1 data sets.png

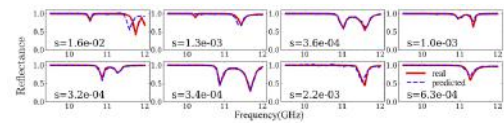


Figure 2 forward prediction.png

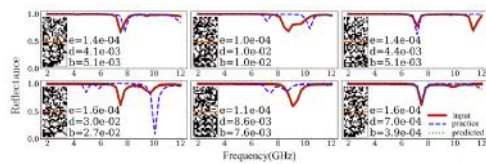


Figure 3 inverse design.png

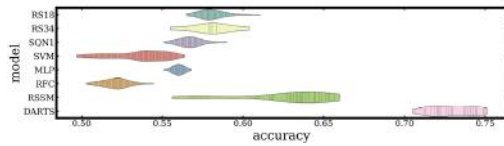


Figure 4 nas.png

Inverse-designed dielectric cloaks for entanglement generation

Tuesday, 25th October - 15:19: Inverse design in photonics - Oral

Mr. Alberto Miguel¹, Prof. Antonio I. Fernández-Domínguez¹, Prof. Francisco José García Vidal¹, Mr. Jaime Abad Arredondo²

1. Departamento de Física Teórica de la Materia Condensada and Condensed Matter Physics Center (IFIMAC), Universidad Autónoma de Madrid, E28049 Madrid, Spain. **2.** – Departamento de Física Teórica de la Materia Condensada and Condensed Matter Physics Center (IFIMAC), Universidad Autónoma de Madrid, E28049 Madrid, Spain

Preparing, preserving, and controlling entanglement in quantum systems is of great importance for quantum communications, teleportation, and quantum computing [1]. In this paper, we show the generation of an entangled steady state in a two-qubit system under continuous incoherent pumping by engineering environment-induced dissipation [2]. To control such system-environment interaction, we use an inverse design approach and create nanophotonic devices with optimized dielectric structures [3]. These are designed using an iterative algorithm, within topology optimization techniques [4], which imposes no constraints on geometrical shapes and involves only a system analysis and a gradient calculation at each step, making the developed procedure very cheap as a computational tool [5, 6].

We show that significant values for the concurrence, a standard measure of the degree of entanglement, can be attained for a wide range of pumping rates and for qubit-qubit distances even larger than the operating wavelength. We also compare with other quantities that refer to the same quantum property and test the robustness of the algorithm. In addition, we obtain strong correlations between qubits through the second-order cross-correlation function, highlighting the quantum nature of the system.

- [1] M. A. Nielsen and I. A. Chuang, Quantum computing and quantum information (Cambridge, 2000).
- [2] A. Miguel-Torcal, J. Abad-Arredondo, F. J. Garcia-Vidal, and A. I. Fernández-Domínguez, “Inverse-designed dielectric cloaks for entanglement generation”, Nanophotonics, 2022 (<https://doi.org/10.1515/nanoph-2022-0231>).
- [3] S. Molesky, Z. Lin, A. Y. Piggott, W. Jin, J. Vuckovic, and A. W. Rodriguez, “Inverse design in nanophotonics”, Nature Photonics 12, 659-670 (2018).
- [4] J. Jensen and O. Sigmund, “Topology optimization for nano-photonics”, Laser & Photonics Reviews 5, 308-321 (2011).
- [5] S. Mignuzzi, S. Vezzoli, S. A. R. Horsley, W. L. Barnes, S. A. Maier, and R. Sapienza, “Nanoscale design of the local density of optical states”, Nano Letters 19, 1613-1617 (2019).
- [6] R. Bennett and S. Y. Buhmann, “Inverse design of light-matter interactions in macroscopic QED”, New Journal of Physics 22, 093014 (2020).

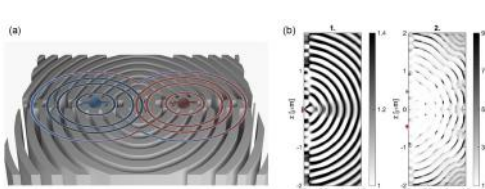


Figure 1: (a) Sketch of the entanglement generation in a pair of quantum emitters through an inverse-designed dielectric cloak. (b) Crosscut of the permittivity map corresponding to the cylindrical-shaped, inverse-designed cloak obtained for emitters (coloured arrows) separated by a distance $d_{12} = 950$ nm (2.5 times its emission wavelength, λ). The white-to-black scale codes the permittivity from 1 to 9.

Dielectric cloaks.jpg

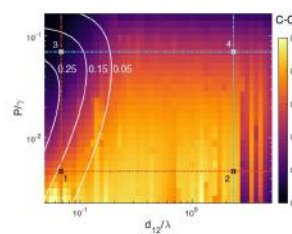


Figure 2: Entanglement generation efficiency, $C-C_0$, versus inter-emitter distance and pumping strength. In 1350 inverse-designed cloaks. White lines plot the free-space concurrence, C_0 , revealing that the QEs are disentangled for $d_{12} > 80$ nm.

Entanglement generation.jpg

Universal active metasurface modulation with ultimate performance in reflection

Tuesday, 25th October - 15:36: Inverse design in photonics - Oral

Dr. Mahmoud Elsayy¹, Dr. Christina Kyrou², Dr. Elena Mikheeva², Dr. Remi Colom², Dr. Jean-Yves Duboz², Dr. Stéphane Lanteri¹, Dr. Patrice Genevet²

1. Université Côte d'Azur, Inria, CNRS, LJAD, 06902 Sophia Antipolis Cedex, **2.** CNRS, CRHEA, Université Côte d'Azur, 06560 Valbonne

Optical metasurfaces are becoming ubiquitous optical components to mold the amplitude, the phase and the polarization properties of light beams. So far, most of these devices are passive in essence, that is, they cannot be arbitrarily reconfigured or optimized according to the user's interest and/or change in their surrounding environment. Here we propose an innovative design strategy relying on the position of topological singularities, namely zeros and poles of the reflection coefficient, to address full phase modulation of light reflecting off an active metasurface with almost unity efficiency. The active metasurface unit cells, consisting of asymmetric Gires-Tournois resonators filled with electro-optics materials comprising either of Liquid crystal or multiple quantum wells, are able to modulate the reflected field from 0 to 2π associated with 100% reflection amplitude despite dealing with extremely low refractive index change on the order of 0.01. The second ingredient to achieve high efficiency modulation consists in optimizing the arrangement of the sub-wavelength unit-cells so as to account for local imperfection and near-field coupling between neighboring structures. Consequently, an advanced optimization method accompanied with high-fidelity full-wave solver are required to identify the refractive index distribution. In our case we rely on a statistical learning optimization technique. It is based on a surrogate model representation which provides a quick estimation to approximate the true function of interest to select the best candidates for the next simulation. Accordingly, programmable beam steering configurations have been designed with ultimate performance in reflection. The realization of active beam splitter and active beam steering devices operating at GHz deflection frequency would open important applications in imaging microscopy, high resolution image projection, optical communication and 3D light detection and ranging (LiDAR).

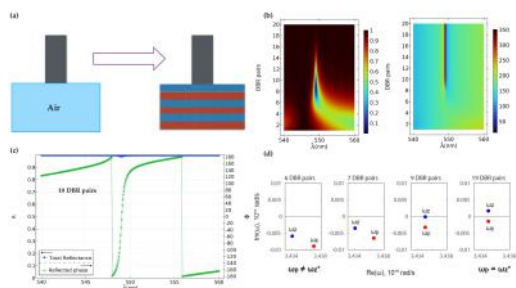


Fig1.jpg

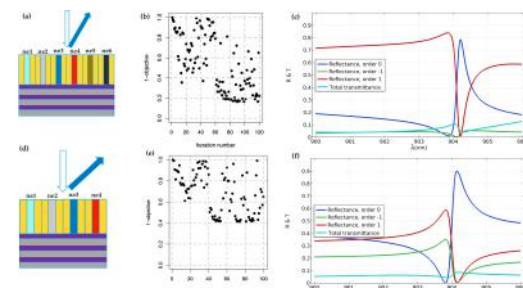


Fig2.jpg

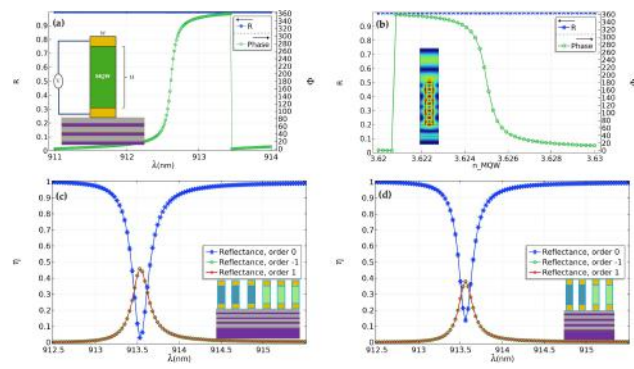


Fig3.jpg

A Chiral Inverse Faraday Effect Mediated by an Inverse-designed Plasmonic Antenna

Tuesday, 25th October - 15:53: Inverse design in photonics - Oral

Mr. Ye Mou¹, Mr. Xingyu Yang², Dr. Bruno Gallas¹, Dr. Mathieu Mivelle³

1. Institut des NanoSciences de Paris - Sorbonne Université, **2.** Institut des NanoSciences de Paris, **3.** Institut des NanoSciences de Paris - CNRS

The inverse Faraday effect (IFE) allows the generation of stationary magnetic fields through optical excitation only [1,2]. This light-matter interaction in metals results from the creation of drift currents via nonlinear forces that light applies to the conduction electrons [1]. The IFE was believed, until now, to be a symmetrical phenomenon, meaning that a right-handed circularly polarized wave will create a magnetic field oriented toward light propagation. In contrast, excitation by a left-handed circularly polarized wave will generate a magnetic field opposite this propagation. Here we demonstrate, via the manipulation of light in the near field of a plasmonic nanostructure, the generation of a chiral IFE. Specifically, using an inverse design algorithm based on evolutionary optimization, we generate a chiral plasmonic nanostructure creating a stationary magnetic field by IFE for one specific light helicity (Figure 1a-c). This chiral behavior is due to the generation of a non-zero spin density for the chosen helicity only.

Furthermore, we demonstrate that using the enantiomer opposite to the optimized structure generates a magnetic field for an opposite helicity of light (Figure 1d-f). Moreover, at the optical powers considered here, the amplitude of the magnetic field generated is 500 mT. The results presented here are remarkable since the plasmonic approach is today the only one allowing the generation of stationary magnetic fields at the nanometer scale and at extremely short time scales [3]. Therefore, using chiral plasmonic nanostructures to generate a chiral IFE opens the door to producing a stationary magnetic field by non-polarized light. The outcomes of these results are multiple, in particular the manipulation of magnetic processes at ultrashort timescales, such as spin precession, spin currents, and skyrmions become possible. This would find applications, for instance, in data storage at an ultrahigh rate.

References

- [1]. Hertel, "Theory of the Inverse Faraday Effect in Metals."
- [2]. Nadarajah and Sheldon, "Optoelectronic Phenomena in Gold Metal Nanostructures Due to the Inverse Faraday Effect."
- [3]. Yang et al., "Tesla-Range Femtosecond Pulses of Stationary Magnetic Field, Optically Generated at the Nanoscale in a Plasmonic Antenna."

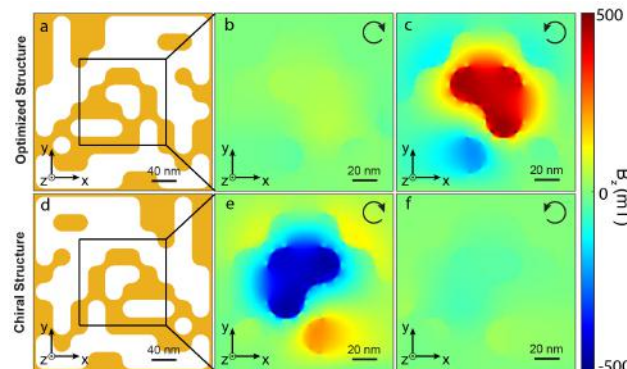


Figure 1. the distributions of stationary magnetic fields for the optimized structure and its chiral structure.jpg

Geometry optimization of the magnetic Purcell factor in high index dielectric nanostructures

Tuesday, 25th October - 16:10: Inverse design in photonics - Oral

Dr. Yoann Brûlé¹, Dr. Peter Wiecha², Dr. Aurélien Cuche³, Prof. Vincent Paillard³, Prof. Gérard Colas des Francs¹

1. ICB - CNRS-Univ. Bourgogne-Franche-Comté, 2. LAAS - CNRS, univ. Toulouse, 3. CEMES - CNRS, Univ. Toulouse

Introduction

Light-matter interaction in the optical regime is principally of electric nature because the magnetic contribution is orders of magnitude weaker. Therefore, engineering optical magnetic dipole emission opens alternative design rules for new types of light sources [1,2].

Methods and results

In this work, we design planar silicon antennas for controlling the emission rate of magnetic or electric dipolar emitters. Evolutionary algorithms coupled to the Green Dyadic Method lead to different optimized geometries which depend on the nature and orientation of the dipoles, but all presenting regular and periodical features [3,4]. In the far-field, we observe circular gratings for all the configurations.

Discussion

As far as the near-field zone is concerned, we observe strong differences for ED and MD emitters, with the presence or not of a Si core, that depends on both the dipole nature and orientation. Similar configurations have been guessed in the literature but our work reveals that they are close to be optimal. To go beyond the “black box” optimization, we also discuss the physical origin of the obtained designs thanks to modal analysis but also in relation to the deterministic design approach recently developed by Mignuzzi *et al.* [5]. We complete our study using finite element method and demonstrate an enhancement of more than three orders of magnitude of the magnetic Purcell factor in europium ions.

Conclusion

Our work brings together random optimizations to explore geometric parameters without constraint, a first order deterministic approach to understand the optimized designs and a modal analysis which clarifies the physical origin of the exaltation of the magnetic Purcell effect.

[1] Bidault *et al*, *Dielectric nanoantennas to manipulate solid-state light emission* J. Appl. Phys. **126**, 094104 (2019)

[2] Staude *et al*, All-Dielectric Resonant Meta-Optics Lightens up, ACS Photonics, 6(4), 802, (2019).

[3] Wiecha *et al*, “pyGDM” -python toolkit for nano-optics full-field simulations, Comput. Phys. Commun. **270**, 10814 (2022)

[4] Brûlé et al, *Magnetic and electric Purcell factor control through geometry optimization of high index dielectric nanostructures*, Opt. Exp. **30**, 20360 (2022)

[5] Mignuzzi *et al*, *Nanoscale design of the local density of optical states*, Nano Lett., **19**, 1613 (2019)

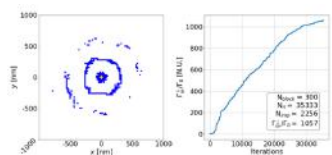


Fig. Left : Evolutionary-optimized structure (orange) ; fixed core emitter, blue : Si nanopillars. Center : Evolution of the magnetic Purcell factor through the optimization iterations.

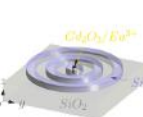


Fig. Left : Evolutionary-optimized structure (orange) ; fixed core emitter, blue : Si nanopillars. Center : Evolution of the magnetic Purcell factor through the optimization iterations.

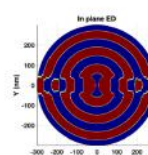


Fig. Left : Evolutionary-optimized structure (orange) ; fixed core emitter, blue : Si nanopillars. Center : Evolution of the magnetic Purcell factor through the optimization iterations.

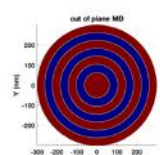


Fig. Left : Evolutionary-optimized structure (orange) ; fixed core emitter, blue : Si nanopillars. Center : Evolution of the magnetic Purcell factor through the optimization iterations.

Zmagpurcellevolution.png

Ldosdesign.png

Optimal nanophotonics: the road from theory to practice

Tuesday, 25th October - 16:55: Plenary Session - Oral

Prof. Alejandro Rodriguez¹

1. Princeton Institute for the Science and Technology of Materials

TBD

Biphoton generation in nanostructures at telecom wavelength

Tuesday, 25th October - 17:35: Plenary Session - Oral

Prof. Rachel Grange¹

1. ETH Zurich

We report nonphase-matched spontaneous parametric down-conversion (SPDC) from LiNbO₃ (LN) microcubes and GaAs nanowires. Both microstructures are free-standing with high bulk quadratic nonlinearities, LN has a wide transparent window (0.4-5.0 μm), and GaAs is a high index semiconductor that can support resonant Mie modes for enhanced localized fields. The signal to noise ratio measured from the coincidence counts indicates the arrival of entangled photons. We discuss the different efficiencies of the SPDC process normalized to the transmission, the power and volume. These efficient compact sources of biphotons could be integrated for quantum cryptography or quantum metrology applications.

Nonlinear Topological Photonics

Wednesday, 26th October - 09:00: Plenary Session - Oral

Dr. Mikael Rechtsman ¹

1. The Pennsylvania State University

The defining property of a topological system is that it exhibits some physical property that is highly robust to perturbations such as disorder. In recent years, it has been demonstrated that such phenomena are not confined to the domain of condensed matter physics (for example, in the quantum and spin Hall effects), but rather can be found in other contexts such as photonics, ultracold atoms, acoustics, polaritonics, etc. In this talk I will present some recent theoretical and experimental results on the interplay between nonlinear photonic structures and topological physics.

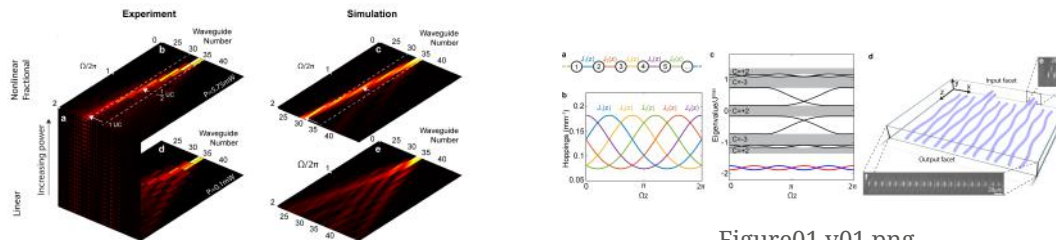


Figure01 v01.png

Figure03 v01.png

TBD

Wednesday, 26th October - 09:40: Plenary Session - Oral

Prof. Laura Na Liu¹

1. University of Stuttgart

TBD

Plasmon Empowered Nanophotonics

Wednesday, 26th October - 10:50: Plenary Session - Oral

Prof. Sergey Bozhevolnyi¹

1. University of Southern Denmark

Surface plasmon polaritons, often shortened to surface plasmons (SPs), represent hybrid excitations involving free electron oscillations in metals and electromagnetic fields in dielectrics that propagate along and strongly bound to metal-dielectric interfaces. These surface electromagnetic waves enable deeply subwavelength confinement of guided modes along with strong enhancement of optical fields, two major features of SP modes that have been and continue being advantageously exploited in plasmon-empowered nanophotonics. It would be impossible to overview, even very briefly, all fascinating topics found within plasmonics that include metasurfaces, graphene and other 2D materials, strong-coupling phenomena, topological plasmonics, quantum plasmonics, hot-electron phenomena, and many other topics even when considering only those presented at the last conference on Surface Plasmon Photonics - SPP9 (see a word cloud compiled from the book of abstracts of SPP9 held in 2019).

In this talk, special attention is given to the progress in ultra-compact photonic circuitry, including modulators and detectors, and plasmonic metasurfaces dynamically controlling propagation of light. In particular, the most efficient and ultrafast electro-optical modulators and deflectors utilizing the commercially viable material, LiNbO₃, in which the radiation transport is controlled using the same metal circuitry for both guiding SP modes and delivering electrical signals, are presented along with the realization of on-chip electrical detection of guided SP modes. Plasmonic metasurfaces, which can be considered as the two-dimensional analogue of metal-based metamaterials, used for room-temperature generation of single-photon streams carrying orbital angular momenta and dynamic control of metasurface-enabled focusing and optical birefringence are also discussed. A personal view on the nearest perspectives for plasmon-empowered nanophotonics concludes this talk.

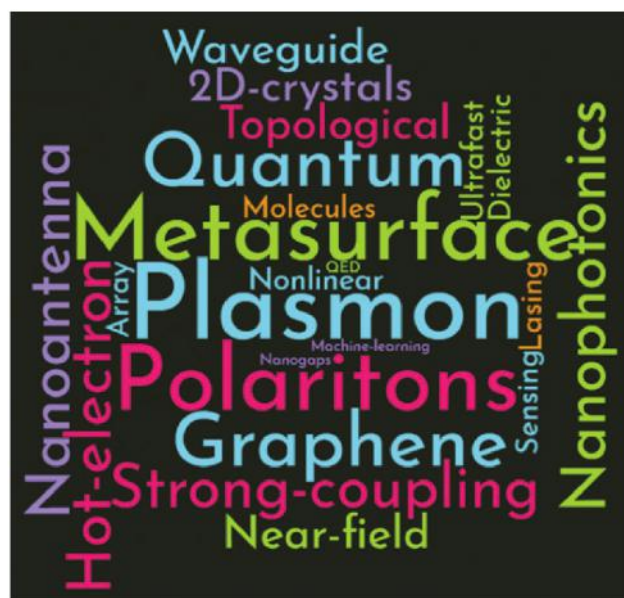


Fig1.png

Topological plasmonics: Watching the ultrafast vector dynamics of plasmonic skyrmions

Wednesday, 26th October - 11:30: Plenary Session - Oral

Prof. Harald Giessen¹

1. Stuttgart University

TBD

Isotropic and anisotropic regime in the limit of weak disorder

Wednesday, 26th October - 13:30: Poster Session - Poster

Dr. Afifa Yedjour¹

1. Faculty of physics, university of sciences and technology of Oran Mohammed Boudiaf

The goal of this work is to examine the scattering mean free path in the presence of interference caused by disordered potential using a numerical calculation. First, we start by examining the behavior of the self energy at the initial state to deduce the an-isotropic factor and comparing it with a classical diffusion. Then, we analyze the scattering mean free path of a cold atoms during the diffusion processes. At the limit of weak disorder, we find that for low momenta, the contribution of the atoms is a constant regardless of the value of disorder amplitude. As predict by Boltzmann, the diffusion is in an isotropic phase. On the other hand, the scattering gives rise to an an-isotropic at large momenta. the atoms start to deviate for each value of disorder amplitude which causes the fluctuations in its trajectory. We show that the interference becomes sensitive at large momentum. Our results are comparable with the experimental results.

New plasmonic-magnetic nanomaterials for Raman analysis of surfaces

Wednesday, 26th October - 13:30: Poster Session - Poster

Prof. Andrzej Kudelski¹

1. Faculty of Chemistry, University of Warsaw, 1 Pasteur Str., 02-097 Warsaw, Poland

The analysis of surface of various materials is important both from the economic and scientific points of view. Such analysis is especially difficult for so-called buried interfaces, which include interfaces of various biological samples in their “natural” environment. Many techniques standardly applied for surface analysis (especially those utilising beams of electrons) require a high vacuum above the surface being analysed. Unfortunately, when introduced into a vacuum, many types of biological samples suffer significant damage (it means that *in situ* characterisation of surfaces of various biological objects is usually not possible using many standard surface science techniques). In 2010, Li *et al.* showed that various surfaces (including surfaces of some biological objects in the *in situ* conditions) may be easily analysed using a modification of surface-enhanced Raman scattering (SERS) spectroscopy, so-called shell-isolated nanoparticle-enhanced Raman spectroscopy (SHINERS) [Nature (2010); 464, 392–395]. In SHINERS measurements, the surface which is analysed is covered with a layer of plasmonic nanoparticles (formed from gold, silver or alloys thereof) protected by a nanometric-thick layer (usually formed from a relatively inert oxide such as SiO₂, Al₂O₃, MnO₂, ZrO₂, or TiO₂), and then the Raman spectrum of the investigated sample is recorded. In this presentation we report the first examples of magnetic nanoresonators for SHINERS measurements in the form of: Au@Fe₃O₄ - see Figure 1, (Fe₃O₄@Au)@SiO₂ - see Figure 2 and (Fe₃O₄@Ag)@SiO₂ nanostructures. Due to the nanomaterials’ strong magnetic properties, they can be easily manipulated using a magnetic field, and it is therefore possible, for example, to form homogeneous layers (with no significant ‘coffee-ring’ effect) of such nanoparticles using a very simple procedure: depositing a drop of a sol of such nanoparticles and evaporating the solvent after placing the sample in a strong magnetic field. Moreover, for the model systems we studied, the spectral Raman backgrounds generated by these SHINERS plasmonic-magnetic materials were only a small fraction (about 1%) of the Raman signal generated by the investigated systems, and we therefore suppose that the materials obtained are very promising nanoresonators for many practical measurements (especially surface investigations).

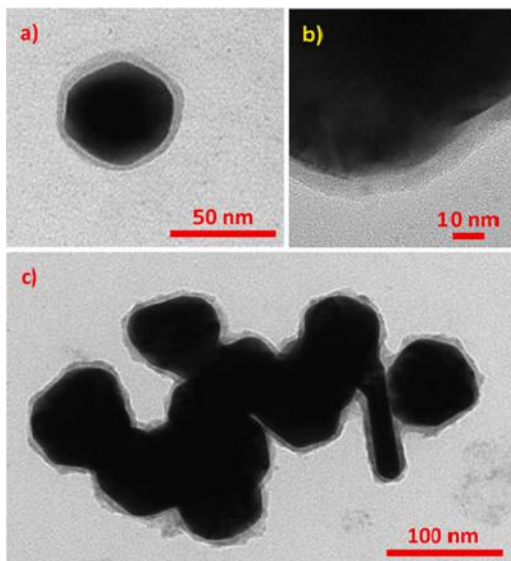


Figure1.jpg

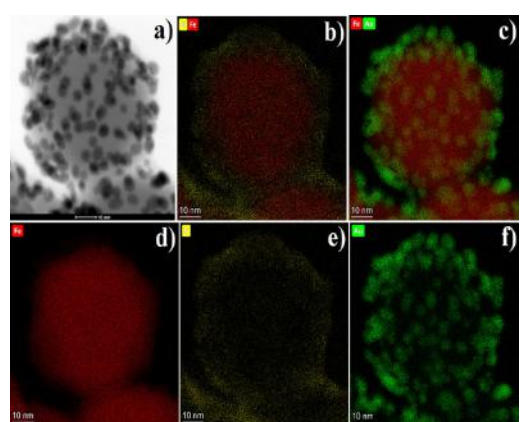


Figure2.jpg

FRET-mediated Collective Blinking of Self-Assembled Stacks of Semiconducting Nanoplatelets

Wednesday, 26th October - 13:30: Poster Session - Poster

Mr. Zakarya Ouzit¹, Dr. Jiawen Liu², Mr. Guillaume Baillard², Mr. Juan Pintor², Dr. Lilian Guillemeney³, Mr. Benoît Wagnon³, Dr. Benjamin Abécassis³, Dr. Laurent Coolen²

1. Sorbonne, **2.** Institut des NanoSciences de Paris - Sorbonne Université, **3.** ENS de Lyon

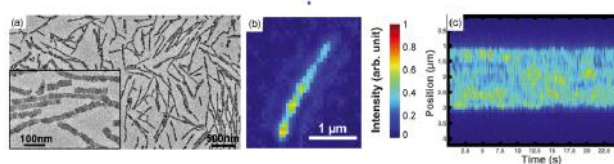
Extensive studies have been performed since the 1980s and 1990s on semi-conducting colloidal nanoparticles, usually on isolated emitters: either ensembles in solution, or single emitters under fluorescence microscopy. When a densely-packed stacking of emitters is considered, interactions between them are expected which must be understood, for instance, for opto-electronic applications such as quantum-dot-LEDs or quantum-dot-sensitized solar cells. However, experimental results are diverse and their interpretation is complex, especially because the level of disorder in stacked structures makes them difficult to model and reproduce.

CdSe nanoplatelets (NPL), also coined colloidal quantum wells, are outstandingly bright and well controlled fluorescent emitters. By a careful choice of ligands and solvents, they can be self-assembled into chains of hundreds of NPLs (up to 4 μm length) [1], with constant platelet center-to-center distance of 6 nm and excellent linear order (fig. 1(a)), therefore constituting a perfect platform for exploring these various collective effects. We have imaged the fluorescence from individual chains and found a FRET (Förster resonant energy transfer : dipole-dipole non-radiative exciton hopping) migration length of 500 nm (around 90 NPLs). From this, a diffusion-equation model leads us to estimate the characteristic time of FRET transfer between neighbour platelets to 1-2 ps, much shorter than all decay mechanisms known to occur in fluorescent semiconductor nanoparticles [2].

Densely-packed nanoparticles can thus be expected to present, because of FRET, totally new photophysical behaviour involving tens or hundreds of emitters collectively instead of each platelet emitting individually. Notably, we have demonstrated that some portions of NPL chains blink collectively (fig. 1(b,c)), showing that a single intermittent quencher platelet is able to block the luminescence from an ensemble of around 70 NPLs as excitons in these NPLs migrate by FRET and reach the quencher. The luminescence decay curves also show signs of FRET-induced effects of quencher defects and metastable traps. Future work will examine to which extent multi-exciton interactions can be influenced by FRET and whether collective optical effects such as superradiance can be obtained.

[1] L. Guillemeney et al, *Comm Chem* **5**, 7 (2022),

[2] Jiawen Liu et al, *Nano Lett*, **20**, 3465-3470 (2020).



Lcoolen fig1.png

Chirality of absorption bands of functionalized CdSe monitored through photoluminescence intensity

Wednesday, 26th October - 13:30: Poster Session - Poster

Ms. Lingfei Cui¹, Mr. Leonardo Curti², Dr. Benoit Fleury², Dr. Yoann Prado³, Dr. Emmanuel Lhuillier³, Dr. Benjamin Abécassis⁴, Prof. Catherine Schwob⁵, Dr. Mathieu Mivelle³, Dr. Bruno Gallas³

1. Institut des NanoSciences de Paris, 2. Institut Parisien de Chimie Molculaire, 3. Institut des NanoSciences de Paris - CNRS, 4. ENS de Lyon, 5. Institut des NanoSciences de Paris - Sorbonne Universit

Circular dichroism (CD) is widely used as a characterization technique of chiral molecules. For most biological molecule, the maximum signal is weak and located in the UV part of the spectrum. To increase the interaction of light in the visible part of the spectrum with biological molecules, it has been proposed to couple the molecules with plasmonic resonators. Here we show an alternative approach for luminescent objects where the CD of the absorption bands can be detected by monitoring the photoluminescence intensity (CD-PL). The CD and CD-PL measurements were realized on a home-made polarimeter (Figure 1(a)). The incident polarization was modulated with a polarizer and a photo-elastic modulator (PEM). A laser at 532 nm was used as an excitation source. A cuvette was placed at the intersection of the CD and CD-PL paths to detect simultaneously the signals. The polarization state after interaction with the sample was detected in transmission using a photodiode. The CD-PL measurements were made perpendicular to the light path of the excitation. A microscope objective (NA 0.42) was placed to collect the photoluminescence. The light was then filtered by a high pass filter to eliminate any spurious signal of the excitation that might have been scattered. The detection was performed using a photomultiplier tube (PMT). The signal of the PMT was demodulated at the modulation frequency of the PEM. The signal of the PMT was demodulated at the modulation frequency of the PEM.

We have measured different samples. The test samples were air and rhodamine. Rhodamine exhibits a strong luminescence at 600 nm and is achiral. The chiral objects consisted in CdSe nanoplatelets suspended in toluene functionalized with enantiomeric pure tartrate. They exhibit a strong chiral band near 532 nm as measured on a JASCO polarimeter (Figure 1(b)) and a strong PL at 565 nm. The PL signal of the nanoplatelets was modulated by the incident polarization at 532 nm, contrarily to rhodamine (Figure 1(c)). This result shows that CD-PL measurements allow detecting the difference in absorption rates of interband transitions in materials as a function of polarization by monitoring the photoluminescence intensity, i.e. at another wavelength. This allows decoupling in wavelength the CD absorption from the detection.

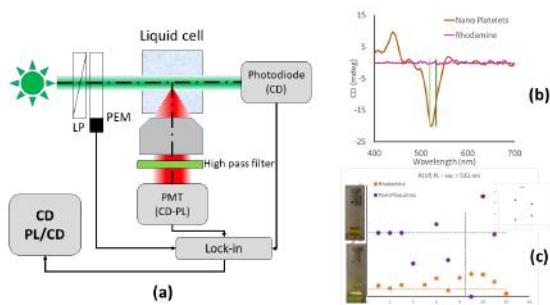


Figure 1: (a) schematic of the experimental setup. (b) CD measured on a JASCO polarimeter for rhodamine and functionalized nanoplatelets. (c) Amplitude of the intensity modulated at 50 kHz measured on the PL signal. The insets show the PL in the cuvettes illuminated at 532 nm.

Fig1.png

Novel ways to image the brain

Wednesday, 26th October - 13:30: Poster Session - Poster

Mr. Sam Crowther¹

1. *Living Systems Institute, University of Exeter*

Where MRI uses external stimuli to image the human body, the objective of this research is to use the emissions from cells to observe the function of the cell. Characterisation associated to metabolic activity, with associated shifts in wavelength through cellular activities has the potential to determine the stress a cell is experiencing. The emissions are classed as ultraweak therefore the high mitochondrial activity associated to the brain provides a basis for initial study utilising a living fossil as the common ancestor to establish practical detection mechanisms.

Effect of charging on electronic structure and plasmonic properties of derivatized anthracenes

Wednesday, 26th October - 13:30: Poster Session - Poster

Mr. Gokul Raj Mini Rajendran¹, Dr. Pavol Tisovský², Dr. Lukáš Félix Paštka³, Dr. Milan Sýkora⁴

1. Laboratory for Advanced Materials, Faculty of Natural Sciences, Comenius University, Ilkovičova 6, 841 04 Bratislava, **2.** Department of Organic Chemistry, Laboratory for Advanced Materials, Faculty of Natural Sciences, Comenius University, Ilkovičova 6, 841 04, **3.** Department of Physical and Theoretical Chemistry, Faculty of Natural Sciences, Comenius University, Ilkovičova 6, 841 04 Bratislava, **4.** Laboratory for Advanced Materials, Faculty of Natural Sciences, Comenius University, Ilkovičova 6, 841 04

Small Polycyclic Aromatic Hydrocarbons (PAHs), such as anthracene exhibit intense absorption in the visible region when charged. Recently it has been proposed that these absorption features can be explained in terms of molecular plasmon resonances [1]. Such resonances are possible in PAHs thanks to the delocalized nature of electrons in the $\pi-\pi^*$ orbitals. It was also shown that the extent of the plasmon character of the optical transitions can be quantified theoretically using the time-dependent density functional theory (TD-DFT) [2,3]. Although the basic principles of the plasmon effects in PAHs have been recently described, little is known about the effects of specific substitutions on the plasmonic properties of small PAHs. In the present work we synthesized series of anthracenes derivatized on the periphery with the carboxylic acid esters and bromine atom and investigated their optical properties in the neutral and charged state using electronic absorption spectroscopy and spectro-electrochemistry. We observed systematic changes in the absorption features of the charged compounds with the peripheral functionalization. The observed absorption features were analyzed with the aid of the TD-DFT modelling to quantify the plasmonic nature of the observed absorption features. The energy and the plasmonic nature of the optical transitions in the anthracene are highly sensitive to the nature of the peripheral substituent. The extent of this effect is quantified. This work was financially supported by the European Union's Horizon 2020 research and innovation program under grant agreement No. 810701, Slovak Research and Development Agency under grant agreement No. APVV-19-410 and Slovak Ministry of education under grant agreement No. 1/0892/21 and Comenius University grants for doctoral students and young scientists No. UK/432/2022.

References

- [1] Lauchner, A.; Schlather, A.E.; Manjavacas, A.; Cui, Y., McClain, M.J.; Stec, G.J.; García de Abajo, F.J.; Nordlander, P. and Halas, N.J. Molecular plasmonics. *Nano letters*, **2015**, 9, 6208.
- [2] Zhang, R.; Bursi, L., Cox, J.D., Cui, Y.; Krauter, C.M.; Alabastri, A.; Manjavacas, A.; Calzolari, A.; Corni, S.; Molinari, E. and Carter, E.A., How to identify plasmons from the optical response of nanostructures. *ACS nano*, **2017**, 7, 7321.
- [3] Langford, J.; Xu, X. and Yang, Y. Plasmon Character Index: An Accurate and Efficient Metric for Identifying and Quantifying Plasmons in Molecules. *J. Phys. Chem. Lett.*, **2021**, 12, 9391.

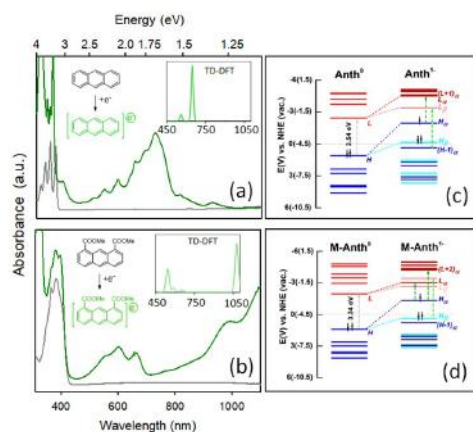


Figure 1. Effect of charging on the absorption spectra and the electronic structure of derivatized anthracenes. Experimental absorption spectra of the neutral (gray) and charged state (green) of anthracene (a) and methoxy anthracene (b). The inset shows the TD-DFT calculated spectra of the charged compounds. The panels (c) and (d) show the calculated molecular orbital diagrams of the neutral and charged compounds shown in (a) and (b).

Nanop figure final.jpg

Fano Resonances in Wire Metamaterials

Wednesday, 26th October - 13:30: Poster Session - Poster

Dr. David Fernandes¹, Mr. Francisco Faim¹, Dr. Sylvain Lannebère¹, Dr. Tiago A. Morgado¹

1. Instituto de Telecomunicações

Wire metamaterials have been one of the most studied metamaterial structures over the last two decades. This class of metamaterials consists of thin straight wires embedded in a dielectric host, and it possesses unique properties such as a strongly spatially dispersive response, extreme optical anisotropy, hyperbolic dispersion or even an anomalously high density of photonic states. In particular, the wire metamaterials offer an extraordinary ability to manipulate the electromagnetic field, permitting exotic wave phenomena such as negative refraction of light, subwavelength imaging, amongst many others.

Throughout the years some modifications of the original wire medium have been proposed and discussed. An interesting one consists of twisting the wires so that they become helical-shaped, originating a magnetic and bianisotropic response. It was also shown that having multiple wires per unit cell (nested wire medium) allows a metamaterial slab to exhibit sharp Fano resonances in its scattering properties. Because of their narrow asymmetric lineshape, Fano resonances can allow for strong selective response, therefore having promising applications in the development of novel types of sensors. The drawback of this configuration is that there must be a high level of structural asymmetry in the unit-cell, either by terminating one sub-set of wires with metallic patches or by using distinct materials in each sub-set. Such restriction can be detrimental to the fabrication process of a prototype, especially for high frequencies. Here, we propose a new configuration wherein both sets of wires are made of the same material and are severed at the interfaces of the slab. The structural asymmetry is ensured by considering one sub-set of wires straight and the other helical-shaped (Figure 1). We developed a homogenization model to study the effective response of the metamaterial, and theoretically and numerically demonstrate that the coupling between the two sub-arrays originates a sharp Fano resonance (Figure 2). The emergence of the resonance is linked to the interference between a narrow quadrupole-type resonance with a broad dipole-type resonance. We envision that the proposed nested wire medium may provide a robust scalable configuration for the experimental demonstration of the effect over a wide range of frequencies of operation.

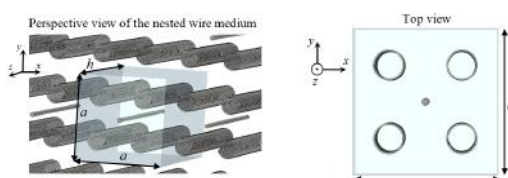


Figure 1.png

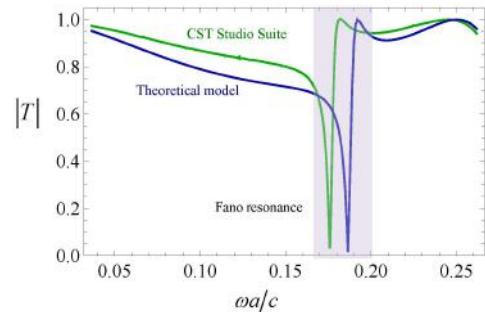


Figure 2.jpg

Label-free detection of virus with specificity by self-assembly single nanostructure

Wednesday, 26th October - 13:30: Poster Session - Poster

Dr. Yali Sun¹, Dr. Zeying Zhang², Prof. Meng Su², Prof. Yanlin Song², Dr. Dmitry Zuev¹

1. ITMO University, 2. Institute of Chemistry, Chinese Academy of Sciences

With the rapid development of nanotechnology, nanoscale optical detection plays essential roles in many areas that has become the forefront of nanophotonics. Among them, the nanostructures-based label-free methods offer great opportunities for improving the detection sensitivity, by virtue of the unique optical resonance characteristics.

However, the rapid, high-throughput and accurate detection of multiple clinical pathogens remains a great challenge, with the increasing complexity of the environment. The applicant has fabricated a series of one-dimensional micro/nanostructure arrays by using the nano-printing technology and have developed a general, label-free and visualized optical detection method at the nanoscale (Fig. 1). In this project, the multi-component optical metastructures can be fabricated at the single-particle level by combining the nano-printing technology and the colloidal self-assembly. After systematically exploring the regulation mechanism of the size, composition and the arrangement of building units on the scattering spectra of the optical metastructures, it enables to construct the simplest optical metastructures with ultrasensitive environment response. Moreover, these optical metastructures have strong local field enhancement that can significantly improve the sensitivity for detecting pathogens. Combined with surface functionalization, it allows for amplification-free detection and recognition of many pathogens with high specificity and stability.

This technology paves the way for the development of the next generation of noninvasive diagnostic and companion diagnostic tests for diseases.

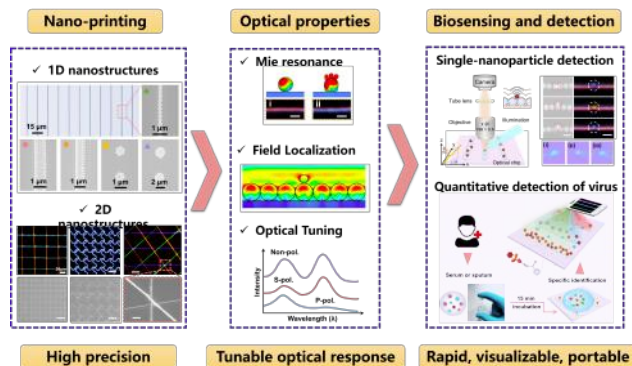


Fig1.png

Superfluorescence from Mie-resonant lead halide superlattices

Wednesday, 26th October - 13:30: Poster Session - Poster

Mr. Pavel Tonkaev¹

1. School of Physics and Engineering, ITMO University

Introduction

Lead halide perovskites possess outstanding optoelectronic properties and present a new class of promising materials been applied as light-emitting devices and solar cells. Perovskite nanocrystals have a high quantum yield of photoluminescence, which makes them a perfect candidate as an optical nanosource. By self-assembling these nanocrystals can form ordered three-dimensional arrays also known as superlattices. Due to a relatively high refractive index of lead halide perovskites, the application of Mie resonances can enhance different processes in nanoparticles. In this work, we study the photoluminescence properties of lead halide superlattices supporting Mie resonances in the optical range.

Methods and Materials

The CsPbBr₃ nanocrystals were obtained by the hot injection method. The synthesized nanocrystals were separated by centrifugation and dispersed in toluene to obtain a colloidal solution for superlattices to be formed. The photoluminescence spectra of the samples were measured using a pump provided by a femtosecond laser with the wavelength of 400 nm for the temperature of 6 K. The 150 fs pulses with a repetition rate of 100 kHz were focused onto the sample surface at normal incidence by a 50x microscope objective.

Results and Discussion

We have studied emissions from separated lead halide perovskites spherical superlattices with diameters from 200 nm to 400 nm at the temperature of 6K. All nanoparticles demonstrated two peaks in photoluminescence spectra. For the nanoparticle with 250 nm radius, the low energy peak is located at 2.39 eV, whereas the high energy peak is located at 2.355 eV. With the increase in particle size, both maxima demonstrate redshift and for the nanoparticle with 380 nm radius, the positions of the maxima are 2.387 eV and 2.338 eV, respectively. We attribute this shift to the polaritonic effect in such an ordered array of quantum dots, which was theoretically described earlier. Our experimental results have good agreement with the theoretical calculations based on the model mentioned. Notably, with temperature increase, the maxima get closer and merge at the temperature of 200 K due to decrease in exciton oscillator strength.

Acknowledgment

This work was performed with financial support of the Russian Science Foundation (project No. 22-22-20077)

Mueller Matrix Ellipsometry for accurate metrology of arrays of Au patches supporting Gap Surface Plasmons

Wednesday, 26th October - 13:30: Poster Session - Poster

Mr. Per Walmsness¹, Mr. Nathan Hale¹, Prof. Morten Kildemo¹

¹. Department of physics, NTNU, Trondheim, Norway

Spectroscopic Mueller Matrix Ellipsometry (MME) is a technique that measures all changes in polarization state of incidence late upon reflection from a sample or transmission through a sample. We have here performed MME at conical incidences (specular reflection at all azimuthal angles of incidence by rotating the sample), of arrays of Au particle patches on a SiO₂ spacer backed by optically thick gold. This type of structure is important with applications to absorber materials, structural colors, sensing, and particularly promising as an important unit in the design of efficient reflective metasurface components [1,2].

The goal of this work is to complement the understanding of the physics and response of this structure through high quality MME measurements of accurately manufactured structures (using Electron Beam Lithography), in addition to enable tight control and monitoring in the manufacture of a new generation of optical components based on metasurface-designs.

Gap surface plasmon (GSP) resonances supported by the array, as well as resonances related to Rayleigh anomalies, were mapped out by full azimuthal rotation of the sample. The experimental data was modelled with the finite element method, and the model was used to identify the main resonances observed in the optical response. The oxidation of Ti-adhesion layers used in the manufacture process causes the optical response to drift significantly in time, and it is thus important to include the adhesion layers when modelling and designing devices based on similar resonators.

We further demonstrate an extreme sensitivity of the Mueller matrix elements to the particle dimensions.

References

[1] P. M. Walmsness, N. Hale and M. Kildemo (2021). JOSA B **38** (2021): 2551-2561.

[2] P. M. Walmsness, N. Hale and M. Kildemo Opt. Lett. **47** (2022): 158-161.

Hyperbolic Meta-Antennas for Light-Matter Interaction Engineering

Wednesday, 26th October - 14:30: Metamaterials and metasurfaces - Oral

Mrs. Sema Ebrahimi¹, Mrs. Sema Ebrahimi², Dr. Alina Muravitskaya³, Dr. Ali Adawi³, Dr. Anne-Laure Baudrion¹, Prof. Pierre-Michel Adam¹, Dr. Jean-Sebastien Bouillard²

1. Light, nanomaterials, nanotechnologies (L2n) Laboratory, CNRS EMR7004, University of Technology of Troyes, F-10004

Troyes Cedex, France, **2.** Department of Physics and Mathematics, University of Hull, Cottingham Road, HU6 7RX, UK, **3.**

Department of Physics and Mathematics, University of Hull, Cottingham Road, HU6 7RX, UK

Hyperbolic Metamaterials are described as an emerging class of highly anisotropic plasmonic materials, providing electromagnetic properties on-demand. Based on their hyperbolic optical dispersion curves, hyperbolic metamaterials can support the propagation of high-k modes and represent a significant increase in the photonic density of states to engineer light-matter interactions [1, 2]. Here, we introduce a hyperbolic meta-antenna based on the multilayer Au/ TiO₂ bowtie nanostructures, supporting a type II hyperbolic dispersion. Effective medium theory (EMT) was used to calculate the effective index and optical responses of the hyperbolic meta-antennas.

We provide a detailed study of the physical mechanisms underlying the meta-antenna optical response. Using electric and magnetic field distributions, both in-plane and out-of-plane, we identify two different modes supported by the multilayer antennas. We find that one mode is purely scattering while the other has a purely absorptive nature (Fig. 1b). The main scattering mode originates from the bonding electric dipolar modes between the two elements of the antenna (Fig. 2b), similar to the pure gold corresponding antenna (Fig. 2a). On the other hand, the absorptive mode at longer wavelengths is absent from the pure gold geometry and solely supported by the meta-antenna (Fig. 2c). Using the field distributions, we propose that this second mode arises from the excitation of magnetic dipolar modes in the meta-antenna.

Additionally, by tuning the metal filling factor in the meta-antenna multilayer system, we obtain full control over the intensity, spectral separation, and ratio of the scattering and absorption modes covering the visible and infrared regions (Fig. 3). The proposed hyperbolic meta-antennas are highly promising for applications in optical sensors, sub-wavelength meta-cavity lasers, photocatalysis, and hot-electron generation processes.

References

- [1] Poddubny, A., Iorsh, I., Belov, P., & Kivshar, Y. (2013). Hyperbolic metamaterials. *Nature photonics*, 7(12), 948-957.
- [2] Maccaferri, N., Zhao, Y., Isoniemi, T., Iarossi, M., Parracino, A., Strangi, G., & De Angelis, F. (2019). Hyperbolic meta-antennas enable full control of scattering and absorption of light. *Nano letters*, 19(3), 1851-1859.

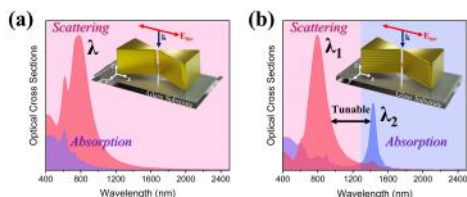


Fig. 1 optical cross sections of a single au nanoantenna and b hyperbolic meta-antenna.jpg

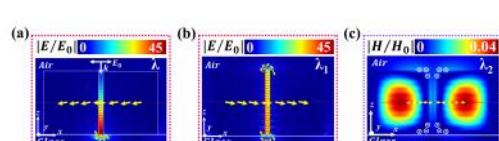


Fig. 2 a b electric near field profiles of scattering modes c magnetic field distribution of absorptive mode.jpg

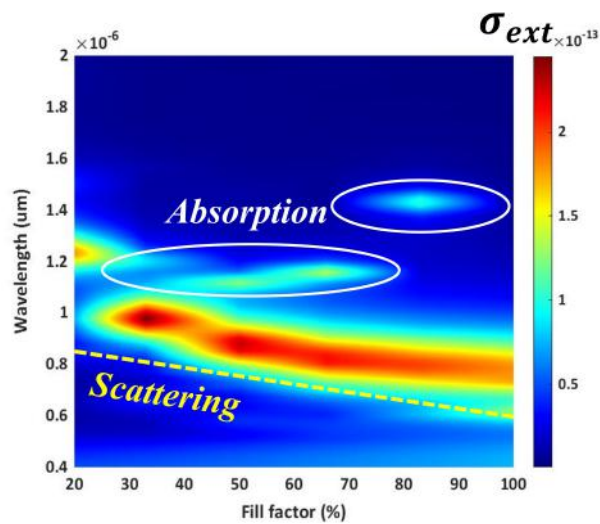


Fig. 3 tunability of the scattering and absorption modes as a function of au fill factor.jpg

Amplified spontaneous emission in CsPbBr₃ decorated metasurfaces

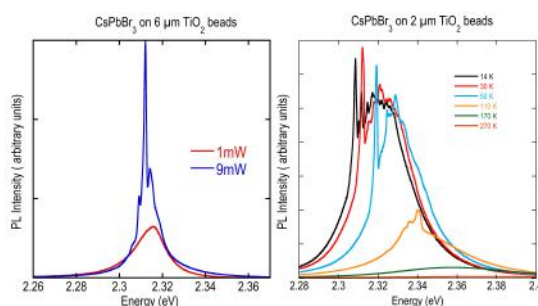
Wednesday, 26th October - 14:47: Metamaterials and metasurfaces - Oral

Dr. Giammarco Roini¹, Mr. Gabriele Calusi², Prof. Ivano Alessandri¹, Prof. Anna Vinattieri³

1. Department of Information Engineering, University of Brescia, via Branze 38, Brescia, Italy., **2.** Department of Physics and Astronomy University Florence, **3.** Department of Physics and Astronomy University Florence

Halide perovskites are extremely interesting semiconductors for innovative optoelectronics devices and sensors. In particular, being direct band-gap semiconductors, they are efficient emitters of both incoherent and coherent light [1]. Therefore the possibility of use as active medium in lasers, light amplification systems (resonators and waveguides) and other photonic devices is driving a large part of research in these years [2]. Among inorganic halide perovskites, CsPbBr₃ is of interest because of its efficient green emission (≈ 2.3 eV) which makes it a valid substitute of indium-gallium nitrides to solve the green gap problem. In this contribution we present experimental results concerning the light emission in a set of CsPbBr₃ films deposited, by spin-coating, on a silicon substrate and on metasurfaces realized by micro/nanospheres having a core of SiO₂ and a shell of TiO₂ (T-Rex) on a silicon substrate [3]. Samples were excited after continuous wave laser excitation at 405 nm and with 300 ps long pulses at 266 nm. We investigate both the linear regime, typical of photoluminescence, and the non-linear regime bringing clear evidence of the presence of Amplified Stimulated Emission (ASE) up to 200 K in a back-scattering geometry without the need of a waveguide configuration (see Figure_PL_and_ASE_CsPbBr₃). Depending on the sample structure and increasing the excitation density a transition from the superlinear regime to a linear/sublinear regime is revealed. The significant differences found between samples, differing in their morphology, allow to distinguish between an amplification due to randomly arranged emitters and an amplification due to quite ordered nanocrystals. In particular an enhancement of the photoluminescence and ASE is found when nanocrystals are arranged on the T-Rex indicating a major role played by the metasurfaces in the light extraction.

- [1] X. Li et al.: “All inorganic halide perovskites nanosystem: Synthesis, structural features, optical properties and optoelectronic applications”, Small 13, 1603996 (2017).
- [2] see “Halide Perovskites for Photonics”, edited by A. Vinattieri and G. Giorgi (AIP Publishing, New York, 2021).
- [3] I. Alessandri, “Enhancing raman scattering without plasmons: Unprecedented sensitivity achieved by TiO₂ shell-based resonators”, Journal of the American Chemical Society 135, 5541–5544 (2013)



Pl and ase cspbbr3.png

Metasurfaces integration for high field of view and ultrafast LiDAR

Wednesday, 26th October - 15:04: Metamaterials and metasurfaces - Oral

Mr. Emil Marinov¹, Dr. Renato Juliano Martins¹, Mr. Aziz Ben Youssef¹, Dr. Patrice Genevet¹

1. CRHEA CNRS

Among 3D computer vision techniques, Light Detection and Ranging (LiDAR) is currently considered at the industrial level for robotic vision. LiDAR is an imaging technique that sends and recovers pulses of light at optical frequencies to sense the space and to recover three-dimensional ranging information. Notwithstanding the efforts on LiDAR integration and optimization, commercially available devices in general have slow frame rate and low image resolution, notably limited by the performance of mechanical or slow solid-state deflection systems. Metasurfaces (MS) are versatile optical components that can distribute the optical power in desired regions of space. Here, we report on an advanced LiDAR technology that uses ultrafast low FoV deflectors cascaded with large area metasurfaces to achieve large FoV and simultaneous peripheral and central imaging zones.

The proposed device relies on the ultra-fast beam deflection capabilities of an Acousto-Optical Deflector, coupled to a passive deflecting metasurface that is used as a beam angle expander to achieve 6 MHz scanning speed, within an extremely large FoV (up to 150° on both vertical and horizontal scanning axes). By exploring the versatility of MS, we were able to mimic the human vision capabilities by simultaneously scanning two field of views simultaneously, one with a high resolution in the central area (mimicking the fovea region) and a second with a much larger field of view for the peripheral image. Random access scanning is also demonstrated, giving the possibility to explore advanced smart scanning schemes. Finally, a pulse encoding technique is implemented to suppress the idle listening time and the signal aliasing responsible of undesired ghost imaging. We show that the implementation of this CDMA technique further improves the speed performances of the LiDAR by a factor of 2. The use of a matched filter to recover the Time-of-Flight extends the SNR regime of work of the by 3 dB as compared to simple peak detection. The use of this disruptive LiDAR technology with advanced learning algorithms offers perspectives to improve further the perception capabilities and decision-making process of autonomous vehicles and robotic systems.

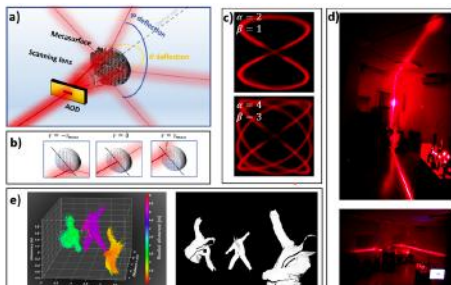


Figure 1 **a)** Detail of the scanning module of the proposed LiDAR, composed of an acousto-optic deflector (AOD) cascaded with a metasurface. The AOD provides an ultrafast light scanning with low FoV ($\sim 2^\circ$). The deflected beam is directed to a scanning lens to scan the laser spot on the metasurface at different radial and azimuthal positions. The transmitted light across the metasurface is deflected according to the position of the impinging beam on the component to cover a scanning range between -75° and 75° . **b)** Representations of beam deflection according to the incident beam positioning on the metasurface. **c)** Lissajous scanning using deflecting functions as $\theta = \text{Asin}(\alpha t + \Psi)$ and $\phi = \text{Bsin}(\beta t)$ for different parameters α and β to illustrate the random laser projection capabilities on a fast beam scanning in a large FoV configuration. **d)** LiDAR line scanning of our laboratory room that show the large FoV on both Elevation (top) and Azimuth (bottom) angles. Note: the top picture showing a scanning line profile covering the whole range from the ground to the ceiling of the testing room over 150 degrees. **e)** 3D ranging demonstration (left): the scene (right) was setup with actors wearing reflective suits positioned in the scene at distance z varying from 1.2 to 4.9m.

Ms lidar principle and results.png

Cascaded-mode optics: generalizing near-field optical design and optical resonators

Wednesday, 26th October - 15:21: Metamaterials and metasurfaces - Oral

Prof. Vincent Ginis¹, Prof. Ileana-Cristina Benea-Chelmu², Dr. Jinsheng Lu³, Dr. Marco Piccardo⁴, Prof. Federico Capasso³

1. Vrije Universiteit Brussel, 2. École Polytechnique Fédérale de Lausanne (EPFL), Lausanne, Switzerland, 3. Harvard University, 4. Istituto Italiano di Tecnologia

In this contribution, we introduce the theory of cascaded-mode optics and show its usability in two important applications.

The core mechanism behind cascaded-mode optics is to create optical devices where an incoming light beam interacts with different components multiple times so that the output of one component becomes the input of another. In this way, the same element can interact with the light several times and have different functionality each time.

First, we show that our theory allows for shaping the near field of electromagnetic waves using remote wave interference. We demonstrate how to structure the longitudinal and transverse variation of the near field, allowing for distributions beyond the conventional monotonic decay of the evanescent field. We provide an experimental realization that confirms our theory. Our method can be applied to fields with multiple polarization states, frequencies, and higher-order spatial mode profiles. It is a new path towards unprecedented three-dimensional control over the properties of the electromagnetic field.

Second, we introduce a new class of optical resonators. In these devices, cascaded-mode resonances exist by designing the optical path through transverse mode coupling facilitated by mode-converting mirrors. The generalized round-trip phase condition leads to resonator characteristics that are different from Fabry-Perot resonators. We show the transmission spectrum of fabricated cascaded-mode resonators and demonstrate that its engineered spectral properties agree with the theory. Cascaded-mode resonators introduce properties not found in traditional resonators and provide a mechanism to overcome the existing resonator trade-offs.

The implications of cascaded-mode optics on optical design potentially permeate all areas of photonics.

Infrared Plasmons in Ultrahigh Conductive PdCoO₂ Metallic Oxide

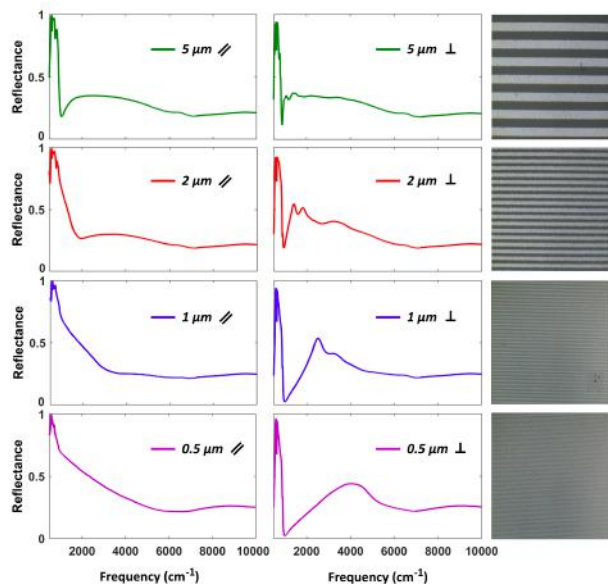
Wednesday, 26th October - 15:38: Metamaterials and metasurfaces - Oral

Dr. Salvatore Macis¹, Dr. Luca Tomarchio¹, Prof. Stefano Lupi¹

1. Sapienza University of Rome

PdCoO₂ layered delafossite is the most conductive compound among metallic-oxides, with a room-temperature resistivity of nearly $2\mu\Omega\text{cm}$, corresponding to a mean free path of about 600\AA [1]. These values represent a record considering that the charge density of PdCoO₂ is three times lower than copper. Despite its notable electronic transport properties, PdCoO₂ collective charge density modes (i.e. surface plasmons) have never been investigated, at least to our knowledge. In this work, we studied surface plasmons in high-quality PdCoO₂ thin films, patterned in the form of micro-ribbon arrays[2]. By changing their width W and period 2W, we select suitable values of the plasmon wavevector q, experimentally sampling the surface plasmon dispersion in the mid-infrared electromagnetic region. Near the ribbon edge, we observe a substantial field enhancement due to the plasmon confinement, indicating PdCoO₂ as a promising infrared plasmonic material[2].

1. Brahlek, M. et al. Growth of metallic delafossite PdCoO₂ by molecular beam epitaxy. *Phys. Rev. Mat.* 3, 093401 (2019).
2. Macis, S., Tomarchio, L., Tofani, S. et al. Infrared plasmons in ultrahigh conductive PdCoO₂ metallic oxide. *Commun Phys* 5, 145 (2022).



Merge grid.png

Tuning of the quasi-trapped mode response of dielectric metasurfaces

Wednesday, 26th October - 15:55: Metamaterials and metasurfaces - Oral

Dr. Andrey B. Evlyukhin¹

1. Leibniz University Hannover

A general strategy for the theoretical tuning of quasi-trapped modes of dielectric metasurfaces composed of nanoparticles with resonant electric and magnetic dipole responses is presented. The developed strategy is based on two stages: the application of the dipole approximation for determining the conditions required for the implementation of a trapped mode at certain spectral positions and then the creation of the energy channel for its excitation by external radiation. Since excitation of trapped modes results in a concentration of electric and magnetic energies in the metasurface plane, the tuning provides possibilities to obtain and control the localization and distribution of optical energy at the sub-wavelength scale and at a required spectral range. A practical realization for spectral tuning of quasi-trapped modes in metasurfaces composed of nanoparticles with a preselected shape is demonstrated [1].

[1] A. B. Evlyukhin, M. A. Poleva, A. V. Prokhorov, K. V. Baryshnikova, A. E. Miroshnichenko, and B. N. Chichkov. *Laser & Photonics Rev.* 15, 2100206 (2021).

Angle-resolved optical properties of the regular arrays of diamond-shaped silver nano-particles

Wednesday, 26th October - 14:30: Bottom-up approach enabled nanophotonics - Oral

Dr. Iryna Gozhyk¹, Mr. Leo Laborie¹, Dr. Paul Jacquet¹, Dr. Barbara Bouteille¹, Dr. Jeremie Teisseire¹, Dr. Rémi Lazzari², Dr. Jacques Jupille², Dr. Philippe Gogol³, Dr. Beatrice Dagens³

1. Surface du Verre et Interfaces, UMR 125 CNRS/Saint-Gobain Recherche, **2.** CNRS, UMR 7588, Institut des NanoSciences de Paris, **3.** C2N, UMR 9001 CNRS / Université Paris-Saclay

Surface lattice resonances are plasmonic modes related to the long-range interactions within the regular arrays of plasmonic nano-particles. These resonances result in the sharp features in the optical spectra of plasmonic nano-composite films, while their wavelength can be tuned through lattice constant and the surrounding medium providing a high potential for near-field sensing applications. Such sharp features in optical spectra of systems with regular surface or volume corrugations can also be a signature of mere grating anomalies. In order to distinguish the surface lattice resonances and grating anomalies in optical spectra, it is necessary to analyze the angle-resolved optical spectra both in reflection and transmission. This task is of tremendous computational difficulty especially for arrays of large nano-particles of non-spherical shape in non-homogeneous environment. Meanwhile, the angle-resolved experimental analysis requires cm-scale arrays of nano-particles and is thus prohibited for several fabrication techniques. Finally, it is virtually impossible to (i) compute the optical properties of the arrays accounting for the exact shape of the nano-particles and the presence of the defects; or to (ii) fabricate the cm-scale nano-composite samples perfectly corresponding to the simplest model system from the computational point of view. In this work we suggest a different approach: experimental study of the angle-resolved optical reflection and transmission of quasi-regular arrays of silver nano-particles on the surface with perfectly regular corrugations.

The provided experimental analysis includes the impact of the polarization of incident light and of the lattice constant on the optical properties of quasi-regular arrays of silver diamond-shaped nano-particles half-embedded into silica substrate, as well as the random arrays of supported truncated sphere-shaped silver nano-particles. We report the presence of sharp features related to grating anomalies (Wood anomalies of I type) and surface lattice resonances (Wood anomalies of II type) of a larger width.

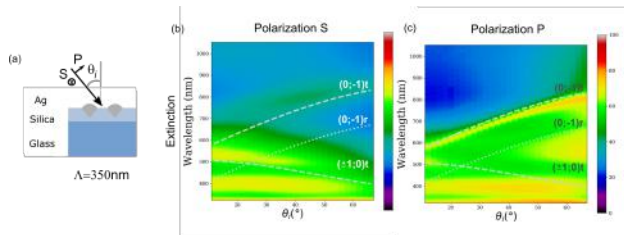


Figure.png

DNA-templated ultracompact optical antennas for unidirectional single-molecule emission

Wednesday, 26th October - 14:45: Bottom-up approach enabled nanophotonics - Oral

Mr. Fangjia Zhu¹, Dr. María Sanz-Paz¹, Dr. Mauricio Pilo-Pais¹, Prof. Antonio I. Fernández-Domínguez², Prof. Fernando Stefani³, Prof. Guillermo Acuna¹

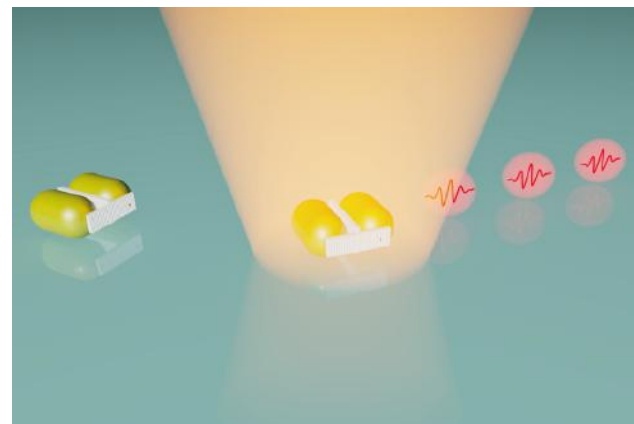
1. University of Fribourg, **2.** Departamento de Física Teórica de la Materia Condensada and Condensed Matter Physics Center (IFIMAC), Universidad Autónoma de Madrid, E28049 Madrid, Spain, **3.** Universidad de Buenos Aires

Optical antennas are nanostructures designed to manipulate light-matter interactions by interfacing propagating light with localized electromagnetic field. Numerous devices have been realized to efficiently tailor the absorption and/or emission rates of fluorophores, but modifying the spatial distribution of their radiation fields remains challenging. In this regard, optical directional nanoantennas based on a Yagi-Uda design have been demonstrated in the visible range ¹. Despite this impressive proof of concept, their overall size ($\sim\lambda^2/4$) and considerable number of elements represent obstacles for the exploitation of these antennas in nanophotonic applications and for their incorporation onto photonic chips.

In order to reduce the size further, several theoretical schemes of ultracompact antennas combined with single emitters have been proposed. However, experimental realization of these designs has remained elusive, since gaps between antenna elements in the range of $\lambda/10$ are required, complicating nanofabrication. Furthermore, excitation of such ultracompact antennas in the right resonant mode to obtain unidirectionality requires positioning of a single emitter with nanometric precision.

Here, we experimentally validate a directional ultracompact antenna design ², which is based on a gold nanorod dimer adapted from the geometry proposed by Pakizeh ³. The design consists of two side-by-side gold nanorods self-assembled via a T-shaped DNA origami, which also controls the positioning of the single fluorophore. Through back focal plane measurements, we confirm that the excitation of the antiphase mode of the antenna by a nanoemitter placed in its near-field can lead to directional emission of fluorophore. Furthermore, in order to verify the feasibility of this design, we numerically investigate the effect on the directionality of several parameters, such as the shape of the nanorods, possible defects in the dimer assembly, and different positions and orientations of the nanoemitter ⁴. Overall, the proposed ultracompact nanorod dimer design provides a new possibility to further study antenna-assisted directional single-photon sources for integrated photonic chips and biosensors.

1. Curto, A. G. *et al. Science* **2010**, 329 (5994), 930-933.
2. Zhu, F. *et al. Nano Lett* **2022**, 22 (15), 6402-6408.
3. Pakizeh, T.; Käll, M. *Nano Letters* **2009**, 9 (6), 2343-2349.
4. Zhu, F. *et al. Nanomaterials* **2022**, 12 (16).



Directional ultracompact antenna on the glass surface.png

A quantum circuit architecture by integrating nanophotonic devices and two-dimensional molecular network

Wednesday, 26th October - 15:00: Bottom-up approach enabled nanophotonics - Oral

Dr. Wei Wu¹

1. University College London

Introduction

Recently spin-bearing molecules have experimentally been demonstrated to have great potentials as building blocks for quantum information processing due to their tunability, portability and scalability. [1] Especially the optically addressable spin-bearing molecules are even more attractive for building quantum circuit architectures for high-temperature operations. [2,3] Nanophotonic devices are important to program the quantum circuit. However, up to now, it is still elusive to even design quantum circuit of this type.

Method

In this work, we have used hybrid-exchange density-functional theory to compute the exchange interactions [2], and performed the analysis for the time evolution of quantum states and the time-resolved electron paramagnetic spectra by using theory of open quantum systems [3].

Results and Discussion

We proposed a quantum computing architecture, by combining the two-dimensional molecular networks with nanophotonic devices. Our design is based on (1) rigorous density functional theory calculations validated by the relevant experimental observations [4] and (2) an open quantum system simulation of the time-resolved electron paramagnetic resonance spectra with realistic experimental parameters. We take the biTYY-DPA molecule (Fig.1) as an example to compute the triplet-mediating exchange interaction between radicals [4]. The resulting optically driven ferromagnetic interaction, computed using hybrid-exchange density functional, is consistent with the previous experiments. We have also computed the time evolution of quantum states when the triplet was present and found that coherence between radicals can be created by using the excited triplet, as indicated by the non-zero off-diagonal terms in the reduced density matrix for radicals (Fig.2). Furthermore, we have designed the quantum circuit by integrating two-dimensional spin-bearing molecular network and nanophotonic devices such that we can realise programmable quantum gate operations (Fig.3).

Conclusions

This work would therefore lay a solid theoretical cornerstone for optically driven quantum computing circuit in radical-bearing molecular network, thus towards high-temperature quantum information processing. In this way, we can not only scale up substantially the quantum circuits but also raise the operation temperature.

References:

- [1] S. L. Bayliss, et. al., Science 307, 309 (2020).
- [2] J. Chang, et. al., arXiv: 2209.04835 (2022).
- [3] L. Ma, et. al., NPG Asia Materials, 14:45 (2022).
- [4] Y. Teki, et. al., J. Am. Chem. Soc. 122 984 (2000)

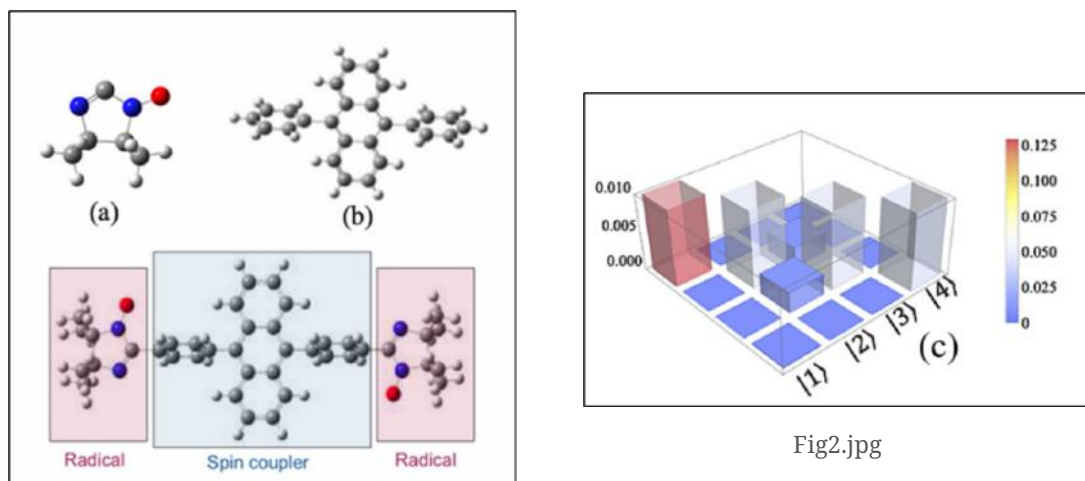


Fig1.jpg

Fig2.jpg

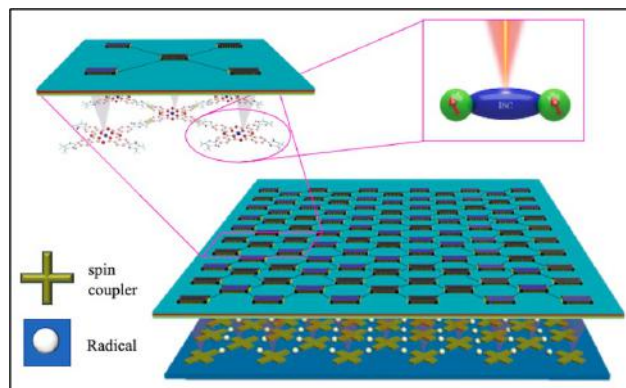


Fig3.jpg

Semiconductors nanocrystals in microcavity for microlasers development

Wednesday, 26th October - 15:15: Bottom-up approach enabled nanophotonics - Oral

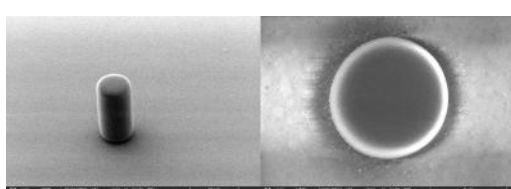
Mr. Charlie Kersuzan¹, Mr. Sergei Celaj¹, Dr. Thomas Pons², Prof. Agnes Maitre¹

1. Institut des NanoSciences de Paris - Sorbonne Université, 2. Laboratoire de Physique et d'Etude des Matériaux - ESPCI

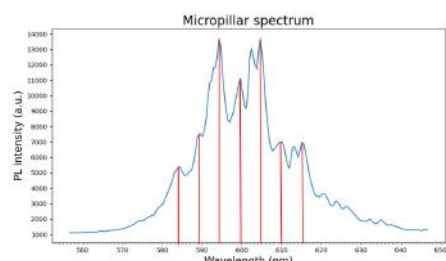
Microcavities and microlasers are being actively developed for a variety of applications. Microcavities provide an important optical confinement and strong light-matter interactions. Microlasers can be used as light sources integrated in photonic circuits, but also for biological detection. Their fabrication process is however generally complex and costly. Here we present the fabrication by optical lithography and the characterization of microcavities loaded with semiconductor nanocrystals (scNCs) as gain media. Indeed, scNCs possess interesting optical properties, such as stable emission tunable in the entire visible and near infrared range. Recent works have also shown the efficiency of scNCs as gain media with low stimulated emission thresholds.

A first critical step consists in modifying the surface chemistry of scNCs to make them chemically compatible with SU8, a negative photoresist with a high refractive index, which is transparent in the visible range and with very low roughness, leading to high quality factors. A 405nm laser is used for photolithography. Exposure by direct focusing of the laser on the sample allows to produce resin cylinders of a few microns in diameter. Precise control of the size and height of the pillars is achieved by controlling the laser focus and the energy delivered to the resin (laser power and exposure time). A solution of chemically modified scNCs is used to infuse the micropillars with scNCs. Under external excitation, the emission of scNCs near the air/cavity interface is trapped by total internal reflection in the whispering gallery modes of the circular cavity. The spectra of the micropillars are obtained by confocal fluorescence microscopy and show peaks corresponding to the gallery modes. Optimization of different parameters such as pillar size, concentration and dissolution of nanocrystals allows to improve the quality factor of these gallery modes.

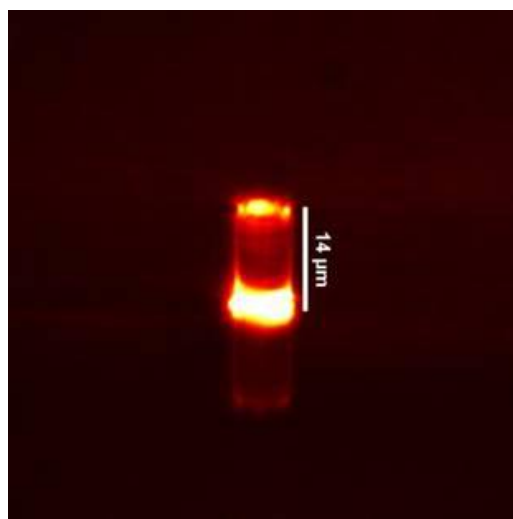
The easy fabrication of high quality, scNCs doped micropillars, will enable us to obtain microlasers, with low laser threshold, lower cost, opening the way to cheap and highly sensitive biological detection methods.



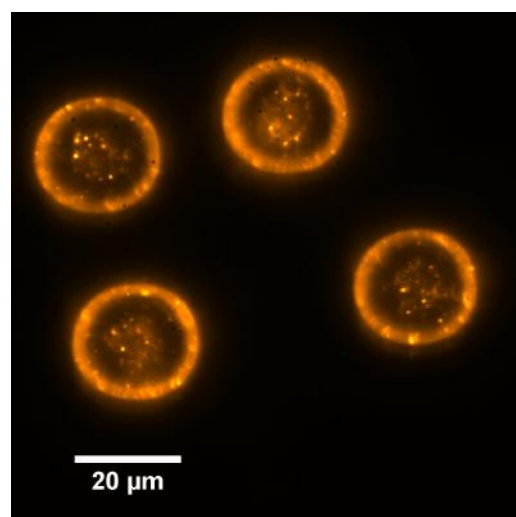
Sem-image-of-a-micropillar.jpg



Microcavity-spectrum.png



Side-view-fluorescence-image-of-a-micropillar.jpg



Fluorescence-image-of-micropillars.jpg

Size-dependent Electronic Properties of Strongly Confined Graphene Quantum Dots

Wednesday, 26th October - 15:30: Bottom-up approach enabled nanophotonics - Oral

Dr. Milan Sýkora¹

1. Laboratory for Advanced Materials, Faculty of Natural Sciences, Comenius University, Ilkovičova 6, 841 04 Bratislava

Using a systematic bottom-up step-wise synthesis we prepared uniform ensembles of small (<2 nm) Graphene Quantum Dots (GQDs) adsorbed on optically transparent, conductive, metal oxide surfaces and investigated the effect of quantum confinement on the electronic structure using optical, electrochemical and spectro-electrochemical methods. Using these techniques, we experimentally show how the bandgap, valence and conduction band offsets, exciton binding energies and densities of states systematically vary with the size of these strongly confined GQDs. The interpretation of the experimental results is supported by detailed DFT modelling. Experimental results indicate that the standard Dirac fermion model and tight-binding modelling approach do not adequately describe the electronic properties of GQDs in the strongly confined regime, which is attributed to stronger carrier-carrier interactions in the GQDs compared to the bulk graphene. Raman spectroscopy studies reveal that even the small GQDs show key D and G spectral features characteristic for periodic graphene structures and that the variation in the ratios of the corresponding band intensities (I_D/I_G) with the GQD size is in good agreement with previous studies of highly defected large area graphenes. This work was financially supported by the European Union's Horizon 2020 research and innovation programme under grant agreement No. 810701, Slovak Research and Development Agency under grant agreement no. APVV-19-410, Slovak Ministry of education under grant agreement No. 1/0892/21, and by the Los Alamos Laboratory Directed Research and Development (LDRD) Program.

References.

- [1] Ji, Z.; Dervishi, E.; Doorn, S. K.; Sykora, M. Size-Dependent Electronic Properties of Uniform Ensembles of Strongly Confined Graphene Quantum Dots. *J. Phys. Chem. Lett.*, **2019**, *10*, 953-959.
- [2] Dervishi, E.; Ji, Z.; Htoon, H.; Sykora, M.; Doorn, S. K. Raman spectroscopy of bottom-up synthesized graphene quantum dots: size and structure dependence. *Nanoscale*, **2019**, *11*, 16571-16581.
- [3] Ji, Z.; Doorn, S. K.; Sykora, M. Electrochromic Graphene Molecules. *ACS Nano*, **2015**, *9*, 4043-4049.
- [4] Ji, Z.; Wu, R.; Adamska, L.; Velizhanin, K. A.; Doorn, S. K.; Sykora, M. In-Situ Synthesis of Graphene Molecules on TiO₂: Application in Sensitized Solar Cells. *ACS Appl. Mater. Interfaces*, **2014**, *6*, 20473-20478.

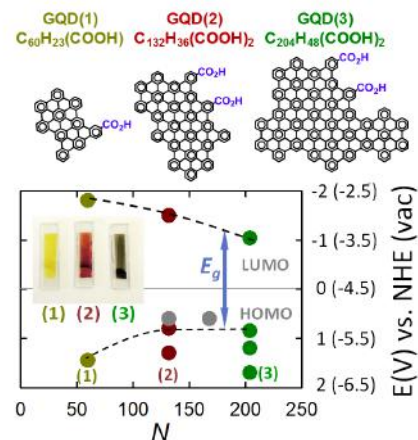


Figure 1. Examples of the strongly confined GQDs prepared by a new “bottom up” synthesis approach and the experimentally determined dependence of the electronic structure on their size.

Figure 1.png

Coupling of strain-induced single-photon emitters in a MoSe₂ monolayer to a low-loss plasmonic waveguide

Wednesday, 26th October - 14:30: Quantum nano-optics - Oral

Mr. Paul Steinmann¹, Mr. Yuhao Zhang¹, Mr. Hans-Joachim Schill¹, Prof. Stefan Linden¹

¹. University of Bonn

Introduction

Monolayers of transition metal dichalcogenides (TMDCs) host excitons with binding energies of several 100 meV. Strain can locally disturb the band structure of the monolayer resulting in the formation of trap states that act as single photon emitters. Here, we report on the coupling of strain-induced single photon emitters in a MoSe₂ monolayer to low loss plasmonic waveguides.

Methods

We used electron beam lithography with the negative-tone resist Medusa82 to fabricate dielectric loaded surface plasmon polariton waveguides (DLSPPWs) on top of a chemically prepared monocrystalline silver platelet. Additional gratings placed at the ends of the waveguides serve as in- and out-coupling structures. A MoSe₂ monolayer was deposited on the centre of one of the waveguides by a dry-transfer technique.

Results and Discussion

Surface plasmon polaritons (SPPs) are launched by a green laser at the input port of the waveguide (see Fig. 1(a)). The SPPs propagate along the waveguide and excite the monolayer. A part of the exciton emission, as well as the emission from the strain induced single photon emitters, couples back to the waveguide and is collected after out-coupling at the exit port.

Fig. 1(b) depicts an optical micrograph of the sample overlaid with photoluminescence images recorded at the two ends of the waveguide as well at the monolayer position at a sample temperature of 4K. The observed photoluminescence shows that the monolayer can be excited via the waveguide and that the monolayer emission couples back to the waveguide. Fig. 1 (c) depicts the photoluminescence spectrum recorded at the exit port and at the bare flake. In addition to the exciton and trion signal, we observe sharp emission lines that we attribute to strain-induced trap states. The second order correlation function of one of the spectrally filtered emission lines was measured with a HBT-setup. The measured value $g^{(2)}(0)=0.4$ indicates the single-photon nature of the emitter.

Our experiments indicate that TMDC monolayers in combination with low loss plasmonic waveguides are an attractive platform for nanophotonic circuits with integrated single-photon sources.

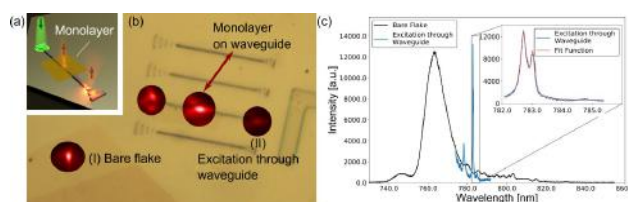


Fig1.jpg

An integrated single photon source at room temperature

Wednesday, 26th October - 14:47: Quantum nano-optics - Oral

Dr. Christophe Couteau¹

1. University of Technology of Troyes

The integration of a single photon source made of solid-state emitters with photonics structures remains to this day a challenging operation. It is however of prime importance to do so for quantum technologies where single photon sources constitute building blocks for many technologies and in particular for quantum photonics. In this work, we demonstrate a new way of integrating a single photon source, in our case made of a single colloidal semiconductor nanocrystal, with a photonics structure made of a glass waveguide obtained by the ion-exchange technique. We demonstrate the integration of a single photon source at room temperature and this is to pave the way towards more relevant emitters such a single colour centre in a single nanodiamond.

Directed and enhanced photoluminescence of quantum nanoemitters using all-dielectric nanostructures

Wednesday, 26th October - 15:04: Quantum nano-optics - Oral

Dr. Romain HERNANDEZ¹, Dr. Mélodie Humbert¹, Dr. Peter Wiecha², Dr. Franck Fournel³, Dr. Vincent Larrey³, Dr. Guilhem Larrieu², Prof. Vincent Paillard¹, Prof. Laurence Ressier⁴, Dr. Aurélien Cuche¹

1. CEMES-CNRS, Université de Toulouse, CNRS, UPS, Toulouse, France, **2.** LAAS-CNRS, Université de Toulouse, CNRS, INP, Toulouse, France, **3.** Université Grenoble Alpes, CNRS, CEA-Leti Minatec, Grenoble, France, **4.** LPCNO, Université de Toulouse, CNRS, INSA, UPS, Toulouse, France

In the framework of quantum technologies, single photon source is a key component for on-chip and long-range quantum communications. In particular, improving their brightness by mean of optically resonant nanoantennas is a major stake for the development of efficient nanodevices.

As a proof of concept, we accurately positioned a few nanodiamonds hosting single nitrogen-vacancy (NV) centers in the gap of silicon dimers, using atomic force microscopy (AFM) nanoxerography [1]. NV centers in nanodiamonds is a model system exhibiting single photon emission properties at room temperature, which are well adapted to test beds in quantum nano-optics. On the other hand, low-loss high-index silicon nanostructures can tailor the Local Density of States (LDOS) in their vicinity and are compatible with CMOS technologies.

Thus, large arrays of nanodiamonds in the gap of silicon dimers with different dimensions have been elaborated by AFM nanoxerography (Figure 1a and b) [2]. The tuning of the experimental parameters allowed to control statistically the number of assembled nanodiamonds. The quantum nature of the sources and their photodynamics have been systematically investigated with time-resolved acquisitions. We notably demonstrated anti-bunched photon statistics down to a single photon emission (Figure 2) along with systematic increased brightness via near-field Purcell enhancement.

In order to go a step further, we explore numerically the control of the directive emission of such quantum sources. Our preliminary results show how to tailor the emission direction of a single dipolar source coupled to antennas made of multiple silicon nanoblocks (Figure 3). The positions of the nanoblocks on the substrate have been optimized with an Evolutionary Algorithm (EA) in order to maximize the intensity of the emitted light within a solid angle (Figure 4). Then, the angular emission distribution of multiple nanostructures coupled to a dipolar source has been simulated with the Green Dyadic Method (GDM), demonstrating the efficiency of such optimized antennas.

[1] M. Humbert et al., Versatile, rapid and robust nano-positioning of single-photon emitters by AFM-nanoxerography, Nanotechnology, 33, 215301 (2022)

[2] M. Humbert et al., Large-scale controlled coupling of single-photon emitters to high index dielectric nanoantennas using AFM nanoxerography, submitted (2022)

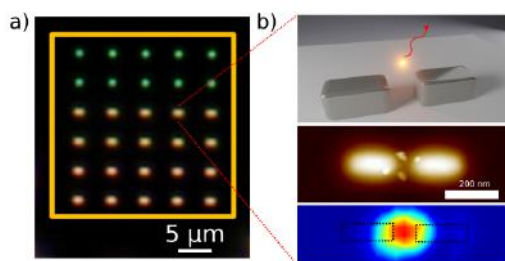


Figure 1. a dark field image of an array of silicon dimers. b schematics afm topography image and associated photoluminescence mapping of a dimer with selectively assembled nanodiamonds in the gap by afm nanoxerography..png

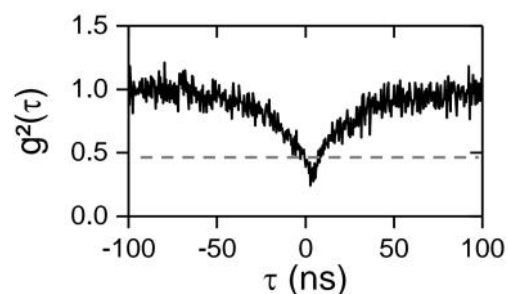


Figure 2. second-order intensity correlation function g^2 mesurement of a single nv center positioned in the gap of a silicon dimer..png

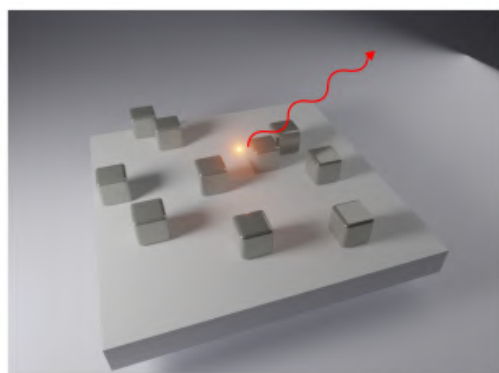


Figure 3. schematics of an optimized silicon antenna made of several resonant nanocubes coupled to a single quantum emitter on top of it..png

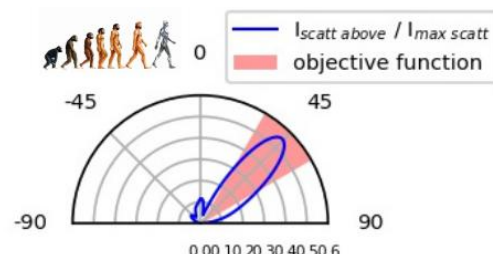


Figure 4. associated radiation pattern of the optimized device in the upper half space blue line and the solid angle objective function filled in red ..png

Deterministic generation of frequency entangled photonic multi-qudit states in modulated qubit arrays

Wednesday, 26th October - 15:21: Quantum nano-optics - Oral

Mr. Denis Ilin¹, Dr. Alexander poshakinskiy², Prof. Alexander Poddubny², Prof. Ivan Iorsh¹

1. ITMO University, 2. Ioffe Institute

Introduction

Frequency multiplexing of signals and ability to transmit them via single channel is the corner stone of modern information processing. A single photon state can also be in a quantum superposition of several frequency channels and act as a flying qudit - a multilevel analogue of qubit which can be used for quantum information processing. While it has been shown that single qudit operations can be effectively realized with passive optical channels, realization of two-qudit gates still poses sufficient challenge. Current protocols are based on post-selection techniques which lead to probabilistic character of the gate operation and suppress the efficiency and scalability. A deterministic scheme would include the elements which demonstrate single photon non-linearity such as single atoms, or artificial two-level systems. Such schemes lack flexibility required for on-demand generation of multi-photon states.

We suggest geometry which combines possibility of on-demand generation of entangled multi-qudit states and flexibility of passive optical elements. The geometry is shown in Fig.1. An array of qubits is coupled to a single one-dimensional photonic bus. Resonant frequency of each qubit is modulated. Due to the modulation photons can non-elastically scatter from the array forming a series of Stokes and anti-Stokes bands in the spectrum.

Methods

To analyze the structure of the scattered multiphoton states we use two complementary techniques: density matrix Master equation and diagrammatic perturbation theory for multiphoton scattering matrix. Details of the calculations can be found in <https://arxiv.org/abs/2203.00414>.

Results.

First we show that for the case of two qubits and π phase shift delay in modulation the system supports parity-protected two-photon correlations between the photons. Namely, if the sum of number of Stokes bands of two scattered photons is odd - they are always antibunched. (See Fig. 2). Moreover, we develop a protocol allowing to deterministically generate maximally entangled M-qudit state for M not exceeding 5. The example for M=2 is shown in Fig. 2(d). The example for 3 photons and different number of qubits N is shown in Figure_3.

The proposed protocol provides a feasible scheme for the on-demand generation of the entangled multi-qudit photonic states indispensable for quantum information processing.

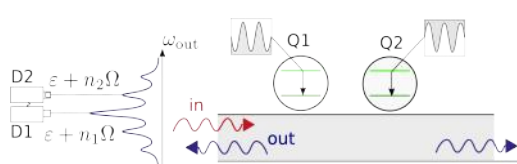


Fig1 geometry.png

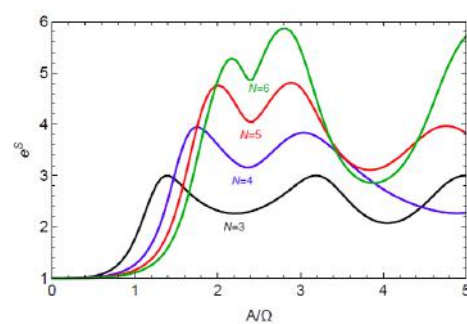


Figure3.png

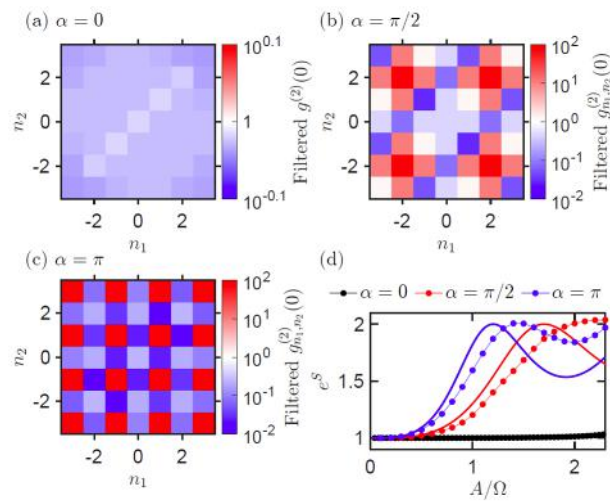


Figure 2 correlations 2photons.png

Electrical Generation of Surface Phonon Polaritons

Wednesday, 26th October - 15:38: Quantum nano-optics - Oral

Dr. Christopher Gubbin¹, Prof. Simone De Liberato¹

¹. University of Southampton

Polar dielectrics are an increasingly attractive platform for mid-infrared nanophotonics as a result of their ability to host sub-diffraction evanescent modes, termed surface phonon polaritons. By storing energy in the optic phonon vibrations of the polar lattice these modes enable nanoscale photon capture and control of light far-below the free space diffraction limit.

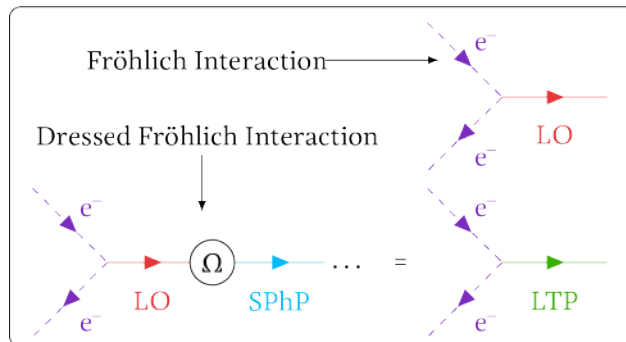
The optical response of polar systems is typically modelled assuming a spatially local relationship between driving fields and material response. In systems where light is confined on lengthscales approaching the lattice spacing this approach can fail, as dispersion of the phonon branches becomes increasingly important. In this regime discrete longitudinal phonons appear, and couple to photons through the screening charges induced at the edge of polar crystals. It has been shown that these phonons can couple to light, leading to the emergence of hybrid modes which possess both a transverse photonic component which is able to couple to the far-field and a longitudinal one which can couple to electrical currents [1]. These modes are termed longitudinal-transverse polaritons (LTPs).

This presents a novel route to design mid-infrared optoelectronic emitters and detectors: electrical currents in the mid-infrared predominantly dissipate energy through Fröhlich emission of longitudinal phonons. If these longitudinal phonons comprised part of a surface phonon polariton they can be utilised to capture this energy and couple it to the far field.

In this work we develop a transparent theory of nonlocality driven electroluminescence, utilising these hybrid modes as resonant interconnects which funnel electrical energy to the far-field through a dressed Fröhlich interaction. We discuss the typical form of such a device and calculate the efficiency of electroluminescence compared to thermal emission [2].

[1] C. Gubbin and S. De-Liberato - Optical Nonlocality in Polar Dielectrics (Phys. Rev. X, 10, 021027, 2020)

[2] C. Gubbin and S. De-Liberato - Electrical Generation of Surface Phonon Polaritons (arXiv:2206.03812)



Dressedfrohlich.png

Collective strong coupling in a plasmonic nanocavity: where is quantum ?

Wednesday, 26th October - 15:55: Quantum nano-optics - Oral

Mr. Alberto Alexander Diaz Valles¹, Dr. Hugo Varguet¹, Dr. Benjamin Rousseaux¹, Prof. Stéphane Guérin¹, Prof. Hans-Rudolf Jauslin¹, Prof. Gérard Colas des Francs¹

¹. ICB - CNRS-Univ. Bourgogne-Franche-Comté

Introduction Quantum plasmonics extends cavity quantum electrodynamics (cQED) concepts to the nanoscale, benefiting from the strongly subwavelength confinement of the plasmon modes supported by metal nanostructures. In this work, we describe in detail collective strong coupling to a plasmonic nanocavity. Similarities and differences to cQED are emphasized.

Methods and results We derive an effective Hamiltonian for an assembly of N_e emitters coupled to a metal nanoparticle bringing a clear physical understanding of the collective coupling process and emphasizing the role of localized surface plasmons (LSP) modes [1,2]. We notably observe that the Rabi splitting can strongly deviate from the standard $N_e^{1/2}$ law. We compare our discrete effective Hamiltonian to continuous models derived considering classical and quantum approaches [2,3].

Discussion The effective model intrinsically includes quantum corrections, whereas the continuous model necessitates their careful estimation. Quantum corrections affect the dipole–dipole coupling and introduce a frequency shift. When they are neglected, the continuous model simplifies to the classical approach. A better understanding of the collective behavior of multiple quantum emitters strongly coupled to a plasmonic nanocavity is crucial for optimizing the hybrid system, towards the generation of non-classical plasmon states in analogy to cQED devices [4] or the control of chemical reactions [5].

[1] Feist *et al*, *Macroscopic QED for quantum nanophotonics: emitter-centered modes as a minimal basis for multi-emitter problems*, Nanophotonics **10**, 477 (2021)

[2] Varguet *et al*, *Collective strong coupling in a plasmonic nanocavity*, J. Chem. Phys. **154**, 084303 (2021)

[3] Hakami *et al*, *Spectral properties of a strongly coupled quantum-dot-metal-nanoparticle system* Phys. Rev. A **89**, 053835 (2014).

[4] Sáez-Blázquez *et al*, *Photon statistics in collective strong coupling: Nanocavities and microcavities*, Phys. Rev. A **98**, 013839 (2018).

[5] Herrera and Owrutsky, *Molecular polaritons for controlling chemistry with quantum optics*, J. Chem. Phys. **152**, 100902 (2020).

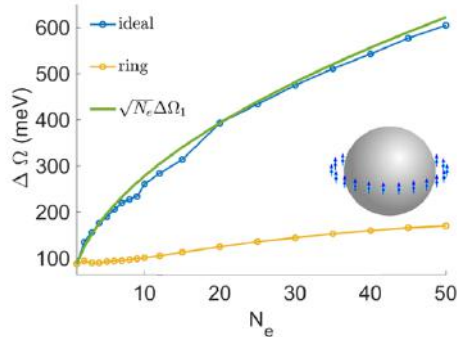


Fig. Rabi splitting as a function of the number of emitters. The blue curve corresponds to all QEs at the same and follows a $\sqrt{N_e}$ law (green curve). The yellow curve represent the Rabi splitting for the ring configuration.

Rabi.png

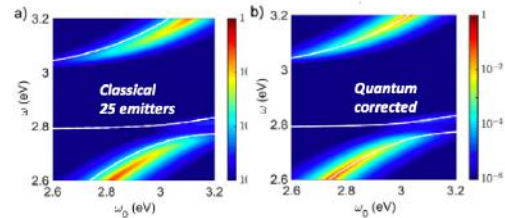


Fig. Emission spectra for QEs coupled to a silver MNP using the continuous model without (a) or with (b) the quantum correction. White solid lines indicate the eigenmode (dressed states) of the effective Hamiltonian.

Rabiquantumclassic.png

DNA origami assembled nanoantennas for manipulating single-molecule spectral emission

Wednesday, 26th October - 16:40: Strong light-matter interactions at the nanoscale - Oral

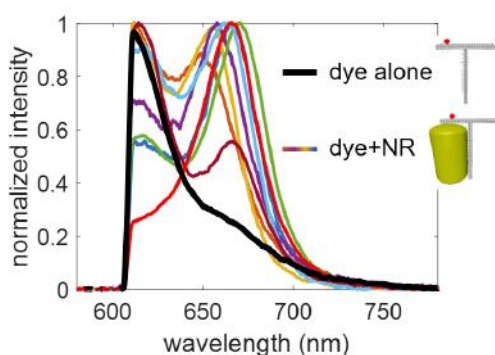
Dr. Maria Sanz-Paz¹, Mr. Fangjia Zhu¹, Dr. Mauricio Pilo-Pais¹, Prof. Guillermo Acuna¹

¹. University of Fribourg

Optical antennas have been widely used for manipulating single-molecule emission properties, including intensity and decay rates, and thus for affecting lifetime, polarization, spectrum, or directivity [1,2]. Investigation of all these properties with high accuracy requires precise positioning of single molecules around the antennas, something that is still quite challenging experimentally. Here, we make use of DNA origami [3,4] as a breadboard to control the interactions between molecules and nanoantennas. By making use of a T-shaped structure, we precisely position a single emitter in the vicinity of a single gold nanorod. We show, both numerically and experimentally, that we can affect the spectrum of a single fluorophore [5,6] in a position-dependent manner. Changes in the fluorescence spectrum are proportional to the resonance wavelength of the nanorods, which can be measured via their photoluminescence spectrum [7].

References

- [1] Novotny, L.; van Hulst, N. F. 2011. *Nature Photonics*, 5, 83-90
- [2] Anger, P.; Bharadwaj, P.; Novotny, L. 2006. *Phys. Rev. Lett.*, 96, 113002
- [3] Rothemund, P. W. K. 2006. *Nature*, 440, 297–302
- [4] Pilo-Pais, M.; Acuna, G. P.; Tinnefeld, P.; Liedl, T. 2017. *MRS Bull.*, 42(12), 936–942
- [5] Ringler, M.; Schwemer, A.; Wunderlich, M.; Nichtl, A.; Kürzinger, K.; Klar, T. A.; Feldmann, J. 2008. *Phys. Rev. Lett.*, 100 (20), 1–4
- [6] Saemisch, L.; Liebel, M.; van Hulst, N. F. 2020. *Nano Lett.*, 20, 6, 4537–4542
- [7] Cai, Y.Y.; Liu, J.G.; Tauzin, L.J.; Sung, E.; Zhang, H.; Joplin, A.; Chang, W.-S; Nordlander, P.; Link, S. 2018. *ACS Nano* 12, 2, 976–985



Reshaping.png

Observation of microcavity fine structure

Wednesday, 26th October - 16:57: Strong light-matter interactions at the nanoscale - Oral

Mr. Corné Koks ¹, **Prof. Martin van Exter** ¹

¹. Leiden University

Optical Fabry-Perot cavities can support many transverse and longitudinal modes. A paraxial scalar theory predicts that the resonance frequencies of these modes cluster in different orders. A nonparaxial vector theory predicts that the frequency degeneracy within these clusters is lifted, such that each order acquires a spectral fine structure, comparable to the fine structure observed in atomic spectra. We will present both the physical origins of this splitting [1] and its experimental observation [2].

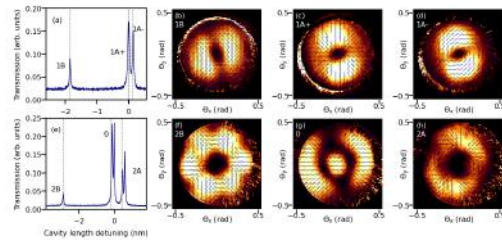
We experimentally observe that resonance spectra of optical microcavities have a fine structure [2]. We use plano-concave Fabry-Perot microcavities consisting of two highly reflective distributed Bragg reflectors. We scan the cavity and identify the polarization-resolved modes in the spectrum. We use close to perfect rotational-symmetric microcavities with very small radii of curvature, to ensure that the intrinsic effects, i.e. emerging from using a nonparaxial vector theory, dominate over external effect which depend only on the mirror shape such as mirror astigmatism.

We were able to distinguish between two intrinsic effects that cause fine structure: (i) an optical spin-orbit coupling and (ii) nonparaxial propagation and reflection. We also show that the relative strength of these effects is inversely proportional with the radius of curvature of the mirror. Finally, we show the existence of even smaller (hyperfine) splittings that originates from a Bragg effect and a second-order effect of astigmatism. All observed effects agree with predictions from a new theory for the nonparaxial modes in a microcavity [1].

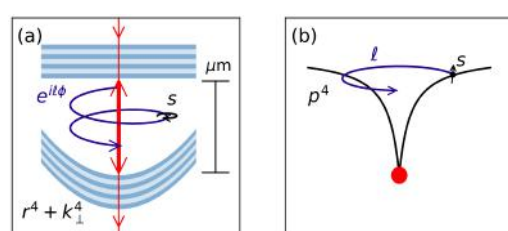
Optical cavity are becoming increasingly smaller to enhance light matter interaction. Therefore, also the effects of nonparaxial fine structure become more dominant. The analogy of fine structure with atomic physics is surprisingly fruitful to predict the resonance spectrum and its predictions are in close agreement to the experiment.

[1] M. P. van Exter, M. Wubs, E. Hissink, and C. Koks, Phys. Rev. A 106, 013501 (2022)

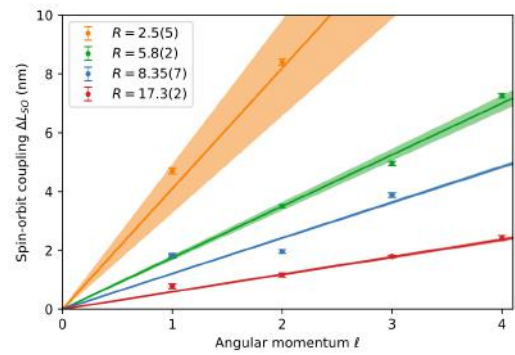
[2] C. Koks, F. B. Baalbergen, and M. P. van Exter, Phys. Rev. A 105, 063502 (2022)



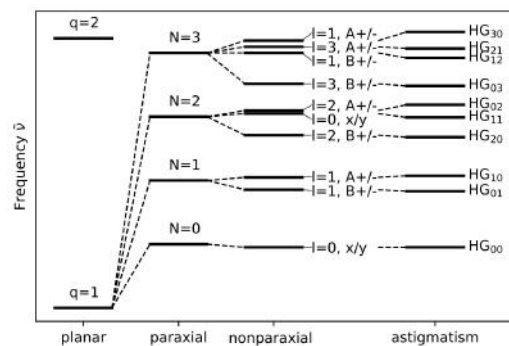
Measured finestructure and polarisation profiles.png



Similarities microcavity and atomic orbitals.png



Spin-orbit coupling measurement and theoretical prediction.png



Theoretical finestructure.png

Strong coupling between polaritons and both vibrational and electronic excitations of organic molecules

Wednesday, 26th October - 17:14: Strong light-matter interactions at the nanoscale - Oral

Mr. Andrei Bylinkin¹, Dr. Francesco Calavalle¹, Ms. María Barra-Burillo¹, Mr. Roman Kirtaev², Dr. Elizaveta Nikulina¹, Dr. Evgenii Modin¹, Prof. James H. Edgar³, Prof. Fèlix Casanova⁴, Prof. Luis E. Hueso⁴, Prof. Valentyn Volkov⁵, Prof. Paolo Vavassori⁴, Dr. Igor Aharonovich⁶, Dr. Pablo Alonso González⁷, Prof. Rainer Hillenbrand⁸, Dr. Alexey Y. Nikitin⁹

1. CIC nanoGUNE BRTA, **2.** Donostia International Physics Center (DIPC), **3.** Tim Taylor Department of Chemical Engineering, Kansas State University Manhattan, **4.** CIC nanoGUNE BRTA / IKERBASQUE, **5.** XPANCEO, Bayan Business Center, **6.** School of Mathematical and Physical Sciences, University of Technology Sydney, **7.** Departamento de Fisica, Universidad de Oviedo, **8.** CIC nanoGUNE BRTA / IKERBASQUE / UPV-EHU, **9.** Donostia International Physics Center (DIPC) / IKERBASQUE

Enhanced light-matter interactions, based on light confinement to a sub-diffraction size spot, are fundamental for surface-enhanced spectroscopy and control of material properties on the nanoscale. The interactions involving vibrational and electronic degrees of freedom, typically taking place at the energies of the mid-infrared (mid-IR) and visible light, respectively, are of particular interest due to controlling chemical reactivity by vibrational strong coupling and photoluminescence by strong plasmon-exciton coupling. However, as the above interactions take place at very different energies and momenta, creating a confined electromagnetic field (a hot spot) - an essential ingredient of the SC - at the same spatial position and with a similar size at different frequencies is demanding, so that using one and the same optical resonator (or optical antenna) is impeded. Here we theoretically demonstrate the strong coupling simultaneously achieved at the same momenta in both visible and mid-IR frequencies in the same spatial location, Fig.1. To that end we engineer a heterostructure composed of metal ribbons, van der Waals crystal slab (h-BN) and a molecular layer (CoPc), which supports ultra-confined polaritons - hybrid light-matter excitations - of the same momenta in the visible and mid-infrared frequency ranges. We visualize the hotspots in both ranges and at the same positions by near-field optical microscopy. We perform far-field spectroscopy to explore SC between the phonon polaritons and molecular vibration in the mid-IR range and between plasmon polaritons and excitons in the visible range. Our results introduce the new concept of exploring the strong coupling between fundamentally different degrees of freedom, which could be used for sensing, local control of chemical reactivity, and quantum optics.

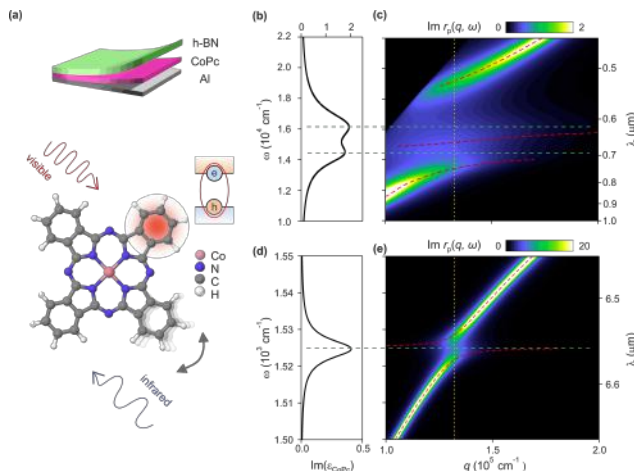


Fig1.png

Polaron-enhanced exciton-polariton optical nonlinearity in perovskite photonic crystal slab

Wednesday, 26th October - 17:31: Strong light-matter interactions at the nanoscale - Oral

Mr. Mikhail Masharin¹, Dr. Vanik Shahnazaryan¹, Dr. Fedor Benimetskiy¹, Prof. Ivan Shelykh¹, Prof. Sergey Makarov¹, Dr. Anton Samusev¹, Dr. Anton Samusev²

1. ITMO University, 2. Technische Universität Dortmund

Introduction

Halide perovskites are one of the most perspective materials for exciton-polariton systems, as it has room-temperature exciton with high oscillator strength. Perovskites embedded in vertical Bragg cavities demonstrate the formation of polaritons and even polariton condensation regimes [1]. However, the microscopic mechanisms of polariton-driven optical nonlinear effects are not well-studied yet. In this work, having in mind further real-world applications, we turn to the planar cavity realizing the perovskite photonic crystal slab based on MAPbI₃. We demonstrate that this material shows large nonlinear polariton blueshifts due to the support of polarons [2,3] mediating polaritonic response.

Methods

Perovskite photonic crystal slab was fabricated using nanoimprint lithography of spin-coated polycrystalline MAPbI₃ thin film [3]. Sample morphology was characterized via SEM and AFM methods. Leaky optical modes of the sample, including polariton states, were studied via the angle-resolved spectroscopy method. A femtosecond laser, coupled to an optical parametric amplifier was used for PL measurements and pump-dependent reflectivity measurements. The sample was mounted in an ultra-low-vibration closed-cycle helium cryostat and maintained at a controllable temperature in the range of 7-300K.

In order to unveil the physical origin of observed nonlinear polariton blueshifts, we develop a microscopic model of exciton-polariton response in MAPbI₃. Our model includes the quantum mechanical description of the exciton-polaron state; the calculation of excitonic nonlinearity rates; the quantitative description of polariton gas temporal dynamics; the many-body renormalization of polariton resonance energy.

Results and Discussion

We experimentally measure exciton-polariton branches for various temperatures via the mentioned method and confirm the strong light-matter coupling regime for temperatures below 200K. Tuning the incident angle and pump wavelength, we resonantly pump polariton states at different exciton fractions and measure polariton nonlinear blueshift at 6K. At the highest exciton fraction, we obtain the record-high value to this date equal to 19.7 meV. Based on the measured data, we develop a microscopic model, which well describes the experimental results. The model shows how polarons modify interaction potential and increase the critical Mott transition density, resulting in enhanced polariton blueshift values. During further work, instead of patterning the perovskite film, we will employ surface acoustic waves to dynamically induce spatially-periodic modulation of the exciton resonance thus giving rise to exciton-phonon-polaritons.

[1] Su, Rui, et al. Nature Materials 20.10 (2021): 1315-1324.

[2] Soufiani, Arman Mahboubi, et al. Applied Physics Letters 107.23 (2015): 231902.

[3] Masharin, M. A. arXiv preprint arXiv:2201.10265 (2022).

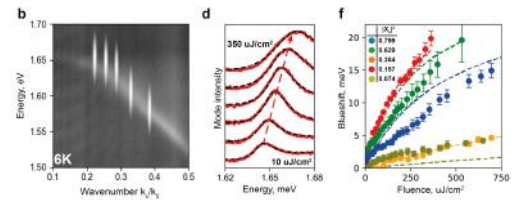


Fig 2 resonant pump polariton blueshift.png

Fig 1 concept.png

Quantum Hydrodynamic Theory for Plasmonics: from Molecule-Coupling to Nonlinear Optics

Wednesday, 26th October - 17:48: Strong light-matter interactions at the nanoscale - Oral

Dr. Cristian Ciraci¹, Dr. Henrikh Baghramyan¹, Dr. Muhammad Khalid¹, Dr. Fabio Della Sala¹

¹ Istituto Italiano di Tecnologia

Metals support surface plasmons at optical wavelengths and have the ability to localize light to sub-wavelength regions. Nano-gap plasmonic systems – in which two or more metallic nanoparticles are separated only few nanometers from each other by an insulating spacer – have been predicted to produce enormous field enhancements (as much as thousands of times that of the incident radiation)¹. For the narrowest (<1 nm) gaps, light can be so tightly confined that the nonlocality associated with the dielectric response of the metal and quantum effects can have a strong impact on the scattering properties of the system, placing strict bounds on the ultimate field enhancement².

A reliable way to theoretically describe and numerically model optical properties of plasmonic nanostructures with different length scales requires methods beyond classical electromagnetism. In this context, it becomes very important to develop simulation techniques to take into account quantum microscopic features at the scale of billions of atoms. A promising solution is given by the hydrodynamic theory, which takes into account the nonlocal behavior of the electron response by including the electron pressure and it can be generalized so that it can describe electron spill-out and tunneling effects^{3,4}. This method allows to explore light-matter interactions in extreme scenarios in which microscopic features can strongly affect the macroscopic optical response.

In this talk, we will present the quantum hydrodynamic theory for plasmonics and will discuss some applications including, photon emission⁵, strong-coupling⁶ and nonlinear optics⁷.

Finally, we point out the limitations of conventional functionals in QHT and propose possible corrections^{8,9}.

References

1. Romero *et al.*, Opt. Express **14**, 9988 (2006);
2. Ciraci *et al.*, Science **337**, 1072 (2012);
3. Toscano *et al.*, Nature Commun. **6**, 7132 (2015);
4. Ciraci, Della Sala, Phys. Rev. B **93**, 205405 (2016);
5. Ciraci, Phys. Rev. B **95**, 245434 (2017);
6. Baghramyan, Ciraci, Nanophotonics **11**, 2473 (2022);
7. Ciraci *et al.*, , Nanophotonics **8**, 1821 (2020);
8. Khalid, Ciraci, Commun. Physics **3**, 214 (2020);
9. Baghramyan *et al.*, Phys. Rev. X **11**, 011049 (2021);

Bimetallic plasmonic metasurface for asymmetric second-harmonic generation

Wednesday, 26th October - 16:40: Nonlinear & ultrafast nano-optics - Oral

Dr. Sergejs Boroviks¹, Mr. Andrei Kiselev¹, Dr. Karim Achouri¹, Prof. Olivier J.F. Martin¹

1. Nanophotonics and Metrology Laboratory, École Polytechnique Fédérale de Lausanne (EPFL)

Photonic metasurfaces enable compact optical devices with diverse functionalities and tunable properties. [1,2] In particular, it is possible to tailor metasurface's directivity and spectral response in both linear and nonlinear regimes. [3,4] Furthermore, it was recently shown that nonlocal metasurfaces [5] allow asymmetric transmission and generation of nonlinear light (sometimes also referred to as nonreciprocal parametric generation). [6-10]

In this talk, we will discuss an experimental demonstration of a plasmonic metasurface that features such asymmetric control of second-harmonic generation (SHG). The concept of the device is illustrated in Figure 1: SHG occurs only when the metasurface is excited from the bottom side. When the excitation direction is reversed, SHG is considerably silenced (approximately by 22 dB in simulations). The metasurface is designed to operate at 800 nm and converts near-infrared light into visible blue (400 nm).

Contrary to previous proposals, in our design, asymmetric SHG functionality is achieved by employing two plasmonic metals – aluminium and silver – as constitutive materials of the metasurface. The unit cell of the metasurface and its simulated performance for both excitation directions are shown in Figure 2. The dimensions of an anisotropic two-layer “T”-shaped nanostructure are selected to support resonances at both fundamental and second-harmonic wavelengths. [11] In combination with the unique plasmonic properties of aluminium, [12] this allows to simultaneously minimize linear transmission for both illumination directions and maximize SHG efficiency for one direction only.

Finally, we will also discuss fabrication methods and optical characterization aspects. Figure 3 shows scanning electron microscope images of the metasurface sample fabricated using the standard electron-beam lithography and ion-beam etching techniques.

1. Appl. Sci. 9, 2727 (2019)
2. Adv. in Opt. and Phot. 11, 380 (2019)
3. Nat. Photon. 9, 180 (2015)
4. Nat. Rev. Mat. 2, 17010 (2017)
5. Laser Photon. Rev. 2100633 (2022)
6. Nat. Photon. 16, 561 (2022)
7. Nat. Commun. 6, 8359 (2015)
8. Sci. Rep. 6, 25113 (2016)
9. Phys. Rev. Appl. 13, 054056 (2020)
10. Plasmonics 16, 77 (2021)
11. New Journ. of Phys. 24, 025006 (2022)
12. Nano Lett. 11, 4674 (2011)

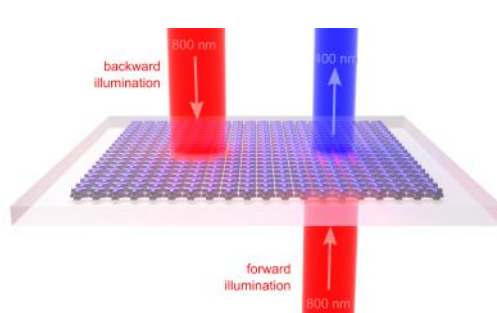


Figure1.png

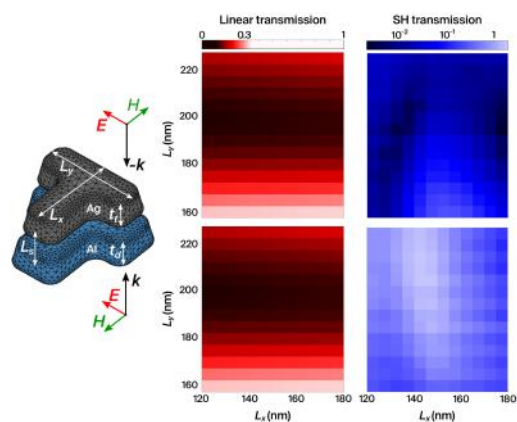


Figure2.png

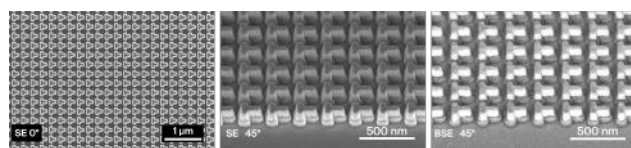


Figure3.png

Non-Hermitian anharmonicity induces photon blockade in hybrid metallocodielectric cavities

Wednesday, 26th October - 16:57: Nonlinear & ultrafast nano-optics - Oral

Dr. Anael Ben-Asher¹, Prof. Antonio I. Fernández-Domínguez¹, Dr. Johannes Feist¹

1. Departamento de Física Teórica de la Materia Condensada and Condensed Matter Physics Center (IFIMAC), Universidad Autónoma de Madrid, E28049 Madrid, Spain

Single-photon sources play a vital role in light-based quantum-information technologies [Nat. Photonics 3, 687–695 (2009)]. One well-known design for such sources is a coupled emitter-cavity system in the strong-coupling regime. Single-photon emission is then achieved through the so-called photon blockade (PB) phenomenon, where the absorption of one photon induces large enough energy shifts in the system to prevent the absorption of subsequent photons [Nature 436, 87 (2005), Nat. Phys. 4, 859 (2008)]. However, this phenomenon is limited by the linewidths of the system's excitations, since larger widths require larger energy shifts. Here we propose a novel mechanism for generating single-photon emission, the non-Hermitian photon blockade (NHPB), which is not limited by the possibly large linewidths of the system's excitations but exploits them. Moreover, in contrast to the well-known (Hermitian) PB mechanism, it operates in the weak-coupling regime, and thus has less stringent experimental requirements for the realization of an efficient single-photon source.

While the Hermitian PB mechanism stems from the anharmonicity of the system's energy levels (Fig.1(a)), the NHPB occurs even though both the first and the second excitation energies are on-resonance with the laser frequency. The origin of NHPB lies in the anharmonicity of the NH energies in the complex plane, i.e., in the difference in linewidth between the first and the second excitations (Fig.1(b)).

Hybrid metallocodielectric cavities, incorporating a narrow photonic mode with a broad plasmonic mode, provide an excellent platform for the observation of the NHPB mechanism. Using a perturbative approach for the low-driving regime [Phys Rev. A 98, 013839 (2018)], we study the statistical properties of the photons emitted from such a cavity weakly coupled to a two-level emitter. The solid lines in Fig.2 depict the obtained (a) intensity I and normalized (b) second- and (c) third- order correlation functions $g^{(2)}_{\tau=0}$ and $g^{(3)}_{\tau=0}$, as a function of the driving laser detuning $\Delta\omega_L$. The dashed lines in Fig.2 represent I , $g^{(2)}_{\tau=0}$ and $g^{(3)}_{\tau=0}$, when all excitations are set to have the same linewidth. As can be seen, high-purity single-photon emission (corresponds to $g^{(n>1)}_{\tau=0} \rightarrow 0$) at high repetition rates is achievable in hybrid metallocodielectric cavities due to the NHPB mechanism.

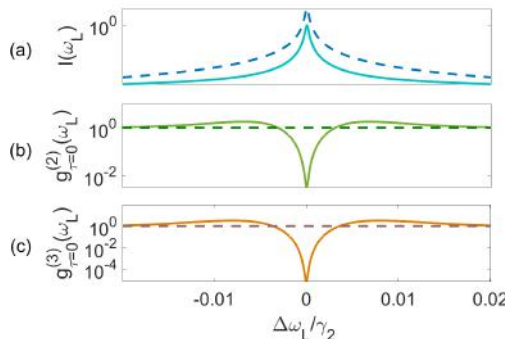


Fig2-correlation functions.png

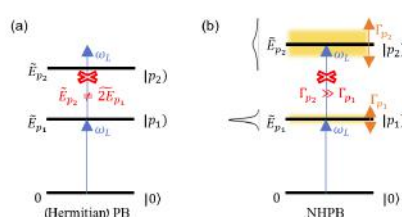


Fig1-two pb mechanisms.png

Plasmon enhanced SHG of BaTiO₃ nanocubes

Wednesday, 26th October - 17:14: Nonlinear & ultrafast nano-optics - Oral

Dr. Laureen Moreaud¹, **Mr. Guillaume Boudan**¹, **Dr. William Djampa-Tapi**¹, **Mr. Aurélien Loirette-Pelous**², **Dr. Alexandra Bogicevic**³, **Dr. Mondher Besbes**², **Prof. Jean-Jacques Greffet**², **Prof. Nicolas Lequeux**³, **Dr. Thomas Pons**³, **Dr. Christine Bogicevic**⁴, **Prof. François Marquier**⁵, **Dr. Simon Vassant**¹, **Dr. Céline Fiorini**¹

1. Univ. Paris-Saclay, CEA, CNRS, SPEC, F-91191 Gif-sur-Yvette, France, **2.** Laboratoire Charles Fabry de l'Institut d'Optique LCFIO, Université Paris-Saclay, Palaiseau, 91120, France, **3.** Laboratoire de Physique et d'Etude des Matériaux - ESPCI, **4.** SPMS, CentraleSupélec, Université Paris-Saclay, CNRS, Gif-sur-Yvette, **5.** Univ. Paris-Saclay, CNRS, ENS Paris-Saclay, LuMIn, F-91190 Gif-sur-Yvette, France

Dielectric nanoparticles have a significant interest as markers in biology. Beyond their stability under high laser power, they show an anisotropic response of the second harmonic generation (SHG) signal. This last point allows the follow-up of protein movements in rotation.[1] It is indeed a parameter of interest in molecular motors dynamics [2] and has significant importance for neurological disease diagnosis.

Barium titanate particles (BaTiO₃ or BTO) are good potential markers: in our study colloidal tetragonal nanocubes were chosen. These particles exhibit high nonlinear second-order properties together with interesting anisotropic properties. In particular, crossing images from a scanning electron microscope (SEM) and SHG measurements demonstrate the correlation between the SHG anisotropy measurements of monocrystalline BTO and their orientation. This correlation is presented in Figure 1.

One known approach to enhance the response of BTO particles is to play on the Mie resonances by playing on the size of the objects.[3] Another way is to study the coupling of NPs of a given size to plasmonic antennas. Such a system ensures a good marking sensitivity, avoiding the need for too big objects.[4] Therefore in this study, we considered single BTO particles coated with 10 nm of gold.

Simulations were performed to determine the laser excitation wavelength enabling to maximization of the SHG enhancement by the gold shell. The incident laser power is carefully controlled to avoid laser-induced reshaping of the gold coating during the measurements. A SHG enhancement by a factor of 3 is evidenced in Figure 2 for different single objects of a given volume range. Although modest compared to previous achievements, references in [3], these results are consistent with calculations that consider the roughness of the gold layer and the associated losses. Interestingly, we show that laser-induced melting of the gold coating is profitable to oppose the same object in the presence or absence of a plasmonic shell.

References

1. Mayer et al., Nanoscale, 5, 18, 8466 (2013)
2. Kaplan et al., Sci. Advances, 4, 3, e16602170 (2018)
3. Timpu et al., ACS Photonics, 4, 76-84 (2017)
4. Karvounis et al., Adv. Optical Mater., 8, 2001249 (2020)

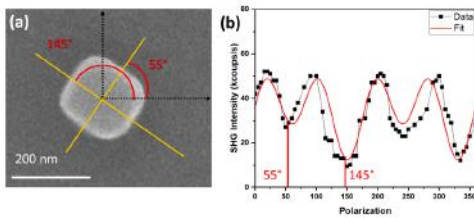


Figure 1: (a) SEM images of a BTO particle indicating its orientation on the substrate. (b) SHG intensity dependence with the incident laser polarization, showing minima for polarizations along the two edges of the crystal, as expected theoretically considering the BTO $\chi(2)$ tensor.

Figure1.png

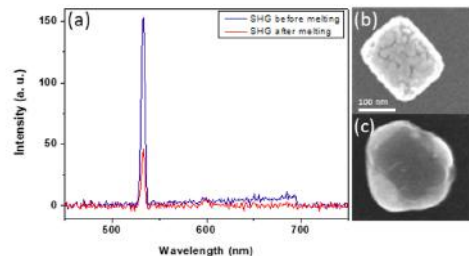


Figure 2: (a) SHG intensity enhancement of BTO nanocubes in the presence of gold coating. (b) SEM images of a BTO particle before and melting the gold shell.

Figure2.png

Nonlinear meta-holograms for the generation of second harmonic vortex beams

Wednesday, 26th October - 17:31: Nonlinear & ultrafast nano-optics - Oral

Ms. Laure Coudrat¹, Dr. Pascal Filloux¹, Dr. Romain Dezert¹, Dr. Adrien Borne¹, Dr. Tana Ranos², Dr. Julien Claudon², Dr. Jean-Michel Gérard², Dr. Aloyse Degiron¹, Prof. Giuseppe Leo¹

1. Université Paris Cité, 2. CEA

We generate second harmonic (SH) beams carrying non-zero orbital angular momentum (OAM) via a dielectric $c^{(2)}$ metasurface, with SH generation and phase control, being achieved at the level of single meta-atoms. The metasurface proposed here relies on dielectric meta-atoms made of (100)-epitaxially grown AlGaAs and reported on a sapphire substrate for the generation of a SH signal with a desired wavefront profile in the forward direction (see Fig. 1). Such metasurface is pumped with a linearly polarized plane wave at $\lambda=1550$ nm, impinging at normal incidence from below the substrate. By varying the meta-atoms geometry, we build a lookup table of nano-resonators with roughly equal SH amplitudes and phases covering the whole $0\text{-}2\pi$ range. Our metasurfaces are arranged as square-lattice 2D gratings, with a period granting for negligible near-field coupling between adjacent resonators.

We first demonstrated experimentally the robustness of the lookup table of meta-atoms by implementing a SH Fresnel lens and a SH beam steering device. Then, an additional specific technological development allowed us to use a larger set of meta-atoms providing more accurate phase sampling along with reduced fabrication tolerances. Finally, as a test of the increased potential of our technological platform, we designed and fabricated a metasurface for the generation of a SH beam carrying OAM. This takes the form of a meta-hologram with the fork-like phase profile depicted in Figure 2a and phases provided by the above lookup table. More specifically, we imprint a SH phase profile that steers a vortex beam of topological charge 5 in ± 1 diffraction orders. Analytical and experimental results are in good agreement, see Figures 2b and 2c.

We fully exploit the tensorial nature of AlGaAs quadratic nonlinearity and its mature fabrication technology to generate SH with engineered wavefront with a metasurface. We have designed and fabricated an all-dielectric $c^{(2)}$ meta-hologram that generates SH vortex beams. The control of the orbital angular momentum of second harmonic beams provides an additional degree of freedom, which promises to increase the capacity of information encoding in compact devices for free-space communications.

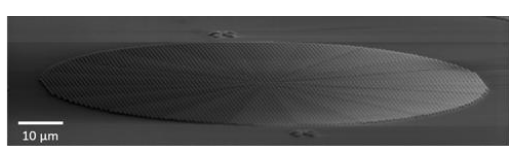


Figure 3: SEM image of one of the fabricated metasurfaces. It has a helical phase profile of topological charge $m=5$.

Picture3.png

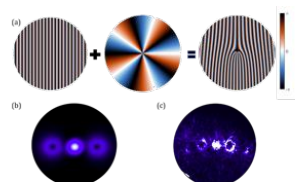


Figure 1 (a) Fork-like phase profile: a sawtooth and helical phase profile are combined to steer a vortex beam of topological charge 5 in the first diffraction order. (b) Analytical and (c) experimental results of the SH vortex beams generated by illuminating a nonlinear metasurface with the phase profile shown in (a).

Picture2.png

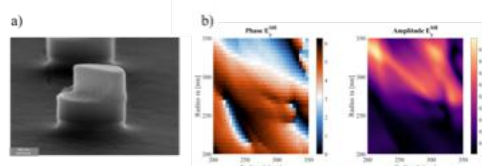


Figure 1.(a) Electron-microscope picture of a meta-atom: a nanocylinder with elliptical basis, height 400 nm and semi-axes r_a and r_b , with $\frac{1}{3}$ of its volume etched away so as to provide it with the shape of a nanochair of height 200 nm. (b) Lookup tables of the phase and normalized amplitude of the SH electric field generated by each nanochair along the vertical direction and diffracted into the 0-th order of the metasurface.

Picture1.png

Photon Pair Correlations in Semiconductor-Superconductor Light Sources

Wednesday, 26th October - 17:48: Nonlinear & ultrafast nano-optics - Oral

Dr. Shlomi Bouscher¹, Mr. Dmitry Panna¹, Dr. Ronen Jacovi¹, Dr. Ankit Kumar¹, Prof. Sebastian Klembt², Prof. Sven Höfling², Prof. Alex Hayat¹

1. Department of Electrical Engineering, Technion – Israel Institute of Technology, Haifa, 3200003, Israel, **2.** Technische Physik, Physikalisches Institut and Wilhelm Conrad Röntgen Research Center for Complex Material Systems, Universität Würzburg, D-97074 Würzburg, Germany

Various applications in the rapidly growing field of quantum information science require reliable and compact quantum light sources. We proposed an efficient approach for generation of entangled photons, based on Cooper-pair luminescence in semiconductors, which does not require isolated emitters [1].

We have experimentally demonstrated superconducting light-emitting diodes (SLED). Our theory predicts that when Cooper-pairs are injected into the pn junction, recombining with a pair of holes, and emitting an entangled photon pair [1]. Such injection of Cooper-pairs into the pn junction is evident through the process of Andreev reflection, which manifests itself as an enhancement of electric conduction below the superconducting gap [2]. We demonstrate enhanced Andreev reflection in a Nb/InGaAs/InP-based device by Cooper-pair tunneling into a semiconductor quantum well resonant state [3]. Moreover, Cooper-pair recombination has also been shown to result in enhanced emission below the superconductor's critical temperature T_c . Our latest SLED design (Fig 1a) exhibits both Andreev reflection in its conductance spectrum (Fig 1b). We have also observed photon-pair correlations $g^{(2)}$ (Fig 1c) and its variance (Fig 1d), with temperature dependence on the order parameter - in good agreement with calculations, corresponding to photon-pair emission from injected Cooper pairs.

Furthermore, incorporation of high-temperature (high- T_c) superconductors can greatly increase operating temperatures to well above LN2 ($\sim 77\text{K}$), thus paving the way for a broad range of commercial applications. We have achieved an important milestone in this direction through the design and fabrication of YBCO/GaN superconductor-semiconductor junctions [4], and have recently observed strong Andreev reflection [5]. These results open new directions for fundamental studies in quantum optics and light-matter interaction and enable a wide range of applications in quantum technologies and quantum information processing.

[1] A. Hayat, et al, Phys. Rev. B 89, 094508 (2014)

[2] D. Panna, S. Bouscher, K. Balasubramanian, V. Perepelok, S. Cohen, D. Ritter, and A. Hayat, Nano Letters, 18, 6764 (2018).

[3] S. Bouscher, D. Panna, K. Balasubramanian, S. Cohen, D. Ritter, and A. Hayat, Phys. Rev. Lett. ,128, 127701 (2022).

[4] D. Panna, et al, Nature Sci. Rep. 8, 5597 (2018).

[5] S. Bouscher, et al. J. Phys. Condens. Matter 32 475502 (2020).

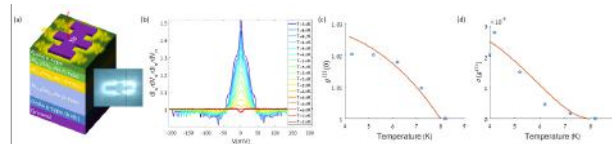


Fig1.png

An Achiral Magnetic Photonic Antenna as a Tunable Nanosource of Superchiral Light

Wednesday, 26th October - 16:40: NanoAntennas - Oral

Ms. Lingfei Cui¹, Dr. Bruno Gallas¹, Dr. Mathieu Mivelle², Mr. Xingyu Yang¹, Mr. Benoît Reynier¹, Dr. Catherine Schwob¹, Dr. Sébastien Bidault³

1. Institut des NanoSciences de Paris - Sorbonne Université, **2.** Institut des NanoSciences de Paris, **3.** Institut Langevin, ESPCI Paris, CNRS

Sensitivity to molecular chirality is crucial for many fields, from biology and chemistry to the pharmaceutical industry. Unfortunately, current enantiomeric selection techniques rely on expensive, slow, high-volume systems working mainly in the UV. Nanophotonics brings innovative solutions to these problems via the generation of superchiral light in the near field, allowing a reduction of the detection volume and a higher sensitivity. Yet, until now, this has been done mainly by using chiral nanostructures, allowing the study of only one type of enantiomer, or nanostructures summing up the near-field and far-field signal, preventing their use in solution. Moreover, in most cases, the distribution of the chirality density around the photonic nanostructure is not uniform, diminishing the interest of the nanophotonic approach. Here, we demonstrate numerically and theoretically how to design a nanosource of pure superchiral light, free of any background and whose chirality sign is tunable on-demand in wavelength and polarization.

Specifically, we demonstrate that the unique properties of this nanoplateform result from an achiral nanostructure, coupled with an achiral light (Figure 1a). Indeed, we demonstrate numerically and theoretically in this work that the coupling between a plasmonic nano-aperture (NA) behaving as a magnetic dipole and a linearly polarized incoming wave generates a chirality density that is both enhanced and uniform across the entire nano-antenna. We also demonstrate that the sign of this chirality density (C) is tunable by changing the excitation wavelength and/or the angle of the incident polarization (Figures 1b, c). Moreover, by its conception as a nano-aperture in an opaque gold layer, this nanosource of superchiral light is thus free of any background, allowing its use for detecting chiral molecules in solution diffusing in the antenna, and this, without any contribution from molecules present in the rest of the volume.

Therefore, we believe that the novelty of this work goes beyond the simple creation of a tunable nanosource of superchiral light but provides a leap forward towards the development of platforms made of achiral magnetic plasmonic resonators for the measurement of circular dichroism in nanovolumes and at the single molecular level.

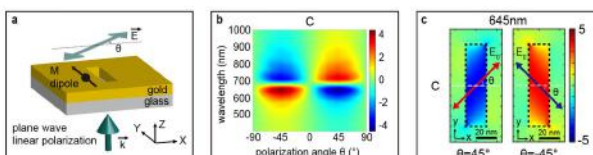


Figure 1. a) 3D representation of the rectangular NA in a thin gold layer of 40 nm thick. The vector k represents the direction of propagation of the linearly polarized incident plane wave, and θ , the angle of this polarization with respect to the NA's transverse axis (Ox). b) variations of C as a function of the incident polarization angle θ and wavelength in the center of the NA. c) Spatial distribution of the chirality density in an XY plane at the middle of the NA in Z, for the wavelength of maximum C and for $\theta = \pm 45^\circ$.

Figure.jpg

An Inverse Faraday effect generated by linearly polarized light through a plasmonic nano-antenna

Wednesday, 26th October - 16:57: NanoAntennas - Oral

Mr. Xingyu Yang¹, Mr. Ye Mou², Mr. Homero Zapata¹, Mr. Benoît Reynier³, Dr. Bruno Gallas², Dr. Mathieu Mivelle³

1. Sorbonne Université, **2.** Institut des NanoSciences de Paris - Sorbonne Université, **3.** Institut des NanoSciences de Paris

The inverse Faraday effect (IFE) generates magnetic fields by optical excitation only. Since its discovery in the 60s, it was believed that only circular polarizations could magnetize matter by this magneto-optical phenomenon. Here, we demonstrate the generation of an IFE via a linear polarization of light.

This new physical concept results from the local manipulation of light by a plasmonic nano-antenna. We show that a gold nanorod excited by a linear polarization generates a non-zero magnetic field by IFE when the incident polarization of the light is not parallel to the long axis of the rod. This dissymmetry generates hot spots of local spin densities (local polarization state), introducing the concept of super circular light, allowing this magnetization. Moreover, by varying the angle of the linear polarization with respect to the nano-antenna, we demonstrate the on-demand flipping of the magnetic field orientation. Finally, this linear IFE generates a stationary magnetic field 25 times stronger than what a gold nanoparticle produces when excited by a circular polarization and via a classical IFE.

The creation of stationary magnetic fields by IFE in a plasmonic nanostructure is nowadays the only technique allowing the creation of ultrashort, intense magnetic field pulses at the nanoscale. This research provides then a new method to locally create an IFE. Thus, it finds applications in the ultrafast control of magnetic domains with applications not only in data storage technologies but also in research fields such as magnetic trapping, magnetic skyrmion, magnetic circular dichroism, to spin control, among others. Therefore, through linear IFE, the ultrafast manipulation of magnetic processes for the same excitation polarization, the same energy density, and the same heat generation, simply by changing the angle of the incident polarization on the plasmonic nano-antenna would be a game-changer in the physics of ultrafast opto-magnetism.

Keyword: Inverse Faraday effect, plasmonic nano-antenna, stationary magnetic field, spin density

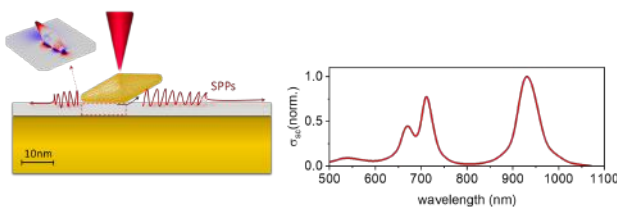
Opening Gap Nanopatch Antenna: A Surface Plasmon Polariton Source

Wednesday, 26th October - 17:14: NanoAntennas - Oral

Ms. Nhung Vu¹, Dr. Bruno Bérini², Dr. Stephanie Buil², Dr. Frédéric Lerouge³, Prof. Emmanuel Cottancin¹, Dr. Michel Pellarin¹, Dr. Julien Laverdant¹

1. Institut Lumière Matière, Université Claude Bernard Lyon 1, CNRS, Université de Lyon, F-69622 Villeurbanne, France, **2.** Université Paris-Saclay, UVSQ, CNRS, GEMaC, 78000, Versailles, France, **3.** Univ Lyon, Ens de Lyon, CNRS, Université Lyon 1, Laboratoire de Chimie UMR 5182, F-69342, Lyon, France

Nanopatch antennas based on metallic nanoparticles-on-mirror configuration offer great advantages as a potential source for launching surface plasmon polaritons (SPPs)¹. In this work, we propose a plasmonic platform consisting of gold bipyramid nanoparticles (AuBPs) deposited over a gold thin film. A sub-10nm TiO₂ gap is introduced between the two metallic structures to prevent conductive contact. The synthesized AuBPs have the ability to support a strong localized surface plasmon resonance along its longitudinal axis which behaves like a radiating dipole^{2,3}. When the nanoparticles are brought to interact with the gold mirror, each AuBP resembles a nanoscale nanopatch antenna with an “opening-mouth”, which allows for effectively launching SPPs over the metallic surface around the bipyramid. In the terms of the experiment, we employ a leakage radiation microscope working in the dark-field configuration to study the scattering of the antenna and also excite and collect the SPPs. Here, we highlight the importance of the orientation effect in the optical response of the AuBPs. A rich mode structure ranging from the visible to the near-infrared regime is opened by tilting AuBP with one tip touching the substrate, whereas other orientations only display a single dipolar longitudinal mode. The plasmon modes exhibit both radiative nature and are confined within the gap. The COMSOL calculation confirmed that the plasmon gap modes resemble behaviors of the Fabry-Pérot resonances. Finally, the bipyramid nanopatch is employed to optically excite SPPs, showing that the efficiency of launching SPPs is resonantly enhanced at the plasmon resonance wavelength of the mode. Especially, in the comparison to the plasmon generated by scattering from a dielectric bead nanoparticle of silica on the same gold substrate, the bipyramid nanopatch induces a greater SPPs efficiency by around 1 order of magnitude. These characteristics of the AuBP nanopatch can pave the way for electrically driven plasmon antennas, for which many applications such as energy harvesting or quantum information, are beneficial.



Abstract image.png

Optoinduced magnetization in metal from the spin and orbital angular momenta of light

Wednesday, 26th October - 17:31: NanoAntennas - Oral

Mr. Vage Karakhanyan¹, Mr. Clément Eustache¹, Dr. Yannick Lefier¹, Dr. Thierry Grosjean¹

1. Femto-ST (CNRS), Université Bourgogne Franche-Comté

Abstract: On the basis of a hydrodynamic model of the conduction electron gas[1,2], we developed a model to predict the generation of static optomagnetic field in metals.

We analytically show the role of the spin and orbital angular momenta of light (SAM and OAM, respectively), as well as the spin-orbit interaction (SOI), in the generation of an optoinduced magnetization.

Introduction: The IFE has attracted much attention for its ability to generate light-induced magnetization, thereby opening the prospect of ultrafast magnetic data storage and a non-contact excitation of spin-waves. We provide SAM and OAM representation of the IFE in metals [3]. The OAM and SOI of light provide additional degrees of freedom in the control of the IFE usually solely attributed to the SAM. We also investigate a resonant IFE within individual nanoantennas [4,5].

Results: Upon illumination, individual subwavelength gold coaxes and cylinders are shown to develop a strong optomagnetic field on the nanoscale that is controllable by the helicity of the light. In a pulse optical regime, this magnetic field is found to reach 0.3 T upon excitation at a light intensity below the damage threshold (see figure).

Our model shows that both the SAM and OAM contributions to the IFE in the metal bulk rely on an optical drag effect [6]: the underlying optoinduced current densities are proportional to the Poynting energy flow inside the metal. Finally, we numerically quantify the relative contributions of the SAM and OAM to the IFE in a thin gold film illuminated with four different focused beams carrying SAM and/or OAM (see table). Except for circular polarization, the OAM of light is found to be the main contributor to the IFE. We also numerically confirm the importance of the SOI of light in the IFE, which manifests both via SAM-to-OAM and OAM-to-SAM conversions at the focus.

[1] J. Hurst, et al. Phys. Rev. B, 98(13):134439, 2018.

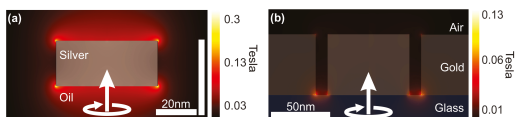
[2] Y. Lefier. Ph.D thesis, Université de Franche-Comté, 2016.

[3] V. Karakhanyan, et al. Phys. Rev. B, 105(4):045406, 2022

[4] V. Karakhanyan, et al. Opt. Lett., 46(3):613–616, Feb 2021.

[5] V. Karakhanyan, et al. OSA Continuum, 4(5):1598–1608, May 2021.

[6] N Noginova, et al. Phys. Rev. B, 84(3):035447, 2011



Particle aperture.png

	$ l=0,s=1\rangle$	$ l=1,s=0\rangle$	$ l=1,s=1\rangle$	$ l=-1,s=1\rangle$
SAM	78%	0.2%	36%	49%
OAM	22%	99.8%	64%	51%

Particle aperture sam oam.png

Giant increase of absorption cross section of CdSe /CdS single nanocrystal within a plasmonic antenna

Wednesday, 26th October - 17:48: NanoAntennas - Oral

Dr. Amit Raj Dhawan¹, Dr. Michel Nasilowski², Prof. Benoit Dubertret², Prof. Agnes Maitre¹

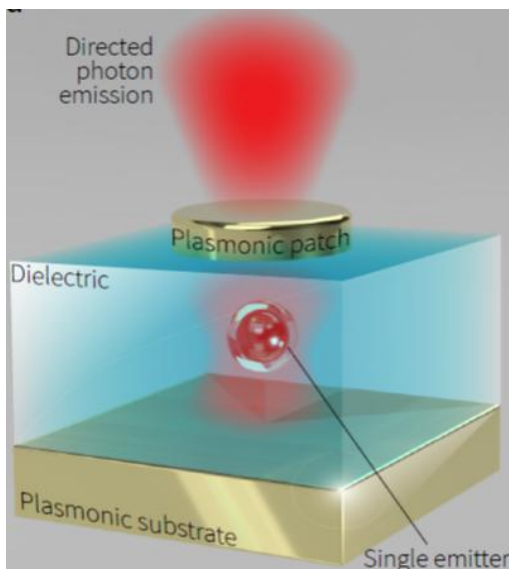
1. Institut des NanoSciences de Paris - Sorbonne Université, 2. Laboratoire de Physique et d'Etude des Matériaux - ESPCI

Nanometric semi-conductor colloidal nanocrystals, like CdSe/CdS ones, are excellent single photon sources. Their emission is stable and bright, with a spectral bandwidth of the order of $\Delta\lambda=20-30\text{nm}$. In specific conditions of high excitation or high confinement, their emission is dramatically changed. They lose their single photon source quality, the dynamic of the emission is accelerated. The spectrum becomes very broad and can reach a few 100nm. Such condition can be achieved either by exciting at high power the emitters or by coupling them to antennas [1], increasing optical confinement.

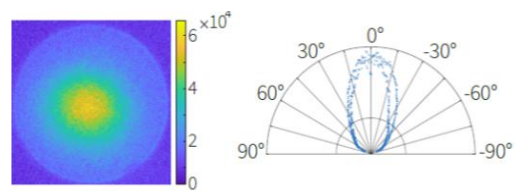
By in situ optical lithography using high order Laguerre Gaussian mode, we deterministically positioned a single colloidal CdSe/CdS emitter [2] between a thick gold layer and thin gold patch. We achieve inside such plasmonic antennas a high interaction between the emitters and the confined field excited inside the antenna. We observe large modification of emission for quantum inside antennas illustrated by directive emission, high brightness and increased efficiency. By exciting the single CdSe/CdS nanocrystal antenna with increasing power we could evidence a emission which can be interpreted up to a certain excitation power as a 2-level system, letting us measuring the absorption cross section of the nanocrystal within antenna. We evidence a increase by 3 order of magnitude of absorption cross-section of emitters inside these antennas by comparison to the one single CdSe/CdS nanocrystal lying on glass. This dramatic increase is reminiscent of the interaction between single nanocrystal and antenna plasmons. At higher excitation, multi excitation recombination becomes radiative and the emission intensity becomes non linear.

[1] Amit Raj Dhawan, and al, *Extreme multiexciton emission from deterministically assembled single emitter sub-wavelength plasmonic patch antennas*, Light: science and application, 9, 33 (2020)

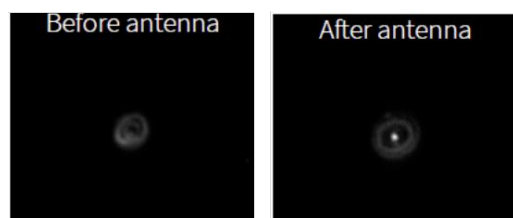
[2] A. R. Dhawan, et al, 'Efficient single-emitter plasmonic patch antenna fabrication by deterministic in situ optical lithography using spatially modulated light', Advanced materials 34, 2108120 (2022)



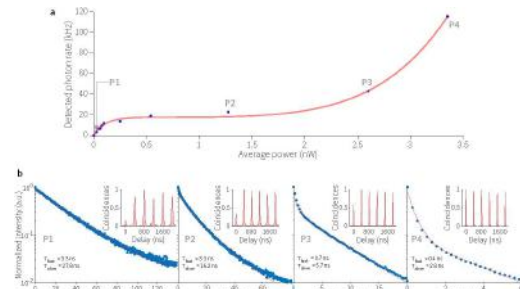
Patch-antenna.png



Emission-diagram-of-antenna.png



Brightness-of-the-antenna.png



Emission intensity and decay curves under increasing excitation.jpg

The glowing fate of hot electrons

Thursday, 27th October - 09:00: Plenary Session - Oral

Dr. Alexandre Bouhelier¹, Dr. Adrian Agreda¹, Dr. Deepak Sharma¹, Mr. Florian Dell'Ova¹, Dr. Konstantin Malchow¹, Dr. HAMDAD Sarah¹, Prof. Gérard Colas-des-Francs¹, Dr. Erik Dujardin¹

1. ICB - CNRS-Univ. Bourgogne-Franche-Comté

Light illumination of a metal generates energetic electron-hole pairs upon photon absorption by the carriers. These out-of-equilibrium carriers are referred as hot carriers. An emerging interesting facet is to utilize these hot carriers for producing minute sources of light by taking advantage of the hot carriers' relaxation process within the metal. A few hundred of femtoseconds after the absorption event the temperature of electron gas reaches thousands of Kelvins, leading to the emission of a nonlinear electromagnetic continuum spanning energies higher than the incident photons. We show in this work how the plasmonic local density of states, given by the material properties and the structural shape, defines the hot-electron generation efficiency as well as the spatial distribution of the nonlinear continuum in the system. We introduce an external control mechanism and demonstrate the successful command of the electron temperature by electrical means. We then show that the radiative decay of an out-of-equilibrium electron gas can be found in other dissipative systems such as electron-fed optical antennas and memristive devices.

Nanoaperture Tweezers: From Single Proteins to Single Quantum Emitters

Thursday, 27th October - 09:40: Plenary Session - Oral

Prof. Reuven Gordon¹

1. University of Victoria

Trapping and analysis of single unmodified proteins (down to 4 kDa in size) will be presented. Innovations in the trapping platform to improve performance (speed of detection, robustness of trapping, ease of nanofabrication) will be highlighted. The application of this technique to drug discovery and biophysics by my own group and by others will be described.

The application of nanoapertures to the analysis of perovskite quantum dots, nanoflakes of 2D materials and lanthanide containing nanocrystals will be presented. The advancement of this technique towards quantum coupling and single photon sources will be discussed.

“Hot” carriers in metal nanostructures – when they matter, and when they do not...

Thursday, 27th October - 10:50: Plenary Session - Oral

Prof. Yonatan Sivan¹

1. Ben-Gurion University of the Negev

In the last couple of decades, “hot” carriers in metal nanostructures have been simultaneously an inspirational concept to which a series of effects were ascribed, but also a source of confusion and hot debates. My talk would be aimed at improving our understanding of the role they play in these various effects.

I will start by presenting a self-consistent theory of the *steady-state* electron distribution in metals under *continuous-wave* illumination which treats, for the first time, both thermal and non-thermal effects on the same footing. I will show that the number of non-thermal electrons (i.e., the deviation from thermal equilibrium) is very small, so that the power that ends up generating these non-thermal electrons is many orders of magnitude smaller than the amount of power that leads to regular heating [1]. I will then review in detail a recent experimental quantitative confirmation of our theory obtained in current measurements through a plasmonic molecular junction [2]; peculiarly, our interpretation of the experimental data is quite different from that offered by in the original paper in which it appeared.

In the second part of the talk, I shall briefly discuss reports of observation of nonthermal electrons in two classes of experiments. First, I will review our re-interpretation of the exciting claims on the possibility to enhance chemical reactions with non-thermal electrons from metals as pure thermal effects [3], showing that in many cases, the role of thermal effects was grossly underestimated. Then, I will show that non-thermal electrons do manifest themselves in metal photoluminescence experiments, explain why they sometime “look” like thermal carriers and resolve several decade-long disagreements in the literature [4].

If time allows, I will conclude by discussing the role played by “hot” carriers generated by *ultrafast pulses*, first in photoluminescence experiments, and then in nonlinear optics and photoemission measurements.

References

- [1] Dubi & Sivan, Light: Science & Applications 2019
- [2] Dubi, Un & Sivan, Nano Letters 2022
- [3] Sivan & Dubi, Applied Physics Letters: Perspective 2020
- [4] Sivan & Dubi, ACS Nano 2021

Purcell Effect in Colloidal Plasmonic and Dielectric Resonators

Thursday, 27th October - 11:30: Plenary Session - Oral

Dr. Sébastien Bidault¹

1. Institut Langevin, ESPCI Paris, CNRS

Light-matter interactions in condensed media at room-temperature are fundamentally limited by electron-phonon coupling. For instance, while the excitation cross-section of an isolated atom, or of a single quantum emitter at cryogenic temperatures, can reach one half of the wavelength of light squared (meaning that ~50% of incoming photons will interact for a diffraction-limited excitation); this value is reduced by 6-7 orders of magnitude for a fluorescent molecule or for a colloidal quantum dot at room temperature because of homogeneous phonon broadening. In order to render the exceptional optical properties of single quantum systems (such as single-photon emission and nonlinearities) efficiently accessible at room temperature and in condensed media, it is essential to enhance and optimize these interaction cross-sections.

In this presentation, I will detail some of our recent work towards this goal. In particular, I will describe how DNA-based self-assembly can be used to introduce, in a deterministic way, a controlled number of quantum emitters in the nanoscale hot-spot of a plasmonic resonator. Using this approach, we can enhance single-photon emission from fluorescent molecules by more than two orders of magnitude in a weak-coupling regime. Using five organic molecules, it is also possible to reach a strong-coupling regime with a single dimer of gold nanoparticles.

An alternative platform to plasmonics, in order to enhance light-matter interactions at room temperature, is the use of nanoscale optical resonators made of high-index dielectric materials such as silicon or gallium phosphide. I will discuss some of our recent work on the use of silicon resonators to enhance or inhibit spontaneous emission from electric or magnetic optical emitters; as well as the development of colloidal dielectric resonators to observe Purcell enhanced linear and nonlinear luminescence from these weakly emitting semiconductors.

Aggregation of Gold Nanoparticles Induced by Halide Salts

Thursday, 27th October - 13:30: Poster Session - Poster

Dr. Vittorio Scardaci¹, Dr. Marcello Condorelli¹, Ms. Lucrezia Catanzaro¹, Prof. Giuseppe Compagnini¹

¹. Department of Chemical Science, University of Catania

Introduction

Metal nanoparticles exhibit unique optical properties due to their interaction with electromagnetic fields, known as Surface Plasmon Resonance (SPR). This is dependent on the environment as well as their size, shape and aggregation state. Gold nanoparticles (Au NPs) have been proposed for applications in a wide range of fields including sensing, medicine, photonics and many others. Their SPR can be tuned by changing their shape into e.g. nanorods, nanoplates or nanostars. Alternatively, SPR can be tuned by controlling their aggregation state. In this study, we present the controlled aggregation of Au NP prepared by laser ablation in liquids (LAL) by addition of halide salts.

Methods

Au NPs are prepared by laser ablation in liquid using an ablation wavelength of 1064 nm at 10Hz pulse frequency. The liquid environment is water kept at pH=9 and containing NaCl 0.1M. The aggregation is induced by addition of KBr and monitored by absorption spectroscopy. FDTD simulations are also employed to interpret spectroscopy results.

Results and Discussion

Fig. 1 shows that by adding KBr a new SPR band is formed and increasing its concentration such band is progressively red-shifted. Simulations suggest that at low KBr concentration (25mM) short NP chains are formed, while longer chains are formed at 30mM. Further increasing KBr concentration produces SPR band that is not related to linear chains, thus we believe that branched or 3D structures are formed, rather than linear chains. We also investigate the effect of temperature on the aggregation process. Fig. 2 shows that for 30mM KBr concentration the aggregation is promoted at lower temperature and prevented at higher temperature, where the new SPR band hardly forms. This is because despite more frequent and energetic collision, at higher temperatures the attachment rate is lower, while at lower temperature the attachment rate is higher and the aggregates that form are more stable.

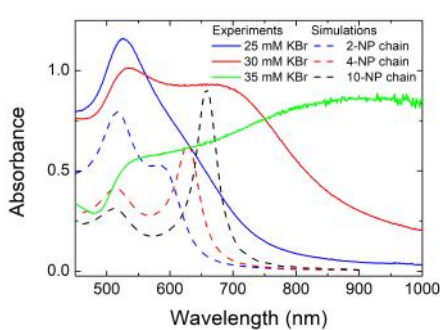


Fig 1 nanop.jpg

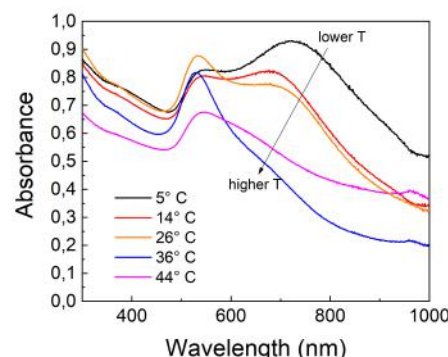


Fig 2 nanop.jpg

Electric field enhancement of dielectric nanoparticle with nanometer-sized low index slot

Thursday, 27th October - 13:30: Poster Session - Poster

Mr. Seokhyeon Hong¹, Mr. Youngsoo Kim¹, Mr. Seung Hyeon Hong¹, Mr. Sanghyeok Yu¹, Ms. Bo Kyung Kim¹, Prof. Soon-Hong Kwon¹

1. Department of Physics, Chung-Ang University

Many studies are being conducted to enhance the local electromagnetic field to enlarge light-matter interaction for the sensitive sensors, light emitters, nonlinear devices, etc. A general method for generating high local electric fields at sub-diffraction limit scales is using plasmonic resonance with metals. However, inherent metallic absorption loss may hinder the control and broaden the linewidth of resonance. So, a method of enhancing a local electric field using a gap mode with a dielectric structure is being studied. The gap mode is a phenomenon in which the electric field is strengthened by the continuity of the electric displacement field in a high refractive index material with a low refractive index gap. In addition, a subwavelength-size dielectric particles show fundamental electric dipole, magnetic dipole, high order modes. The resonant wavelength of Mie resonance can be tuned by controlling the size, shape and effective refractive index of nanoparticles. Especially. The magnetic dipole mode of the dielectric particles shows the circular displacement currents excited inside the particle by the incident wave.

We propose a split dielectric antenna consisting of the high refractive index cylinders ($n = 3.48$) with low refractive index ($n = 1.44$) gap as shown in Figure 1, which shows a high local vertical electric field intensity at low index gap. The smaller the gap size, the stronger the intensity of the e-field in the gap tends to be due to the continuity of the electric displacement field in Figure 2. In addition, the 10-nm thick gap (G) shows the highest electric field intensity with up to 16x in air. We can increase the value up to 39x as shown in Figure 3 by coupling additional electromagnetic energy from an underlying perfect electric conductor - metal substrate. Our structure has low energy loss and high efficiency. Which can be used in combination with biosensor, light emitter.

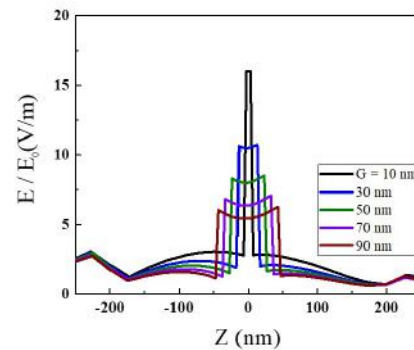
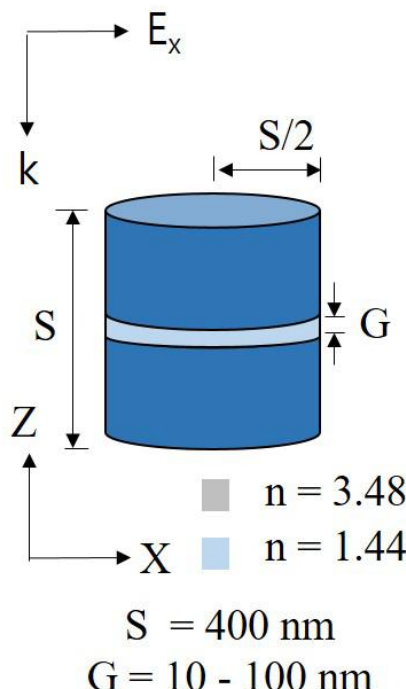


Figure 2.jpg

Figure 1.jpg

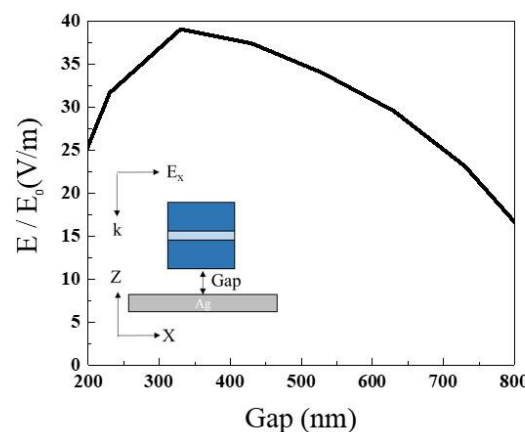


Figure 3.jpg

PSF distortion and mislocalization by dielectric nanoparticles in single-molecule microscopy

Thursday, 27th October - 13:30: Poster Session - Poster

Mr. Masih Fahim¹, Mr. Teun Huijben², Dr. Kim I. Mortensen¹, Prof. Jonas N. Pedersen¹, Prof. Rodolphe Marie¹

1. Department of Health Technology, Technical University of Denmark (DTU), Denmark, **2.** Technical University of Denmark

Colloidal micro- and nanoparticles are often used for biosensing and drug delivery. They are typically functionalized with biomolecules on their surfaces, and their performance depends on the coverage and distribution of these biomolecules. Current analysis methods are based on ensemble averaging and lack the ability to reveal particle-to-particle variation of the functionalization efficiency.

Single molecule localization microscopy (SMLM) can resolve individual binding sites and analyze such heterogeneity but scattering of light by the nanoparticle is expected to distort the point spread function (PSF) and cause localization errors [1].

Here we show that PSF distortion occurs in a typical SMLM experiment using 200 nm polystyrene beads (Fig 1 A). The green, fluorescent beads are conjugated with 9 bases-long oligonucleotides and deposited on a plasma-treated glass surface. DNA-PAINT [2] movies are captured using TIRF illumination at 100 ms exposure for 10000 frames in the presence of 1 nM imager strands labelled with ATTO655. The green signal is used to localize each bead and correct for drift.

From analytical PSF calculations, we predict that the distortion of the PSF caused by the nanoparticle can be captured by fitting a symmetric Gaussian function to the DNA-PAINT signal. The spot width is smallest for an emitter placed at the equator of the bead (Fig. 1 B), independently of the focus condition within the diameter of the bead. More surprisingly, the PSF distortion results in a spot width smaller than the PSF in absence of the nanoparticle. In our experiments, we indeed observe two populations of spots where one has a constant width. The other corresponds to emitters close to the equator of the bead, and they have a spot width close or below the diffraction limit (Fig. 1 C). This spot size reduction could wrongly be interpreted as high localization precision but is a combined effect of defocusing and PSF distortion.

With these calculations and experiments, we hope to improve localization by combining exact knowledge of the focal plane and accounting for PSF deformation due to the dielectric colloid.

[1] Raab, M., et al. Nature Communications (2017).

[2] Schueder, F., et al. Nature Methods (2019).

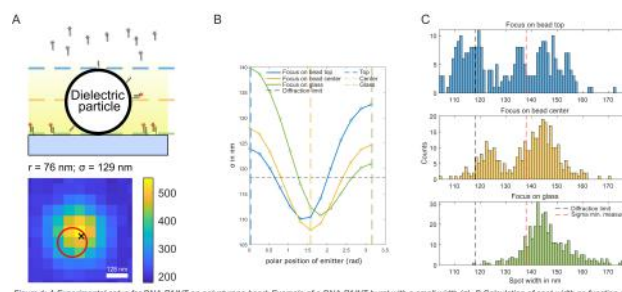


Figure 1: A Experimental setup for DNA-PAINT on polystyrene bead. Example of a DNA-PAINT burst with a small width (σ). B Calculation of spot width as function of emitter position on the bead for three different focus conditions. C Measured spot width of the same three focus conditions with $N_{\text{burst}} = 407$, $N_{\text{emitter}} = 398$ & $N_{\text{gap}} = 290$.

Psf distortion and mislocalization by dielectric nanoparticles.png

Single-photon superradiance: effects of the dielectric environment and accuracy of the rotating-wave approximation

Thursday, 27th October - 13:30: Poster Session - Poster

**Mr. Mads A. Jørgensen¹, Dr. Devashish Pandey¹, Dr. Sanshui Xiao¹, Dr. Nicolas Stenger¹,
Dr. Martijn Wubs¹**

1. Department of Electrical and Photonics Engineering, Technical University of Denmark

Introduction:

The electromagnetic environment influences the spontaneous-emission rate of a quantum emitter, but also the collective decay (superradiance and subradiance) of a collection of emitters. In a solid, dephasing due to phonons often but not always spoils the collective decay. The present study of collective decay in a 2D material close to a plasmonic surface is especially relevant for a remarkable class of lifetime-limited defect emitters in hexagonal boron nitride.

Methods:

We employ a multiple scattering theory where collective emission is described by the Green function of the macroscopic Maxwell wave equation. We calculate the propagator between various quantum emitters positioned in a multilayer medium [in preparation, 2022]. We also determine how much the propagator differs from the Green function when making the common rotating-wave approximation (RWA) [*J. Phys. B* 55, in press (2022)].

Results:

We consider emitters embedded in a thin high-index dielectric layer with either air or metal as a substrate. Both configurations allow for guided modes. The guided and surface-plasmon modes are shown to play a significant role in the collective decay (super- and subradiance) of emitters at all lateral separations considered. The relative orientation of the emitters w.r.t. each other and to the interfaces of the medium determine whether the guided modes enhance or inhibit collective decay. The largest effect is found for dipoles oriented along the plane. Making the RWA only affects the real part of the induced inter-emitter interactions. For free space, the RWA may lead to induced interatomic interactions that are wrong by up to a factor of two, in contrast to a scalar model where the “RWA error” even diverges in the near field.

Discussion:

Collective emission in layered systems is affected by guided modes, with the strongest effect for dipoles oriented along the planes, which is the most common orientation for emitters in 2D materials. Making the RWA in the light-matter interaction has subtle effects: it affects neither single-emitter spontaneous-emission rates, nor the collective emission rates of two identical emitters. But for three or more identical emitters or for two slightly detuned emitters, the RWA does influence the calculated collective rates.

The Handedness (Chirality) Of A Neuronal Molecule Using Plasmonic Chains

Thursday, 27th October - 13:30: Poster Session - Poster

Mrs. Shahin Ghamari¹, Dr. Hsin Yu Wu¹, Prof. Frank Vollmer²

1. 1 Living Systems Institute, University of Exeter, Stocker Road, Exeter EX4 4QD, United Kingdom **2** Department of Physics and Astronomy, University of Exeter, Stocker Road, Exeter EX4 4QL, United Kingdom, **2.** 1, Living Systems Institute, University of Exeter, Stocker Road, Exeter EX4 4QD, United Kingdom **2**, Department of Physics and Astronomy, University of Exeter, Stocker Road, Exeter EX4 4QL, United Kingdom.

Most naturally occurring molecules are chiral. Chiral molecules have two possible three-dimensional (3D) structures, known as enantiomers, with a property of broken mirror symmetry. Detection and characterization of enantiomers are critical in biomedical science and pharmaceuticals since the two enantiomeric forms, e.g., the l- and d-isomer of a biomolecule, could have dramatically different impacts on our living systems. Cysteine (Cys) is an example that has gained much attention among chiral species due to its vital biological functions in neuronal tissues, the brain, and metabolism.

Circular dichroism (CD) spectroscopy is generally used for analyzing the optical activity of chiral molecules, which typically measures the slight differences in the interaction of left- and right-circularly polarized light with a chiral substance. The CD spectra of a set of enantiomers show mirror-image curves with the same magnitude. The most significant chiroptical signal of chiral molecules is often located in the UV spectral range, associated with the molecule absorption band. However, the chiroptical signals of enantiomers are extremely weak. To develop susceptible chiral analysis techniques, plasmonic structures can amplify the weak optical signals of chiral molecules and provide an elegant way for achieving intense optical activity in the visible spectral region. Theoretical calculations and experimental work have shown that the chiral plasmonic signal intensities are proportional to the concentration of AuNRs in the nanochains, as depicted in Figure 3. The characterization of the plasmonic chains and the attachment of the enantiomers on the surface of AuNRs confirm by UV-Vis spectra and transmission electron microscopy (TEM) depicted in figure 1 and Raman spectroscopy (figure 2), respectively. The assemblies of Au NRs induced by L- and D-isomer exhibit strong CD signals in the visible region, which is attributed to the chiral current inside AuNRs. No CD signal was displayed for discrete NRs. After triggering self-assembly with L- and D-Cys, distinct CD signals were immediately observed in the LPB region of the spectrum, shown in figures 3 and 4. In this work, the UV and CD spectra of assembled AuNRs induced by L- and D-Cys stated that the enantiomers of Cys could be identified in plasmonic nanochains.

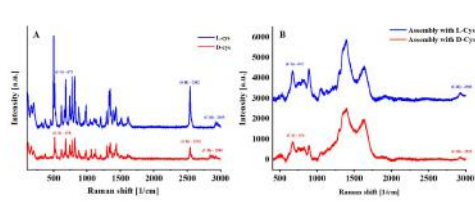


Fig. 2: (A) D-Cys (red), L-Cys (blue) induced Raman spectra in crystalline phase; (B) Raman spectroscopy of assembled AuNRs induced by D-Cys (blue), L-Cys (blue). Disappearance of c-H band at ~1250 (cm⁻¹) and appearance of c-H(=O) ~ 360 (cm⁻¹) and c-H(=O) ~ 900–750 (cm⁻¹) pointed out the attachment of L- and D-Cys on the surface of the AuNRs.

Raman.jpg

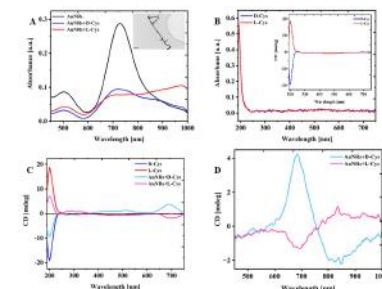


Figure 1: (A) UV-Vis spectra of AuNRs and bare AuNRs, mixture of AuNRs and L-Cys (red), and mixture of AuNRs and D-Cys (blue); (B) UV-Vis spectra of AuNRs and bare AuNRs, mixture of D-Cys (blue), and mixture of L-Cys (red); (C) CD spectra of AuNRs and L-Cys (blue), mixture of AuNRs and L-Cys (pink), and mixture of AuNRs and D-Cys (red); (D) CD spectra of mixture of AuNRs and L-Cys (pink), and mixture of AuNRs and D-Cys (cyan) in the VIS-NIR region.

Figure 1.jpg

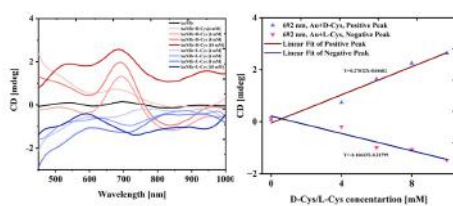


Fig 4: (A) The CD spectral changes of mounted AuNRs mounted by D-Cys (red) and L-Cys (blue) for different concentrations of L- and D-Cys. (B) The linear relationship between CD signal at 692 nm and the added concentration of D-Cys and L-Cys.

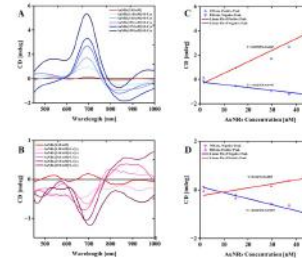


Fig 5: (A) and (B) The CD spectra of assembled AuNRs in the presence of D-Cys (not efficient) and L-Cys (not so people) for different concentrations of AuNRs. (C) and (D) Magnitude of pheomeric CD signals versus the concentration of AuNRs in the presence of D-Cys and L-Cys respectively.

Figure 4.jpg

Au vs cd figure3.jpg

Efficient Si metasurface mirror design for practical realization

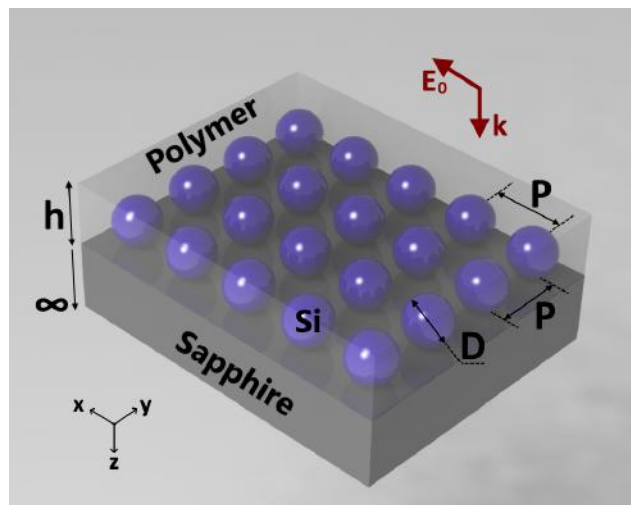
Thursday, 27th October - 13:30: Poster Session - Poster

Ms. Mariia Matiushechkina¹, Dr. Andrey B. Evlyukhin², Dr. Vladimir Zenin³, Prof. Boris Chichkov², Prof. Michèle Heurs¹

1. Max Planck Institute for Gravitational Physics / Leibniz Universität Hannover, **2.** Leibniz University Hannover, **3.** University of Southern Denmark

A wide variety of metastructures are being developed with the purpose of manipulating light behaviour. The optimization of dimensional parameters of these structures and the use of particular material properties endow to apply them in a broader range of quantum experiments. One of such projects considers the development of highly efficient reflective coatings at the telecom wavelength with low optical and mechanical losses for the future generation of gravitational wave detectors. We suggest using a monolayer of periodically arranged silicon nano-spheres as a coating on sapphire substrates. Due to their electric and magnetic dipole resonant responses to the incident light field [1], the so-called metasurface can exhibit perfect reflection. Our investigation goes one step further as we also consider the influence of the substrate and a polymer layer, that fixes the position of nano-spheres, on the sustainability of optical properties. We estimate functionality and accuracy by analyzing structural and dimensional imperfections. The theoretical and numerical results are going to be checked in the future with the experimental realization of the metastructure.

[1] Andrey B. Evlyukhin, Mariia Matiushechkina, Vladimir A. Zenin, Michèle Heurs, and Boris N. Chichkov, Opt. Mater. Express **10**, 2706-2716 (2020)



Schematic view of silicon metasurface.png

Fabrication of dielectric metasurfaces with 2π phase control

Thursday, 27th October - 13:30: Poster Session - Poster

Ms. Shan Song¹

1. Institute of solid state physics, Leibniz Universität Hannover, Appelstraße 2, 30167 Hannover

Recently, researchers have shown an increased interest in tailoring light by metasurfaces in quantum technologies. A metasurface is a two-dimensional ultra-thin layer, artificially fabricated by planar structures on a sub-wavelength scale. Compared to conventional optical elements, metasurfaces are capable to manipulate the light wavefront accurately by specific nanostructures and integrated with single photon emitters by microfabrication process. The efficient imaging of quantum emitters by metasurfaces is the focus of interest, which can be achieved by high numerical aperture metasurfaces with 2π phase control. Here, we optimize the fabrication process of dielectric metasurfaces, which are composed of polysilicon nanodiscs with various diameter (200 – 350 nm) and periodicity (380 – 700nm) on a quartz glass substrate. The fabrication process includes mainly the deposition of a thin polysilicon layer by low-pressure chemical vapor deposition, the pattern determination by application of hydrogen silsesquioxane negative resist in electron beam lithography, the pattern transfer on polysilicon layer by reactive ion etching and covered with thin polydimethylsiloxane layer. Besides, the phases of metasurfaces are measured by a interferometer using a laser with wavelength of 632 nm. In scheme, based on different designs with various nanodisc diameters and periodicity, we are developing a diameter-dependent phase library, where the proper phases and their corresponding parameters of nanostructures are chosen to design and fabricate a high numerical aperture metasurfaces generating a full 2π phase shift.

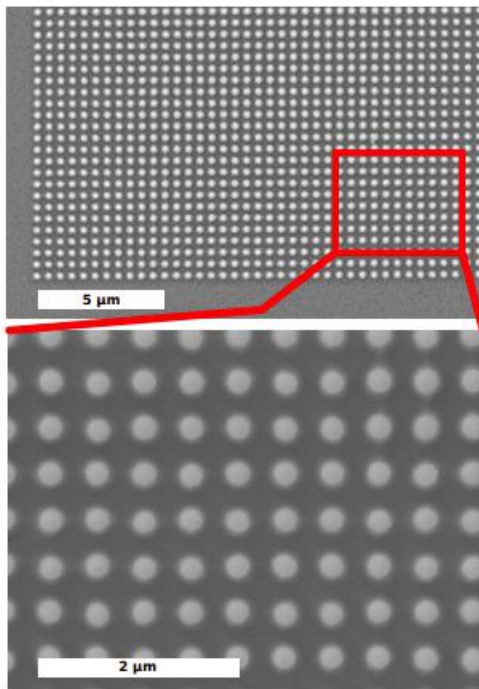
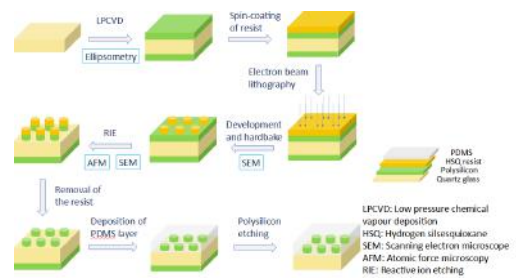


Figure 2: Silicon nanodisks produced using electron beam lithography and reactive ion etching. The diameter is about 230 nm and the period is 460 nm.



2.png

1.png

Thermo-optical simulation of Bragg gratings for monolithically integrated extended cavity diode lasers

Thursday, 27th October - 13:30: Poster Session - Poster

Dr. Igor Nechepurenko¹, Ms. Yasmin Rahimof¹, Mr. Sten Wenzel¹, Dr. Bassem Arar¹, Dr. Andreas Wicht¹

1. Ferdinand-Braun-Institute (FBH)

Monolithically integrated extended cavity diode lasers (mECDL) are high-profile photonic devices on the grounds of their cutting-edge attributes such as electro-optical efficiency, robustness and miniaturization capabilities [1]. The consequent functionality improvement of diode lasers by monolithic integration comes at the cost of soaring required numerical and theoretical comprehension so as to streamline the design process. Designing a semiconductor laser chip chiefly relies on the numerical simulation of its dynamic behavior, which is governed by complex and interlinked electro-optical and thermal phenomena. The opted multiphysics approach to numerically study the semiconductor laser chip avails of various simulation tools, i.e. waveguide mode and thermal solvers along with the calculation of material parameters such as the refractive index and current density. Finally, the used modules and tools will be interconnected together through numerical loops and self-consistency requirements.

In this particular study, the distribution of the optical field and heat were investigated, which in turn will aid the mECDL design process in terms of thermal and waveguide design, including the design of the Bragg grating. Therefore, in our study a numerical multiphysics description of a GaAs-based semiconductor laser chips operating at 1064 nm optical wavelength with a total length of 8 mm as the cornerstone of mECDL assessment was developed. The absorption heating in the Bragg gratings section was taken into account.

As a result of the heating, it was shown that a thermally induced chirp is observed. The presence of the chirp changes the reflection spectrum of the gratings, thus changing the field distribution in the longitudinal direction and consequently the heating distribution. In order to simulate such a system, a coupled thermo-optical ridge waveguide description is required. This can be done with the coupled mode theory and 3D thermal modeling. As a result of the modeling, a thermo-optical response of Bragg gratings was demonstrated. Application of such a multi-physical model will allow further improvement of Bragg grating design techniques for extended diode lasers.

References:

- [1] Wenzel, S., et.al.. CLEO (2021): ATh4G-3.

Glyphosate IR spectroscopy with a plasmonic sensor optical transductor based in functionalized semiconductor nanoantennas

Thursday, 27th October - 13:30: Poster Session - Poster

Dr. Anis Taleb Bendiab¹, Mrs. Cécile Pohar¹, Dr. Marion Mortamais², Dr. Nicola Marchi³, Dr. Julie Perroy³, Dr. AMARIA BAGHDADLI⁴, Prof. Thierry Taliercio¹, Dr. Fernando Gonzalez-Posada Flores¹

1. IES - Univ. Montpellier - CNRS, **2.** INM, Univ. Montpellier, INSERM, CeAND, France., **3.** IGF, CNRS UMR 5203, Inserm U1191, Univ. Montpellier, **4.** Univ. Paris-Saclay, UVSQ, Inserm, CESP, CeAND, Fac. Medecine, Univ. Montpellier

Glyphosate is the most used pesticide in the world since the last century, but the most difficult to detect in the environment.[1] Emerging epidemiological studies suggest that exposure to pesticides associates with atypical neurodevelopmental trajectories, representing a risk factor for autism spectrum disorders (ASD) in particular [2]. In this multidisciplinar and transactional projet, a path towards autism spectrum disorder origins is presented in relation to environmental pesticides and genetic predisposition. The project is divided in clinical, experimental and techronological approaches and constitutes a solid consortium. The clinical approach entails the relation between the exposure to pesticides of pregnant-women, new born to 10 years-old children included in the ELENA French cohort [3]. The experimental approach focuses in the neuropathology and comportamental analysis of mice with and without ASD-prone gene-modified exposed to glyphoste in their food. The technological approach seeks a practical solution for glyphosate biosensors for rapid control of levels in accordance with regulations for environmental control and protection. We propose a plasmonic optical sensor transductor with all-semiconductor plasmonic nanoantennas made of epitaxially grown, highly doped InAsSb on GaSb substrates. Large arrays of nanoantennas were fabricated by optical lithography and dry etching. [4] The optical properties were studied experimentally by Fourier transform IR spectroscopy and in simulations using the rigorous coupled wavelength analysis. We evaluate a functionalization of the semiconductor surface based in silane compounds and EDC/NHS chemistry is used to immobilize glyphosate on the surface. Different glyphosate solutions (~mM), usually applied to soils in the form of aqueous solutions, are tested to find the enhancement of the characteristic IR absorption features. In the figure A, a SEM image of dry glyphosate, figure B shows the immersion of InAsSb optical transductor in a 1mM concentration glyphosate dilution in DI H₂O, figure C and D show dried glyphosate dilution on top of InAsSb nanoantennas and Au surface. Finally, Figure E shows preliminary results in spectroscopy on both surfaces.

[1] A.L.Valle et al, Environmental Chemistry Letters (2019)17:291

[2] J.R. Roberts, et al. Pediatric Research (2019)85:234

[3] J. S. Ongono et al. Journal of Psychiatric Research (2022)145:197

[4] F. Barho et al. Nanophotonics (2018)7:507

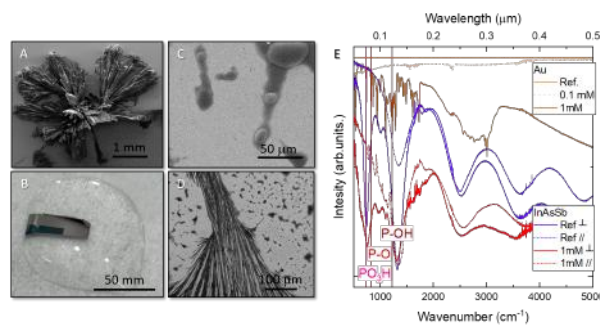


Image gly.png

Plasmonic nanoparticles for the exploration of strong field physics

Thursday, 27th October - 14:30: Hot Electrons - Oral

Dr. Sylvie Marguet¹, Prof. Bruno Palpant², Dr. Ludovic Douillard³

1. Univ. Paris-Saclay, CEA, CNRS, NIMBE, F-91191 Gif-sur-Yvette, France, **2.** Univ. Paris-Saclay, CNRS, ENS Paris-Saclay, CentraleSupélec, LuMIn, F-91190 Gif-sur-Yvette, France, **3.** Univ. Paris-Saclay, CEA, CNRS, SPEC, F-91191 Gif-sur-Yvette, France

At small scale, the interaction of light with a metallic object leads to the occurrence of remarkable resonances within the absorption spectrum, the plasmonic modes. They correspond to coherent collective oscillations of charge carriers [Mie 1908] and generate localized fields of high amplitude. In short, plasmonics offer the option to explore new physical properties in extreme regimes in particular the physics of strong fields.

Here we report on the use of common colloidal Au nanorods as versatile hot electron sources in various emission regimes. The electron emission mechanism can be continuously switched from non-linear photoelectric emission in the weak field regime to a cold field tunnelling emission in the strong field regime. The investigation is conducted at the individual object level by monitoring the kinetic energy of electrons emitted at the hot spots of individual nanoparticles shined at their plasmon longitudinal resonance [Dombi 2013]. The kinetic energy cut-off of the ponderomotively accelerated electrons follows a linear behaviour with the irradiance of the pulsed laser source. A cut-off energy of the order of 10 eV is easily obtained for a modest light irradiance in the 1 GW/cm² range. Figure 1 shows the electronic kinetic energy distribution curves of the electrons emitted by an individual Au nanorod excited at its longitudinal plasmon resonance for different laser irradiances. The relevance of plasmonic particles to strong field physics will be discussed.

Methods. Au nanorods are prepared by colloidal chemistry; light matter interaction at the nanometer scale is investigated by photoemission electron microscopy PEEM [Hrelescu 2011].

[Dombi 2013] P. Dombi, et al. Nano Lett. 13 (2013) 674

[Hrelescu 2011] C. Hrelescu, et al. Nano Lett. 11 (2011) 402

[Mie 1908] G. Mie, Ann. Phys. (Leipzig) 25 (1908) 377

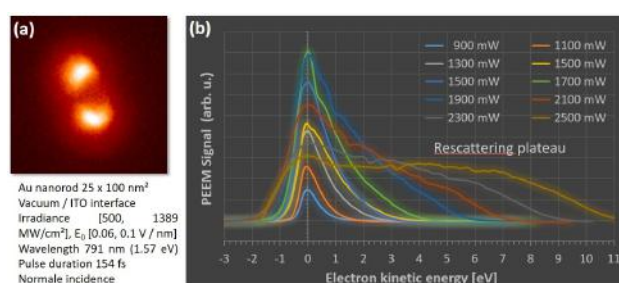


Figure 1.(a) Near field map of a Au nanorod shined at its longitudinal plasmon resonance – PEEM imaging, (b) Electron kinetic energy distribution curves for different laser powers – PEEM spectrometry.

Nanop2022 ldouillard figure1.jpg

Extremely large broadband emission of CdSe/CdS nanocrystals under high excitation

Thursday, 27th October - 14:47: Hot Electrons - Oral

Mr. Damien Simonot¹, Mr. Poncia Nyembo¹, Dr. Celine Roux-Byl², Dr. Thomas Pons², Dr. Simon Huppert¹, Prof. Agnes Maitre¹

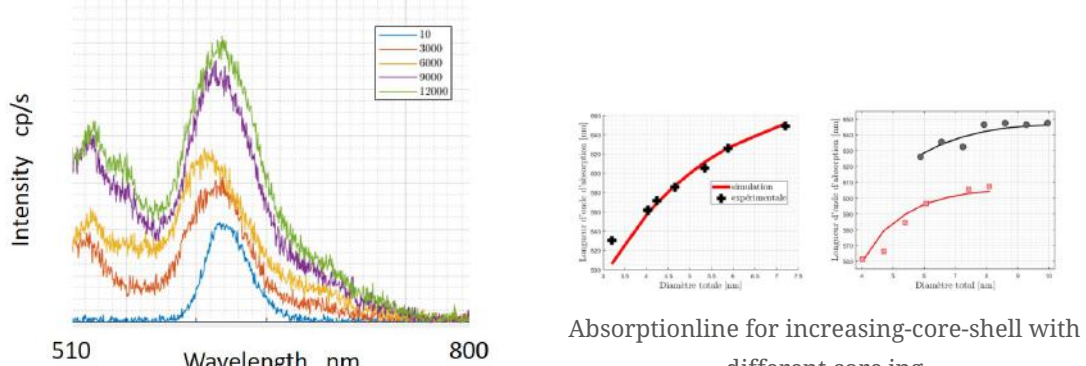
1. Institut des NanoSciences de Paris - Sorbonne Université, 2. Laboratoire de Physique et d'Etude des Matériaux - ESPCI

Single core/shell CdSe/CdS colloidal nanocrystals are usually used as efficient single photon sources working at room temperature, with a narrow spectrum of $\Delta\lambda=20\text{nm}$. For large shell, they evidence a strong resistance to high excitation and can withstand a few 10^6W/cm^2 . Under high excitation their emission change dramatically, emission evolves non linearly with laser excitation power and the spectrum range can reach a few 100nm. Therefore, emission cannot be anymore explained as excitonic recombination issued from a two-level system and other radiative recombinations have to be considered and demonstrated.

In order to understand such a behavior, we use a statistical description of the electrons and holes population as fermi dirac distributions over the range of discrete energy levels and continuum states level of electrons and holes of spherical core shell quantum dots. Radiative recombination of excitons following those distributions opens the way to large spectral range emission.

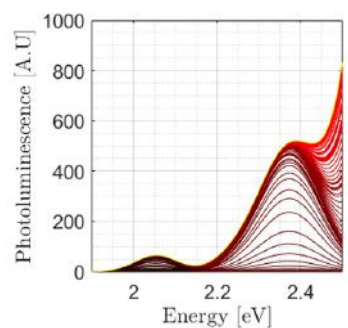
In order to develop such a model, the first step is to solve Schrödinger equation for holes and electrons in such a core shell structure, taking into account different parameters such as the presence of ligands, and the pressure induced by the shell on the core, which induces shifting and bending of the electrons and holes energy levels. The key parameter governing the excitons recombinations is the alignment between CdSe and CdS first excited electron state. Unfortunately this parameter remains mainly indeterminate in the scientific literature. Our model combined with absorption spectroscopy realized with core –shell nanocrystals, of different size, made it possible to determine experimentally this offset, which value has been confirmed by XPS spectroscopy.

Taking all those parameters into account, after predicting thick shell CdSe/CdS energy levels, we predict the evolution of emission intensity and spectrum under increasing laser excitation. As well spectral broadening could be described by our model in accordance to experimental results. Non linear increase of intensity emission with increasing excitation power could be also evidenced theoretically and experimentally.

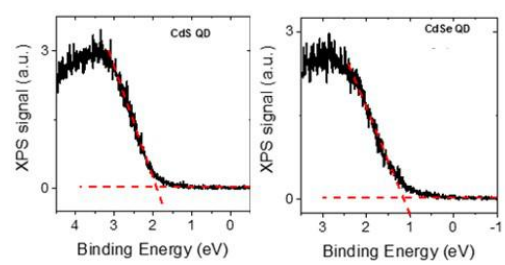


Absorptionline for increasing-core-shell with different core.jpg

Experimental-spectrum-under-increasing-excitation.jpg



Theoretical-spectrum-under increasing
excitation.png



Xps-spectrum-for-cds and cdse-cores.jpg

The nonlinear optical response and non-equilibrium electron dynamics in ITO

Thursday, 27th October - 15:04: Hot Electrons - Oral

Dr. Subhajit Sarkar¹, Dr. Ieng-Wai Un¹, Prof. Yonatan Sivan¹

¹. Ben-Gurion University of the Negev

Introduction: Low electron density Drude (LEDD) materials such as transparent conducting oxides, plasmonic nitrides, have emerged as popular candidates for high-efficiency nonlinear optical applications, due to their unique “epsilon near zero” point near Infra-Red wavelengths. Their nonlinearity is extremely large as it can change the refractive index/permittivity by 100’s of percent. Particularly, despite the large body of impressive experimental demonstrations of these effects, their theoretical modeling was mostly coarse, and has not yet conclusively elucidated the origins of this giant optical response. Here, we close this knowledge gap and provide a “first principles” modeling of the electronic response of LEDD materials to ultrafast illumination. For concreteness, we focus on Indium Tin Oxide (ITO).

Methods: We use the well-accepted Boltzmann equation (BE) approach, including all the key ingredients necessary for the faithful description of the electron dynamics. This model is complemented by proper verification of energy and charge conservation, and a coarse-grained effective two temperature model.

Results and Discussion: We find the electron heat capacity to be smaller in ITO in a manner commensurate with the lower electron density, but the electron-phonon energy transfer rate to be comparable to that in noble metals. This leads to stronger heating of the electrons, and to a faster cooling compared to noble metals [Fig. 1(a)]. Surprisingly, because of the intense illumination and associated high electron temperature, the effective chemical potential dramatically decreases and becomes negative, thus, effectively converting the Drude metal into a semiconductor [Fig. 1(b)]. We find that the drastic increase of the real part of the permittivity causes a significant detuning of the pump from the resonance such that the absorptivity drops rapidly with increased illumination intensity [Fig. 2(a)]. Consequently, the maximum values of phonon temperature increases sub-linearly with the pump peak-intensity, reaching the melting point of at 500 GW/cm² [Fig. 2(b)]. This explains, for the first time to our knowledge, the experimental observation of the high damage threshold of ITO. This further shows that the type of nonlinearity observed in ITO is not saturable (i.e., it doesn’t have a pure electronic origin), but rather thermal as for noble metals.

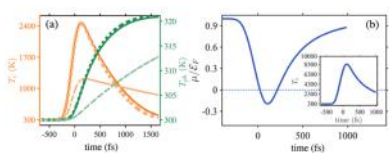


Fig. 1: (a) Effective electron temperatures (orange lines) and phonon temperatures (green lines) as a function of time for Gaussian pulse of width 220 fs and peak intensity, 2.5 GW/cm². Solid and dashed lines correspond to temperatures obtained from the eTM simulation using BE and the solution of the eTM, respectively. Dot-dashed lines correspond to the temperature dynamics of gold (Au) obtained from the eTM simulation. (b) The instantaneous chemical potential following illumination by a Gaussian pulse of width 220 fs with peak intensity is 50 GW/cm², obtained from the effective electron temperature shown in the inset.

Effective temp.png

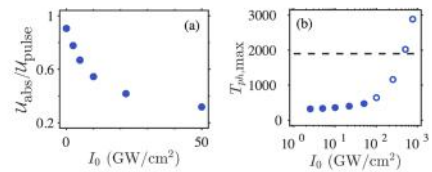


Fig. 2 (a) The total absorbed pump energy (normalized to the pump pulse energy) as a function of the pulse peak intensity. (b) The maximum phonon temperature that can be achieved for different pump peak intensities. The filled dots represent the data obtained from the simulation; and the open dots represent the estimated upper bound of the maximum $T_{ph,max}$ for I_0 up to 750 GW/cm².

Absorbed power.png

Raman amplification for trapped radiation in crystalline Si single nanoparticle

Thursday, 27th October - 14:30: Nano-optical trapping - Oral

Dr. Giovanni Mannino¹, Dr. Marcello Condorelli², Prof. Giuseppe Compagnini², Prof. Giuseppe Faraci³

1. CNR, IMM Catania, 2. Department of Chemical Science, University of Catania, 3. Department Physics and Astronomy, University of Catania

Introduction

In this work, we were able to study the interaction of light with single silicon nanoparticles using micro-Raman spectroscopy.

The precious properties of nanoparticles, as amplifier systems, have been emphasized in many papers, regarding a large variety of materials, such as Si, C, Ge, and others. We limit here to mention only Si nanostructures, showing incredible amplification properties, observed e. g. by Raman spectroscopy, as discussed in several review papers. Of course, any effort to determine the amplification mechanism of radiation absorption, scattering, and/or emission is very valuable, and not only in the visible range, being related to energy production spectroscopy.

Methods

Si nanocrystal has been synthesized by an inductively coupled plasma chemical vapor deposition equipment, obtaining monocrystalline, isolated, and monodisperse structures. Each observed crystalline particle has an octahedral shape of 100-200 nm (fig 1)(TEM and AFM). Single particle Raman scattering has been excited by using three laser wavelengths (532, 633, and 785 nm), finding an outstanding enhancement of the phonon signal compared to bulk (fig.2).

Discussion

Such an intense signal amplification is attributed to multiple reflections during the radiation traveling path inside each nanoparticle. Moreover, laser beam-induced thermal effects have been observed during the measurements at high laser fluences, some of them determining the fundamental particle melting. To better understand the behavior of the electromagnetic field inside the nanocrystal, theoretical calculation of the electromagnetic field strength and its propagation inside the nanostructure were carried out with a Finite Difference Time Domain method (FDTD). Photon trapping in a single Si nanoparticle could imply electron excitation enhancements from the valence to the conduction band since the photon energy largely exceeds the Si band gap and the evident electron concentration amplification in the conduction band could be used to increment a photovoltaic current in a device of solar energy conversion.

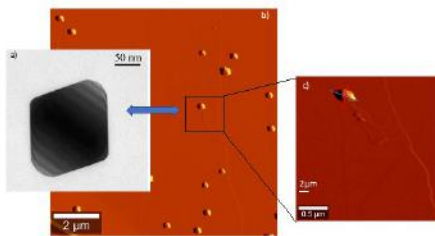


Fig 1 afm and tem images.jpg

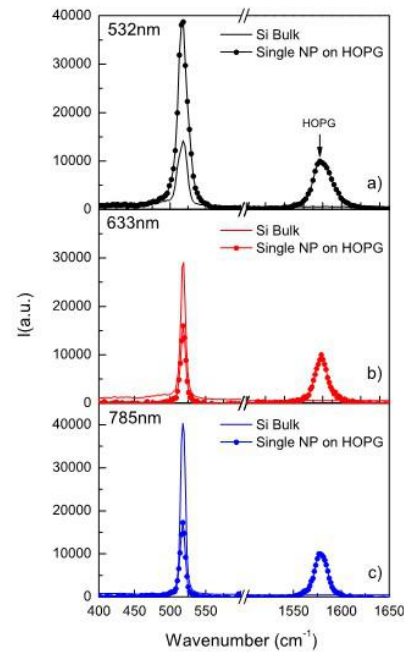


Fig. 2. raman spectra at three laser wavelengths
of a single si-np and si bulk dot-line .jpg

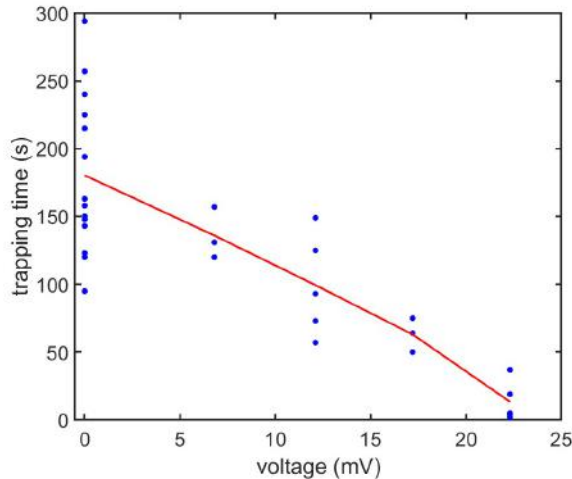
Speeding up trapping of nanoparticles in nanoaperture optical tweezers by applying a voltage

Thursday, 27th October - 14:47: Nano-optical trapping - Oral

Ms. Elham Babaie¹, Prof. Reuven Gordon¹

1. University of Victoria

Trapping single nanoparticles and biomolecules were demonstrated using optical tweezers in plasmonic apertures before. Trapping nanoparticles in a short time has been challenging due to surface charging and thermophoretic effects. Our measurements show speeding up by a factor of up to 12 in trapping is achieved for 20 nm polystyrene nanoparticles by applying an electric potential difference between the solution and the gold film where the apertures are located (Figure1). The generated electric field in the region close to the aperture makes trapping faster by electrophoresis. Proteins and biomolecules do not show similar responses to this method.



Trapping time of 20 nm polystyrene vs applied voltage.jpg

Comprehensive in-situ study of solution-based quantum dots with plasmonic tweezers

Thursday, 27th October - 15:04: Nano-optical trapping - Oral

Ms. Parinaz Moazzezi¹, Mr. Hao Zhang¹, Dr. Juanjuan Ren², Ms. Brett Henderson¹, Dr. Cristina Cordoba¹, Mr. Vishal Yeddu¹, Prof. Arthur Blackburn¹, Prof. Maksud Saidaminov¹, Prof. Irina Paci¹, Prof. Stephen Hughes², Prof. Reuven Gordon¹

1. University of Victoria, **2.** Queen's university

Cesium lead halide perovskite quantum dots (PQDs) are known as pure single-photon sources [1]. A long coherence time in addition to efficient single photon emission makes colloidal CsPbBr₃ semiconductors an appropriate candidate for quantum information technology applications [2]. Also, their strong quantum coupling initiates non-classical emission phenomenon [3]. Size analysis and coupling between QDs are two parameters which we focus on in this work.

We use an optical trapping setup [4] as an in-situ approach to analyze QDs size and coupling between two PQDs. An optical tweezer with a double nanohole aperture can determine the heterogeneity of PQDs. From the Brownian motion characteristic signal collected by an avalanche photodiode, we calculate the standard deviation and autocorrelation time constant of each single trapping event, as is shown in Fig. 1(a), which has a slope of -0.67 on a log-log plot, as expected from theory. This allows for sizing the PQDs and correlating with emission wavelength. Also, we sequentially trapped two dots in a single trap and measured the change in emission wavelength and intensity. Two-photon photoluminescence distribution for single and double PQDs trapping is shown in Fig 1(b). The intensity for double PQDs is double the single PQD trapping, and also there is a systematic red-shift in the emission peak wavelength.

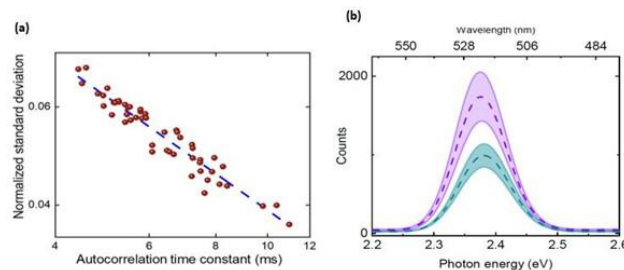
[1] C. Zhu *et al.*, “Room-Temperature, Highly Pure Single-Photon Sources from All-Inorganic Lead Halide Perovskite Quantum Dots,” *Nano Lett.*, vol. 22, no. 9, pp. 3751–3760, 2022.

[2] H. Utzat *et al.*, “Coherent single-photon emission from colloidal lead halide perovskite quantum dots.,” *Science*, vol. 363, no. 6431, pp. 1068–1072.

[3] G. Rainò, M. A. Becker, M. I. Bodnarchuk, R. F. Mahrt, M. V Kovalenko, and T. Stöferle, “Superfluorescence from lead halide perovskite quantum dot superlattices.,” *Nature*, vol. 563, no. 7733, pp. 671–675, Nov. 2018.

[4] A. L. Ravindranath, M. S. Shariatdoust, S. Mathew, and R. Gordon, “Colloidal lithography double-nanohole optical trapping of nanoparticles and proteins.,” *Opt. Express*, vol. 27, no. 11, pp. 16184–16194, May 2019.

[5] S. Wheaton and R. Gordon, “Molecular weight characterization of single globular proteins using optical nanotweezers,” *Analyst*, vol. 140, no. 14, pp. 4799–4803, 2015.



Picture1.jpg

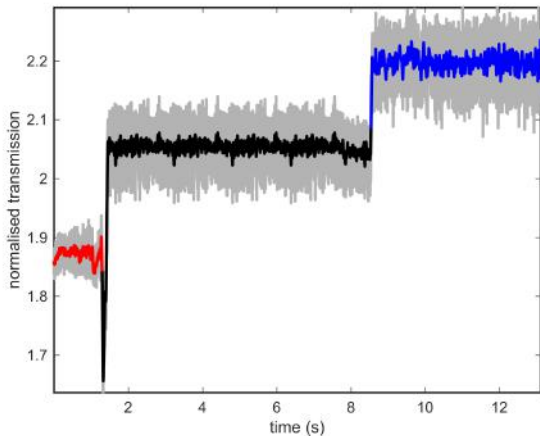
Double nanohole optical tweezers probe for protein-ligand binding

Thursday, 27th October - 15:21: Nano-optical trapping - Oral

Mr. Samuel Mathew¹, Prof. Laura Itzhaki², Prof. Ivet Bahar³, Mr. Anupam Banerjee⁴, Dr. Moshin Naqvi², Dr. Janet Kumita², Dr. Michael Ohlmeyer⁵, Dr. Demelza Wright¹, Ms. Elham Babaie¹, Mr. Mirali Seyed Shariadoust¹, Prof. Reuven Gordon⁶

1. University of Victoria, Canada, **2.** University of Cambridge, Cambridge, **3.** University of Pittsburgh, Pittsburgh, **4.** University of Pittsburgh, Pittsburgh, **5.** Atux Iskay LLC, Plainsboro, New Jersey, **6.** University of Victoria

Techniques that analyse small molecule interactions with single proteins are useful for drug discovery. Here, we specifically look at the small molecule activators of PP2A (SMAPs). In the past, we have looked at tolbutamide and phenytoin binding to off-target human serum albumin (HSA) [1]. Other groups like the Alexandrakis' group have studied immunotherapy targets using the double nanohole aperture (DNH) technique [2]. The double nanohole technique has also been used to investigate enzyme activity [3]. In the present work we look at PP2A interaction using its 65 kDa α -subunit otherwise known as pr65 [4]. We get trapping and observe a trapping signal, then we add small molecules and observe a binding signal.



Dnh signal with double jump step.png

Topological engineering of plasmonic waveguide arrays

Thursday, 27th October - 14:30: Topological photonics & Non-reciprocal nano-optic - Oral

Mrs. Anna Sidorenko¹, Mrs. Helene Wetter¹, Prof. Stefan Linden¹, Dr. Julian Schmitt¹

¹. University of Bonn

Introduction

Arrays of evanescently coupled plasmonic waveguides are a powerful platform to study the topological properties of one-dimensional lattices. Here, we present a real- and Fourier space investigation of the anomalous π -mode supported by the driven Su-Schrieffer-Heeger (SSH) model and report on the observation of localized topological states at the boundaries of a lattice with tailored losses.

Methods

Arrays of dielectric loaded surface plasmon polariton waveguides (DLSPPWs) were fabricated on a thin gold film. The coupling strength J between adjacent DLSPPWs was controlled by the relative separation. Additional losses (loss rate γ) for specific waveguides could be introduced by depositing a thin layer of chromium below the respective DLSPPWs. The evolution of the surface plasmon polariton (SPP) intensity in the arrays was characterized in real- and Fourier space by leakage radiation microscopy (LRM).

Results and Discussion

We present a joint experimental and theoretical study of the driven SSH model with periodically varying coupling strength. This model supports for suitable driving frequencies a topologically protected edge state (see Fig. 1(a)), the so-called anomalous π -mode, that is absent in the static system. By using real- and Fourier-space LRM in combination with edge- and bulk excitation (see Fig. 1(b) and (c), respectively), we can unequivocally identify the π -mode and study its frequency dependence.

Next, we study the topological properties of a lattice of equally coupled waveguides with a tailored loss distribution. The unit cell of the lattice comprises four waveguides. If one adds an equal amount of losses to the two central waveguides of the unit cell, we anticipate that the lattice becomes topologically nontrivial (see Fig. 2 (a)). In contrast, a topologically trivial lattice is expected if the same losses are assigned to either to the first or the last two waveguides. Our experiments confirm the anticipated behaviour. Localized edge states are observed both at the boundary of the nontrivial lattice as well as at the interface between the nontrivial and the trivial lattice (see Fig. 2 (b)). Conversely, the boundary of the trivial lattice does not support a localized edge mode providing conclusive evidence for the open-system control of topological properties.

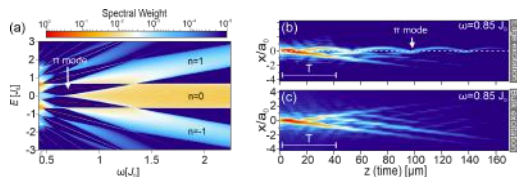


Fig 1 topology.png

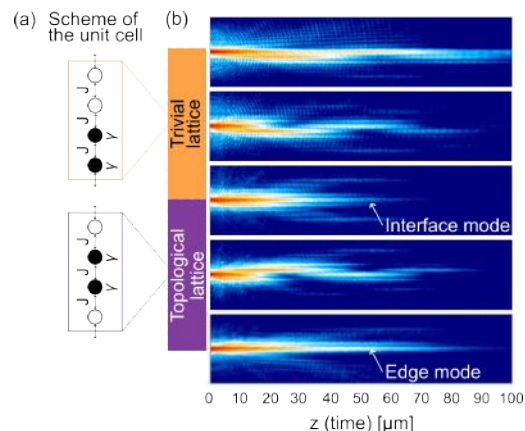


Fig 2 nhl.png

Enhanced second-harmonic generation from photonic crystal slabs via double-resonance bound states in the continuum

Thursday, 27th October - 14:47: Topological photonics & Non-reciprocal nano-optic - Oral

Mr. Ji Tong Wang¹, Dr. Feng Xia Li², Prof. Nicolae C. Panoiu¹

1. University College London, 2. Xidian University

Optical bound states in the continuum (BICs) provide a promising way to control and manipulate light-matter interactions in photonic structures, enabling large local field enhancement, which is highly desirable for efficient nonlinear frequency conversion processes at the nanoscale. Here, we utilize BICs to engineer resonances with high quality-(*Q*) factors in silicon nitride photonic crystal (PhC) slabs (Fig. 1). By investigating the angle-resolved reflection spectra and corresponding eigenmode analysis, we demonstrate, as per Figs. 2(a) and 2(b), that a photonic crystal slab supports a BIC-type resonance (BIC 1) at the fundamental frequency (FF) and a BIC-like resonance (resonance 2) at the second harmonic (SH), respectively. In the eigenmode analysis summarized in Fig. 2(c), the dispersion curve of the FF BIC with doubled frequency crosses that of the SH resonance precisely at the Γ point (~ 401 THz), where we simultaneously achieve the maximum *Q* factor for both resonances. To gain deeper insights, we present in Fig. 2(d) their electric field patterns at the Γ point and the field confinement along the out-plane (*z*) direction.

This double-resonance phenomenon is subsequently used to significantly enhance the second-harmonic generation (SHG) from PhC slabs. To quantify the efficiency of the nonlinear frequency conversion processes, Fig. 3(a) shows the dispersion map of normalized SHG intensity. The presence of two resonances in the SHG intensity map reveals the strong light-matter interaction facilitated by the FF BIC and the high-*Q* resonance at the SH. We define the angle-dependent enhancement factor, η , as the ratio between the peak value of SHG intensity at a given angle of incidence and the SHG intensity under normal incidence at the same frequency. The maximum η is nearly eight orders of magnitude, cf. Fig. 3(b), indicating the efficiency of our proposed nonlinear frequency conversion scheme. In addition, the field pattern obtained from nonlinear simulation, shown in Fig. 3(c), is consistent with that of the resonance at the SH. All simulations are based on the finite element-method implemented in Comsol Multiphysics. We believe that our approach based on double-resonance BICs provides a novel way to realize enhanced nonlinear optical interactions in photonic nanodevices.

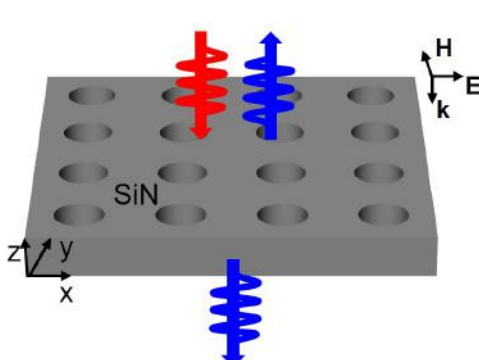


Fig. 1 schematics of a nonlinear phc slab.jpg

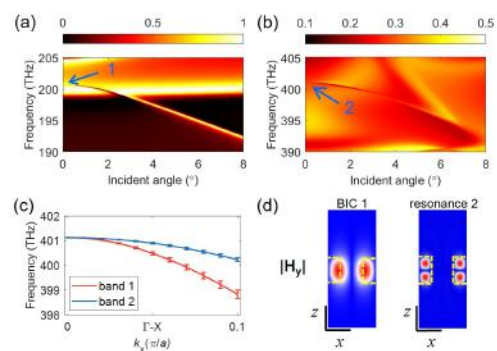


Fig. 2 a b angle-dependent reflection spectra in the linear and nonlinear regimes respectively. c eigenmode analysis. d field patterns of the eigenmodes at the point.jpg

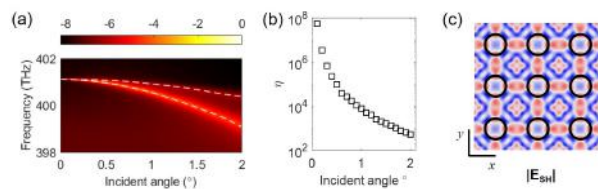


Fig. 3 a dispersion map of normalized shg intensity. b enhancement factor of shg intensity. c ab initio simulation of field pattern at the sh.jpg

Tip-induced and electrical control of the photoluminescence yield of monolayer WS₂

Thursday, 27th October - 15:04: Topological photonics & Non-reciprocal nano-optic - Oral

Dr. Ricardo Javier Peña Román¹, **Dr. Rémi Bretel**², **Dr. Delphine Pommier**², **Dr. Luis E. Parra López**³,
Dr. Etienne Lorchat⁴, **Dr. Elizabeth Boer-Duchemin**², **Dr. Gérald Dujardin**², **Prof. Luiz F. Zagonel**¹,
Dr. Guillaume Schull³, **Prof. Stéphane Berciaud**³, **Dr. Eric Le Moal**²

1. Institute of Physics “Gleb Wataghin”, Department of Applied Physics, State University of Campinas-UNICAMP, **2.** Université Paris-Saclay, CNRS, Institut des Sciences Moléculaires d’Orsay, **3.** Institut de Physique et de Chimie des Matériaux de Strasbourg, Université de Strasbourg, CNRS, **4.** NTT Physics and Informatics Laboratories, NTT Research

Monolayer transition metal dichalcogenides (TMDs) are two-dimensional (2D) direct bandgap semiconductors that have the potential to lead to breakthrough applications in nanodevice technologies due to their unique optical and electronic properties [1]. The photophysics of monolayer TMDs is governed by the dynamics of bound electron-hole pairs (i.e., excitons) and their interactions with charge carriers [2]. Manipulating the creation, diffusion, and recombination of excitons is essential for the performance of monolayer TMD-based devices. In particular, locally controlling the radiative quantum yield and the formation of charged excitons (i.e., trions) in these materials has been a long-sought-after goal. Attempts to achieve such nanoscale control have been reported, for example using the plasmonic tip of an atomic force microscope [3]. Nevertheless, most of the techniques based on a scanning probe that are used to locally control or excite excitons in 2D materials do not provide any direct information about the local diffusion and recombination processes of these excitons, a key aspect for the integration of these materials into devices.

In this communication, we present a novel method to locally and electrically control the radiative quantum yield of monolayer TMDs on a transparent electrode (i.e., indium tin oxide-coated glass) using a scanning tunneling microscope equipped with a tungsten tip. Using a combination of scanning tunneling microscopy and wide-field laser-induced photoluminescence microscopy, we demonstrate and we spatially and spectrally resolve the reversible effects of the biased tip-sample junction on the excitonic properties of a WS₂ monolayer [4]. The near-field non-radiative electromagnetic energy transfer from the excitons to the tungsten tip quenches the luminescence in a diffraction-limited area below the tip. Moreover, bias- and current-dependent luminescence quenching and enhancement occur in a micrometer-scale region around the tip position. These “long-range” effects result from the electron-tunneling-induced lateral spatial gradients of the charge carrier density in the monolayer, which modify the relative contributions of excitons versus trions and the radiative quantum yield of the excitons.

[1] Mak et al, Phys. Rev. Lett. 2010, 105, 136805

[2] Wang et al, Rev. Mod. Phys. 2018, 90, 021001.

[3] He, et al, Sci. Adv. 2019, 5, eaau8763.

[4] Peña Román et al, submitted

Direct investigation of trivial and non-trivial photonic modes in symmetry protected edge states at telecom wavelengths at the nanoscale

Thursday, 27th October - 15:21: Topological photonics & Non-reciprocal nano-optic - Oral

Ms. Sonakshi Arora¹, Dr. Thomas Bauer², Mr. Rene Barczyk³, Prof. Ewold Verhagen³, Prof. L. Kuipers⁴

1. Delft university of technology, 2. University of amsterdam, 3. AMOLF, 4. TU Delft

Topological photonics emulating the quantum valley Hall effect has recently gained attention due to its potential to offer immense control over optical signals and light-matter interactions stemming from robustness against backscattering. Recently, a concept for topological slow light devices has been put forward: a bearded topological photonic crystal interface supports a topological and a trivial mode around the K and K' valleys of the Brillouin zone. This raises the interesting question of whether the onset of Anderson localization caused by multiple scattering, which plagues slow-light applications in conventional photonic crystal architectures can be delayed or even avoided. Here we present a direct investigation of the onset of Anderson localization in topologically non-trivial photonic crystals with and without the engineered disorder.

We use amplitude- and phase-resolved near-field microscopy to visualize light propagation along the bearded interface (Fig.1 SEM). We observe the photonic manifestation of localization, illustrated by the appearance of localized high-intensity patches, only when we introduce engineered disorder in the structure. The real-space amplitude distributions as a function of frequency reveal different localized states associated with varying factors of quality. Using amplitude and phase-resolution we experimentally measure the two modes below the light cone in the dispersion relation and compare it with the numerical calculations. We quantitatively investigate a degree of merit called the backscattering mean free path (BMFP) for a range of geometrically engineered disorders and confirm that the BMFP falls with an increase in disorder.

More importantly, the results of the experimentally determined BMFP for a topological vs trivial mode differs. This proves that the trivial mode within the same structures is more susceptible to the spatial disorder than the topological mode.

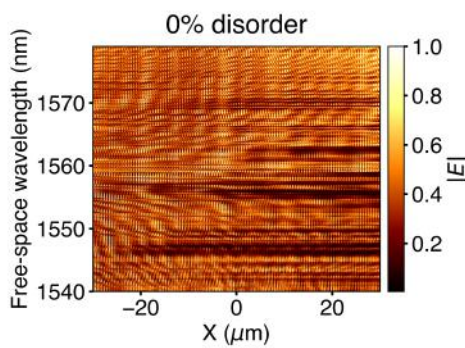


Fig3 a disorder0.png

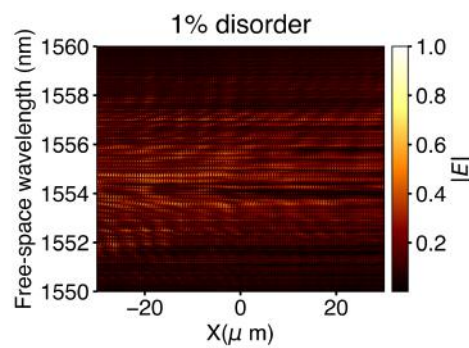


Fig3 b disorder1.png

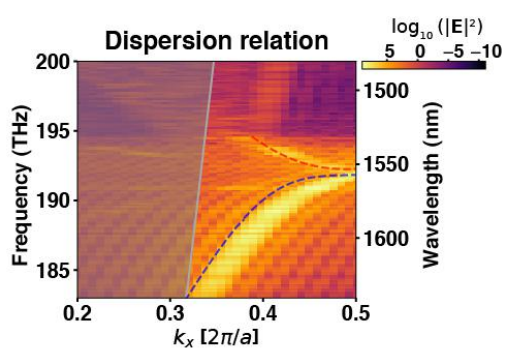


Fig2 dispersion.jpg

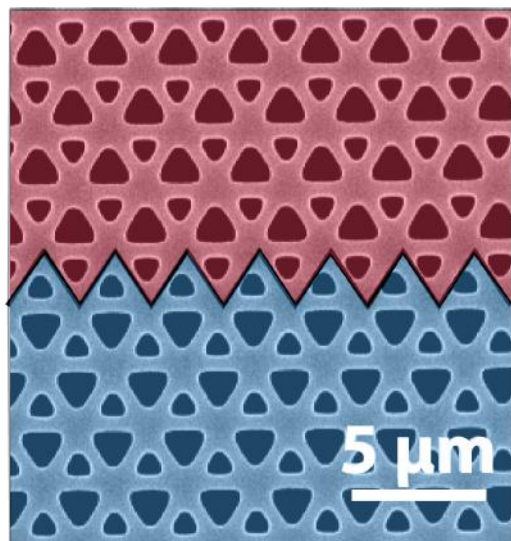


Fig 1 sem.png

Mie-exciton polaritons with monolayer WSe₂ hybridized by van der Waals nanophotonic structures

Thursday, 27th October - 15:38: Topological photonics & Non-reciprocal nano-optic - Oral

Dr. Yadong Wang¹, Mr. Sam Randerson², Dr. Panaiot Zotev², Dr. Xuerong Hu², Dr. Yue Wang³, Prof. Thomas Krauss³, Prof. Alexander Tartakovskii²

1. The University of sheffield, **2.** The University of Sheffield, **3.** University of York

Dielectric nanostructures exhibit low optical losses and a wealth of distinct Mie resonances in contrast to their plasmonic counterparts (*Science* **354** (6314), aag2472, 2016; *Nature communications* **10** (1), 5119, 2019). Meanwhile, the strong light-matter coupling has attracted long-standing interest due to its fundamental importance in Bose-Einstein condensation, polariton lasing, and potential in quantum optics applications. However, strong coupling with relatively broad Mie resonances has been rarely observed. Here, we achieve relatively narrow Mie resonances by combining high-refractive-index WS₂ nanoantennas and demonstrate strong exciton-photon coupling in monolayer WSe₂.

We fabricate nanoantennas by etching 30-nm WS₂ on a gold substrate and then stack a monolayer WSe₂ onto them using a dry transfer method. We use nanoantennas with radii from 83 to 155 nm, which allows gradual tuning of the Mie resonance through the WSe₂ exciton energy (Figure 1a). Thanks to the high refractive index of WS₂ and the gold substrate, Mie resonances with a narrow bandwidth of $\Gamma_M \sim 105$ meV are achieved in WS₂ nanoantennas, suitable for observation of the strong coupling with WSe₂ excitons. As shown in Figure 1b, the Mie resonances in the hybrid monolayer WSe₂/nanoantenna structures undergo significant changes compared with bare WS₂ structures. Typical anti-crossing behaviour is observed using dark-field scattering spectroscopy. The energy splitting between the upper (UBP) and low (LPB) polariton branches is fitted as $\Gamma_p \sim 86$ meV (Figure 1c), which is higher than the value reported in plasmonic systems (~50 meV). Considering the linewidth of Mie resonance and neutral exciton, the strong coupling condition is thus satisfied at room temperature. Our results provide a novel route for the manipulation of excitons in semiconductors and a promising platform for the realization of the strong coupling in nanophotonic structures and controlled light emission in nanophotonics (Nat. Commun. **12** (1), 6063, 2021; ACS Photon. **8** (3), 721, 2021; ACS Nano **16** (4), 6493–6505, 2022).

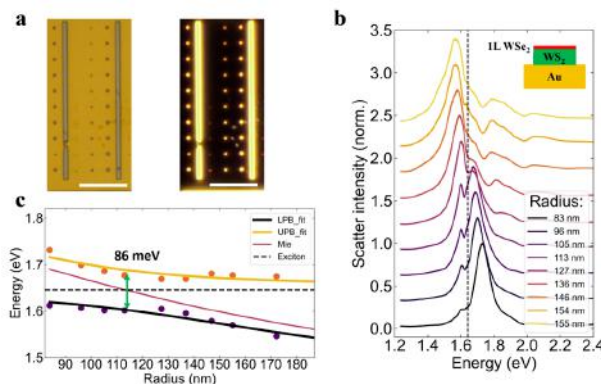


Figure1.png

Authors Index

Abad Arredondo, J.	54	Benimetskiy, F.	107
Abdelmalek, A.	25	Benisty, H.	39
Abécassis, B.	69, 70	Bennet, P.	50
Achouri, K.	110	Benson, O.	7
Acuna, G.	86, 103	Berciaud, S.	153
Adam, P.	78	Besbes, M.	113
Adawi, A.	78	Bidault, S.	12, 36, 118, 127
Agreda, A.	124	Blackburn, A.	148
Aharonovich, I.	106	Boer-Duchemin, E.	153
Aho, A.	33	Bogicevic, A.	113
Aissaoui, N.	12	Bogicevic, C.	113
Aizpurua, J.	4	Borne, A.	115
Alessandri, I.	80	Boroviks, S.	110
Amara, E.	25	Boudan, G.	113
Amaro de Faria Jr, A.	23	Bouhelier, A.	124
Amirtharaj, S.	46	Bouillard, J.	78
Andres-Penares, D.	34	Bouscher, S.	117
ANG, R.	52	Bouteille, B.	85
Ang, Y.	52	Bozhevolnyi, S.	38, 64
Arar, B.	32, 138	Bretel, R.	153
Arora, S.	154	Brodbeck, S.	6
Autore, M.	4, 35	Brottons-Gisbert, M.	34
Babaei, E. (University of Victoria)	147	Brzobohaty, O.	3
Babaei, E. (University of Victoria, Canada)	149	Brûlé, Y.	58
BAGHDADLI, A.	139	Buil, S.	120
Baghramyan, H.	109	Buyanova, I.	26, 33
Bahar, I.	149	Bylinkin, A.	35, 106
Baillard, G.	69	Bérini, B.	120
Banerjee, A.	149	Caixeiro, S.	16
Barczyk, R.	154	Calavalle, F.	22, 35, 106
Bargheer, M.	7	Calusci, G.	80
Barra-Burillo, M.	4, 22, 106	Capasso, F.	82
Basov, D.	1	Carcenac, F.	42
Baudrion, A.	78	Casanova, F.	4, 22, 35, 106
Bauer, T.	154	Catalano, S.	4
Bedu, F.	28	Catanzaro, L.	128
Beermann, J.	38	Celaj, S.	90
Bellot, G.	12	Centeno, E.	27, 50
Ben Youssef, A.	81	Chadeyron, G.	27
Ben-Asher, A.	112	Charron, E.	36
Benea-Chelmus, I.	82	Chen, P.	26

Chen, W. (Laboratory of Quantum and Nano-optics, Ecole Polytechnique Fédérale de Lausanne, CH-1015 Lausanne, Switzerland)	46	Duchan, M.	3
Chen, W. (Linköping University)	26, 33	Dujardin, E.	124
Chichkov, B.	135	Dujardin, G.	153
Ciraci, C.	109	Dutta, A.	31
Claude, J.	41, 43	Désert, A.	27
Claudon, J.	115	Ebrahimi, S. (Department of Physics and Mathematics, University of Hull, Cottingham Road, HU6 7RX, UK)	78
Colas des Francs, G.	58, 101	Ebrahimi, S. (Light, nanomaterials, nanotechnologies (L2n) Laboratory, CNRS EMR7004, University of Technology of Troyes, F-10004 Troyes Cedex, France)	78
Colas-des-Francs, G.	124	Edgar, J.	35, 106
Colom, R.	55	Elsawy, M.	55
Compagnini, G.	29, 128, 145	Esteban, R.	4
Condorelli, M.	29, 128, 145	Eustache, C.	121
Conteduca, D.	34	Evlyukhin, A.	84, 135
Coolen, L.	69	Fahim, M.	19, 131
Coquillat, D.	48	Faim, F.	74
Cordoba, C.	148	Faraci, G.	145
Corti, C.	12	Feist, J.	112
Cottancin, E.	120	Fernandes, D.	74
Coudeville, J.	39	Fernández-Domínguez, A.	54, 86, 112
Coudrat, L.	115	Filloux, P.	115
Couteau, C.	95	Fiorini, C.	113
Crowther, S.	71	Fleury, B.	70
Cuche, A.	58, 96	Fournel, F.	96
Cui, L. (Institut des NanoSciences de Paris)	70	Gaimard, Q.	39
Cui, L. (Sorbonne Université)	118	Galland, C.	46
Curti, L.	70	Gallas, B. (Insti)	36, 70
D'Urso, L.	29	Gallas, B. (Institut des NanoSciences de Paris - Sorbonne Université)	57, 118, 119
D. Gonçalves, P.	5	García de Abajo, F.	5
Dagens, B.	85	García Vidal, F.	54
De Liberato, S.	100	Garreau, A.	39
Degiron, A.	115	Gather, M.	16
Dell'Ova, F.	124	Gayet, E.	12
Della Sala, F.	109	Genevet, P. (CNRS, CRHEA, Université Côte d'Azur, 06560 Valbonne)	55
Demirdjian, B.	28	Genevet, P. (CRHEA CNRS)	81
Destouches, N.	40	Gerardot, B.	34
Dey, S.	8	Ghamari, S.	133
Dezert, R.	115	Giessen, H.	65
Dhawan, A.	122	Ginis, V.	82
Diaz Valles, A.	101	Gobbi, M.	22
Djampa-Tapi, W.	113	Gogol, P.	85
Dolci, M.	10		
Douillard, L.	141		
Duarte, L.	31		
Dubertret, B.	122		
Duboz, J.	55		

Gonzalez-Posada Flores, F.	42, 48, 139	Juliano Martins, R.	81
González, P.	35, 106	Jupille, J.	85
Gordon, R.	125, 147–149	Jákl, P.	3
Gozhyk, I.	85	Jørgensen, M.	132
Grange, R.	61	Karakhanyan, V. (Femto-ST (CNRS), Université Bourgogne Franche-Comté)	121
Greffet, J.	113	Karakhanyan, V. (Femto-ST, Université Bourgogne Franche-Comté)	50
Groenhof, G.	31	Kee, C.	52
Grosjean, T.	50, 121	Kersuzan, C.	90
Gubbin, C.	100	Kewes, G.	7
Guillemeney, L.	69	Khalid, M.	109
Guina, M.	33	Khaywah, M.	27
Guselnikova, O. (National Institute For Materials Science)	44	Kildemo, M.	77
Guérin, S.	101	Kim, B.	129
Gérard, J.	115	Kim, Y.	129
Hakkarainen, T.	33	Kirtaev, R.	106
Hale, N.	77	Kiselev, A.	110
Hayat, A.	6, 117	Klembt, S.	117
Heinrich, M.	17	Koks, C.	104
Henderson, B.	148	Koopman, W.	7
Henkel, C.	7	Kotsedi, L.	25
Henry, C.	28	Krauss, T.	34, 156
Henzie, J.	44	Kudelski, A.	67
HERNANDEZ, R.	96	Kuipers, L.	20, 154
Heurs, M.	135	Kumar, A.	117
Hillenbrand, R.	4, 22, 35, 106	Kumita, J.	149
Hiura, S.	33	Kurdiumov, S.	18
Hobbs, J.	34	Kwon, S.	129
Hong, S.	129	Kyrou, C.	55
Hu, X.	156	Laborie, L.	85
Huang, Y.	33	Lamberti, V.	10
Hueso, L.	4, 22, 35, 106	Landau, N.	6
Hughes, S.	148	Lannebère, S.	74
Huijben, T.	19, 131	Lanteri, S.	55
Humbert, M.	96	Larrey, V.	96
Huppert, S.	142	Larrieu, G.	96
Höfling, S.	6, 117	Laverdant, J.	120
Höjer, P.	33	Lazzari, R.	85
Ilin, D.	98	Le Moal, E.	153
Iorsh, I.	98	Le, V.	40
Ishikawa, F.	26	Lefier, Y.	121
Isoaho, R.	33	Lefkir, Y.	40
Itzhaki, L.	149	Leo, G.	115
Jacovi, R.	117	Lequeux, N.	113
Jacquet, P.	85	Lerouge, F.	120
Jauslin, H.	101		

Lhuillier, E.	70	Mortensen, K.	19, 131
Li, F.	151	Mou, Y.	57, 119
Li, P.	35	Mullin, N.	34
Liang, Y.	39	Muniaín, U.	4
Linden, S.	94, 150	Muravitskaya, A.	78
Liu, J.	69	Murayama, A.	33
Liu, S.	35	Na Liu, L.	63
Loirette-Pelous, A.	113	Najem, M.	42, 48
Lorchat, E.	153	Naqvi, M.	149
Lu, J.	82	Nasilowski, M.	122
Lupi, S.	83	Nechepurenko, I.	32, 138
Lupu, A.	39	Nikitin, A.	35, 106
Lörtscher, E.	46	Nikulina, E.	106
Maaza, M.	25	Noordam, M.	20
Macis, S.	83	Nooteboom, S.	8
Mahajan, S.	19	Novotny, L.	2
Mahiou, R.	27	Nyembo, P.	142
Maitre, A.	90, 122, 142	Ohlmeyer, M.	149
Makarov, S.	107	Ou, J.	18
Malchow, K.	124	Ouerdane, Y.	27
Manganelli, C.	22	Ouzit, Z.	69
Mannino, G.	145	Ozerov, I.	28
Marchi, N.	139	Paci, I.	148
Marguet, S.	12, 141	Paillard, V.	58, 96
Marie, R.	19, 131	Palpant, B.	141
Marinov, E.	81	Pandey, D.	132
Markesevic, N.	31	Panna, D.	6, 117
Markovic, O.	36	Panoiu, N.	151
Marquier, F.	113	Papasimakis, N.	18
Martin, O.	110	Parola, S.	27
Martín-García, B.	22	Parra López, L.	153
Masharin, M.	107	Pašteka, L.	72
Mathew, S.	149	Pedersen, J.	131
Matiushchikina, M.	135	Pedireddy, S.	14
Miguel, A.	54	Pellarin, M.	120
Mikheeva, E.	55	Perera, K.	14
Mini Rajendran, G.	72	Perroy, J.	139
Mivelle, M. (Institut des NanoSciences de Paris - CNRS)	70	Peña Román, R.	153
Mivelle, M. (Institut des NanoSciences de Paris)	36,	Piccardo, M.	82
	57, 118, 119	Pilo-Pais, M.	86, 103
Moazzezi, P.	148	Pintor, J.	69
Modin, E.	106	Poddubny, A.	98
Moreau, A.	27, 50	Pohar, C.	139
Moreaud, L.	113	Polojärvi, V.	33
Morgado, T.	74	Pommier, D.	153
Mortamais, M.	139	Pons, T.	90, 113, 142

poshakinskiy, A.	98	Simonot, D.	142
Potdevin, A.	27	Simpson, S.	3
Prado, Y.	70	Sivan, Y.	126, 144
Pulvirenti, M.	29	Smaali, R.	27, 50
Qureshi, H.	31	Song, S.	136
		Song, Y.	75
Rahimof, Y.	32, 138	Sortino, L.	34
Ramdane, A.	39	Spirito, D.	22
Randerson, S.	34, 156	Stefani, F.	86
Ranguis, A.	28	Stehr, J.	26
Ranos, T.	115	Steinmann, P.	94
Rechtsman, M.	62	Stenger, N.	132
Ren, J.	148	Stete, F.	7
Ressier, L.	96	Su, M.	75
Reynier, B. (Institut des NanoSciences de Paris - Sorbonne Université)	118	Subramanian, S.	14
Reynier, B. (Institut des NanoSciences de Paris)	36, 119	Sun, Y.	75
Rodriguez, A.	60	Svak, V.	3
Roini, G.	80	Synanidis, A.	5
Rousseaux, B.	101	Szameit, A.	17
Roux-Byl, C.	142	Sýkora, M.	72, 92
roy, p.	41, 43	Taboada-Gutiérrez, J.	35
Réveret, F.	27	Takayama, J.	33
Saidaminov, M.	148	Taleb Bendiab, A.	139
salemi, l.	29	Taliercio, T.	42, 48, 139
Samperi, O.	29	Tartakovskii, A.	34, 156
Samusev, A.	107	Teisseire, J.	85
Sanz-Paz, M.	86, 103	Teytaud, O.	50
Sarah, H.	124	Tiainen, V.	31
Sarkar, S.	144	Tichauer, R.	31
Sato, S.	33	Tisovský, P.	72
Scardaci, V.	128	Titze, V.	16
Schill, H.	94	Tomarchio, L.	83
Schmitt, J.	150	Tonkaev, P.	76
Schneider, C.	6	Toppari, J.	31
Schnell, M.	35	Un, I.	144
Schubert, M.	16		
Schull, G.	153	van Exter, M.	104
Schwob, C.	70, 118	Varguet, H.	101
Severs Millard, T.	34	Vassant, S.	113
Seyed Shariadoust, M.	149	Vavassori, P.	106
Shagar, M.	34	Verhagen, E.	154
Shahnazaryan, V.	107	Vinattieri, A.	80
Sharma, D.	124	Volkov, V.	106
Shelykh, I.	107	Vollmer, F.	14, 133
Sidorenko, A.	150	Vu, N.	120

Wagnon, B.	69	Yang, X. (Institut des NanoSciences de Paris)	36, 57
Walmsness, P.	77	Yang, X. (Sorbonne Université)	119
Wang, J.	151	Yeddu, V.	148
Wang, X.	26	Yedjour, A.	66
Wang, Y. (Eindhoven University of Technology)	8	Yezekyan, T.	38
Wang, Y. (The University of sheffield)	156	Yu, S.	129
Wang, Y. (University of York)	34, 156	Zagonel, L.	153
Wenger, J.	41, 43	Zapata, H.	119
Wenzel, S.	32, 138	Zemanek, P.	3
Wetter, H.	150	Zenin, V.	38, 135
Wicht, A.	32, 138	Zeyneb, B.	25
Wiecha, P.	58, 96	Zhang, B.	26
Wilk, A.	39	Zhang, H.	148
Wolterink, T.	17	Zhang, T.	52
Wright, D.	149	Zhang, Y.	94
Wu, H.	133	Zhang, Z.	75
Wu, W.	88	Zheludev, N.	18
Wubs, M.	132	Zhiyuan, X.	46
Xiao, S.	132	Zhu, F.	86, 103
Yamauchi, Y.	44	Zijlstra, P.	8, 10, 19
Yang, X. (Institut des NanoSciences de Paris - Sorbonne Université)	118	Zotev, P.	34, 156
		Zuev, D.	75



Conferences, Events & Workshops